論文 / 著書情報
Article / Book Information

題目(和文)	
Title(English)	CO2 Gasification of Biomass for High Efficiency and Carbon-negative Power Generation
著者(和文)	PRABOWOBAYU
Author(English)	Bayu Prabowo
出典(和文)	学位:博士(工学), 学位授与機関:東京工業大学, 報告番号:甲第9595号, 授与年月日:2014年6月30日, 学位の種別:課程博士, 審査員:吉川　邦夫,加茂　徹,高橋　史武,時松　宏治,梶谷　史朗
Citation(English)	Degree:Doctor (Engineering), Conferring organization: Tokyo Institute of Technology, Report number:甲第9595号, Conferred date:2014/6/30, Degree Type:Course doctor, Examiner:,,,,
学位種別(和文)	博士論文
Type(English)	Doctoral Thesis

Doctoral Thesis

CO_2 Gasification of Biomass for High Efficiency and Carbon-negative Power Generation

Bayu Prabowo

11D29066

Advisor: Professor Kunio Yoshikawa

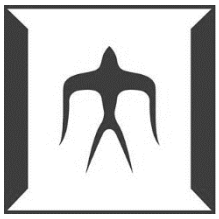

Department of Environmental Science and Technology

Interdisciplinary Graduate School of Science and Engineering

Tokyo Institute of Technology

June 2014

Abstract

With a strong growth of energy demand and the increase of environmental anxiety, one of the world's ultimate challenge for the 21st century is to develop a sustainable and low-carbon energy supply technologies. Bioenergy with carbon capturing and storage (BECCS) offers an opportunity for responding the challenge by ensuing the net removal of atmospheric CO_2 while at the same time as fulfilling energy requirements. However, the gap between the scale of biomass conversion system that in many cases is required to be small and the CCS that is merely feasible for the relatively large scale process is potentially hinder the implementation of BECCS. In this study we recognize the potential utilization of biomass CO_2 gasification as a compatible method for BECCS. CO_2 gasification can produce high purity of CO and CO_2 mixture which combustion product can be sequestrated in a simple process and/or recycled back to gasifier as gasifying agent. To more deeply investigate and optimize this potential, the following three parts were studied in this thesis.

First, the performance of CO_2 gasification in producing nitrogen-free producer gas was examined in a lab-scale downdraft gasifier. The effect of the temperature and the gasifying agent mixing with steam and/or O_2 on gas evolution and the thermal efficiency were investigated to obtain the knowledge of the reaction behavior and find the optimum operating condition. The result shows that CO_2 as a gasifying agent and heat carrier, especially in direct gasification process, is potentially be more efficiently utilized in N_2-free producer gas production than steam.

Second, the operability and performance of CO_2 gasification was examined in a pilot scale downdraft gasifier. Findings in previous chapter was used as basic conditions while further examination was performed to investigate the effect of the CO_2 flow rate on the reactor temperature, the producer gas composition and the energy yield. CO_2-O_2 gasification was stably operated for around 70 min in pilot scale downdraft gasifier under 0.6 - 1.6 CO_2/C ratios and around 0.4-0.6 equivalence ratio. The enhancement of CO evolution through CO_2-char reaction and dry reforming was observable.

At last, CO_2-recycled biomass gasification system was proposed. The performance of the power system was analyzed using the thermal equilibrium model. Validation and adjustment of the model was performed on the gasifier component based on the result of previous chapter. The parameter of CO_2 recycle ratio was examined under various gasifier target temperatures and turbine inlet and exit temperatures to find the optimum operating condition. Compared with the conventional air gasification, the proposed system could produce 11.93 % higher efficiency. The system also potentially implement carbon-negative power generation with intensity around -484.25 to -1372.23gCO_2/kwh with maximally 6.12 % efficiency penalty.

Acknowledgement

In the name of Allah the most merciful. I would like to express my praise to Allah for His guidance to finish this research on the CO2 Gasification of Biomass for High Efficiency and Carbon-negative Power Generation.

This research would not be completed without the full support of many people; therefore I would like to acknowledge the gratitude to:

1. Prof. Kunio Yoshikawa, as my supervisor,
2. Assoc. Prof. Fumitake Takahashi and Assoc. Prof. Koji Tokimatsu, for the valuable discussion during the study,
3. Assist. Prof. Marco J. Castaldi, Prof. Herri Susanto, and especially Assist. Prof. Kentaro Umeki, for the precious collaboration and opportunity for conducting experiment in their laboratory,
4. Japanese Government Monbukagakusho Scholarship scheme, for the financial support during my study,
5. All supportive staffs and friends in Department of Environmental Science and Technology, Tokyo Institute of Technology for the help and close friendship,
6. Friends in ITB, LTU, CU and other people that I can not mention one by one, and

Last but not least to all my family, my parents, my beloved wife Tanty and my daughter Jehan. This thesis would be too short to describe their love, efforts and support for me not only for this thesis but also for my entire life.

Tokyo, 4 June 2014

Bayu Prabowo

Table of Contents

List of Figures

Chapter I

Chapter II

Chapter III

Chapter IV

List of Tables

Chapter I

Introduction

1.1 Social Background

1.1.1 Energy supply and demand

As a crucial part of human life, energy is evolving to match with the contemporary human development and requirements. Over the last 200 years, the global population has risen by a factor of 6 while the per capita energy consumption is estimated to have risen by a factor of 20 [1]. It shows that not merely population growth that makes the future compounded, but the inevitable need to expand economic output also placed enormous demands on natural and environmental resources.

In 2005, the United Nation estimated that the world population will increase around 40% by the year of 2040, from 6.5 billion to 9.1 billion. Moreover, the average of GDP per capita, indicates the level of economic activity, is predicted to grow by roughly 3% annually in the non-OECD area and 1.7% in the OECD area over the next half century [2]. Thus, as shown in Fig.1.1, it is projected that the world energy demand will increase as much as 56% between 2010 and 2040, 524 to 820 quadrillion Btu [3]. Based on these projections, the efforts on increasing energy supplying capacity and sustainability is essential for securing energy supply.

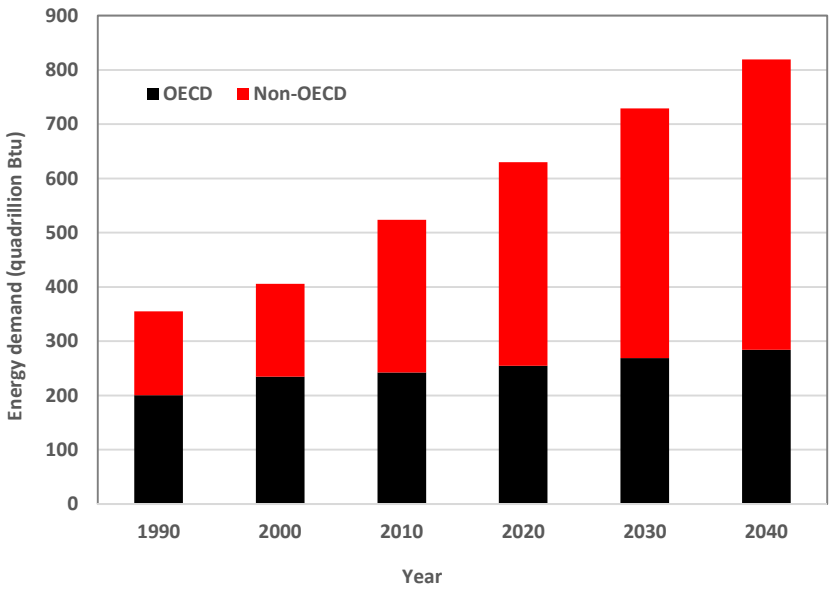

Figure 1.1 World energy demand history and projection [3]

Currently, more than 80% of world energy demand is fulfilled by fossil fuel. Petroleum oil is the biggest energy contributor with the contribution around 175 quadrillion Btu per day in 2010, followed by coal, 150 Btu per day, and then natural gas, 120 quadrillion Btu per day [3]. However, in contrast with their contribution, the reserves of the fossil is highly limited. World Energy Outlook (WEO) 2006 estimated the consumption/reserve ratio of around 39, 43 and 164 years for oil, natural gas and coal, respectively. Considering the modified rate of production or consumption, a recent proposed model in 2005 even calculated the reserves sustainability down to 35, 37 and 107 years for oil, natural gas and coal, respectively [4]. This means at this rate coal reserves will be available until at least 2112, and it will be the single fossil fuel in the world after 2042.

Based on the summarized circumstances, one of ultimate challenge for the 21st century is to develop a new methods of generating and using energy that meet the needs of growing global civilization.

1.1.2 Climate changes and other environmental problems

In addition to the energy supply depletion, the world is now on the path to violate the governments' agreement to limit the rise of the average global temperature to 2 degrees Celsius by 2050. To achieve the target, CO_2 concentration in atmosphere by that time needs to be as low as 450 ppm but recently in May 2013, CO_2 level in the atmosphere already exceeded 400 ppm which is the first time in several thousand years. Average global temperatures have already increased by 0.8 °C compared with pre-industrial levels and without further climate action, it is projected that the long-term temperature increase will be around 2.8 °C to 4.5 °C [5]. These temperature increases are reversible and potentially create several permanent damages on human's health and ecosystem as shown in Fig. 1.2.

On the other hand, world energy-related carbon dioxide emission is projected to rise 46% from 31.2 billion metric tons in 2010 to 45.5 billion metric tons in 2040 [3]. With a strong economic growth and continued heavy reliance on fossil fuels, the global action for limiting the global temperature rise to 2 °C is extremely challenging. The growth in global energy-related CO_2 emission needs to be halted and start to be reduced within the current decade. The development of high efficiency and low-carbon energy supply technologies is urgently crucial.

1.2 Bioenergy with Carbon Capturing and Storage (BECCS)

Biomass-based energy generation offers an opportunity for responding the problem of energy sustainability and global warming. First, biomass has relatively short life-cycle compared to fossil fuel so that the productivity is technically expandable. The potential contribution of bioenergy that is currently 45-55 EJ/year (2004) may be increased to the 200-400 EJ/year up to 2050 [7]. The second feature is the carbon neutrality. Biomass is considered to be net CO_2 emission free since the entire

carbon precursor in biomass was assimilated from atmospheric CO_2 during its growth via photosynthesis. The use of biomass is expected to cut emissions by 80 to 90% compared to the fossil energy baseline scenario [8].

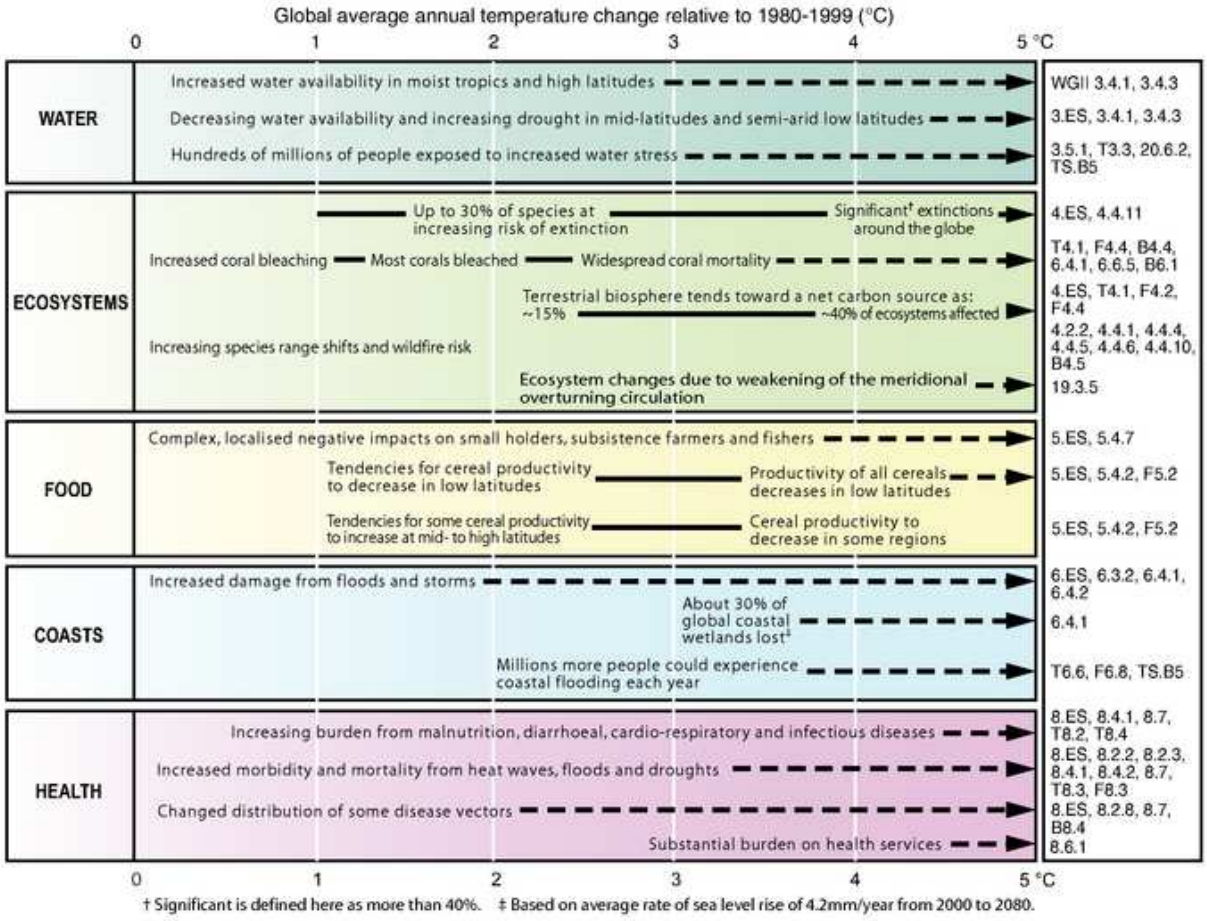

Figure 1.2 Effect of global warming [6]

Considering the carbon neutrality, bioenergy can go further to carbon-negative by reducing the release of carbon emission from the conversion process to the atmosphere, as shown in Fig. 1.3. This concept can be realized by integrating the carbon capture and storage (CCS) process to the biomass conversion system, so called bioenergy with carbon capturing and storage (BECCS). This option offers a unique opportunity for the net removal of atmospheric CO_2 while at the same time as fulfilling energy requirements. The negative CO_2 emissions that result from BECCS operations have four main implications [9]:

1. BECCS can mitigate emissions from any CO_2 emission source so that it can be used to abate the emissions that are difficult and expensive to cut back on, such as CO_2 from transportation sector or small scale emissions.

2. BECCS can abate the emissions which have already occurred in the past.
3. BECCS can be used as a climate mitigation risk management tool, which may be needed due to the uncertainties of climate scenario modelling as well as uncertainties related to the long-term efficiency of greenhouse gas (GHG) mitigation policies.
4. BECCS can be added as a supplement to other processes such as on top of bio-energy use. The application of BECCS would make it possible to reach agreed climate targets at lower costs, and also involves opportunities to raise the ambitions for emission reductions and the pace of climate mitigation work.

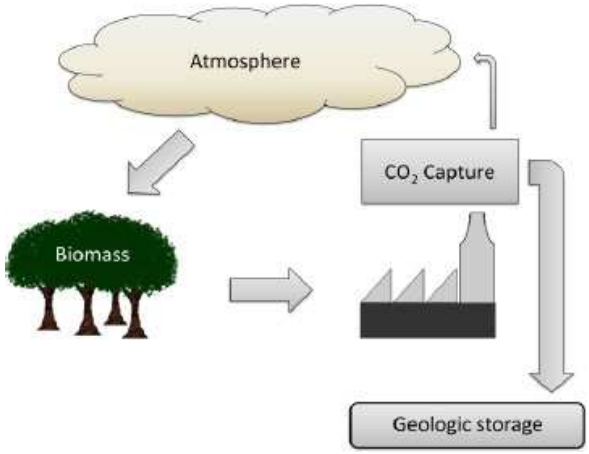

Figure 1.3 The concept of Bio Energy with Carbon Capturing and Storage (BECCS) [9]

Due to those implications, BECCS stands out as a viable, cost effective method to significantly reduce atmospheric CO_2 concentrations. Other mitigation methods alone are said to be insufficient or too expensive to reach rigorous climate mitigation targets to 450 ppm while with BECCS, it is possible to reach below 350 ppm [9].

As shown in Figs. 1.4 and 1.5, BECCS could be used in a wide range of applications either for biomass to biochemical or biomass to bioenergy, respectively. For the conversion method, in general the high moisture content biomass is suitable for biochemical conversion while the dry biomass is suitably converted by thermochemical conversion mostly through gasification.

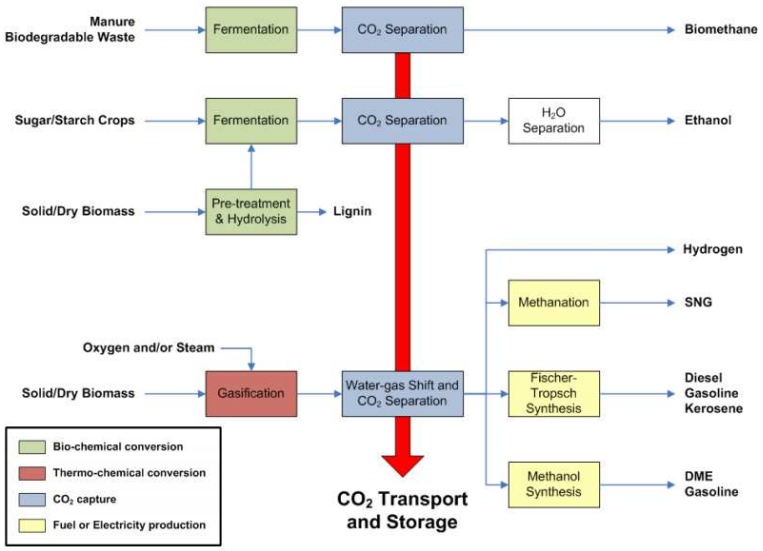

Figure 1.4 Schematic of BECCS deployment in biomass to biochemical conversion [10]

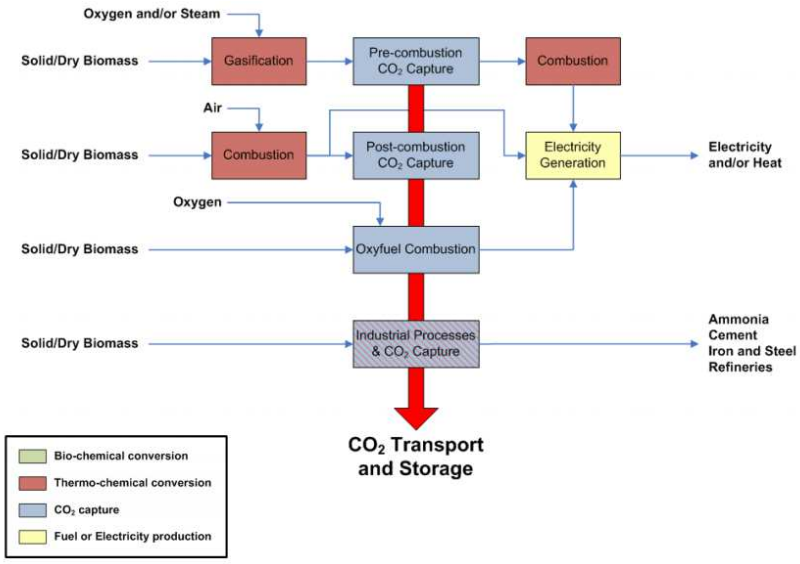

Figure 1.5 Schematic of BECCS deployment in biomass to bioenergy conversion [10]

However as a new emerging concept, BECCS still has large gaps to the implementation. From the aspect of policy and economic, it still remained many constraint such as incentive, biomass availability, land use, CO_2 storage location, etc. [11]. From the technical issue, it is well studied that the attachment of CCS will be resulted in 8-12 % efficiency reduction and the available technology also required some complex equipment. Hence, CCS is merely feasible for the relatively large scale and multicomponent process, i.e. IGCC process for coal. On the other, due to the low energy density that increase its transportation cost, the scale of biomass conversion system in many cases is required to be small [12]

thus might not be suitable for a complex process. The balance between these factors is largely unexplored [11]

Currently there are only several projects on BECCS on the operation. BECCS projects are started in 2010, where around 16 initiated projects are mostly located in Europe and North America. The world's first BECCS project is situated in Illinois, in the United States. The first ton of carbon dioxide emerges as a by-product in ethanol production was sequestered in this facility on 4th of November 2011. Presently carbon dioxide is injected at a rate of 30-0 tons per year but the project will be terminated in 2016 without additional funding. Another project at the University of North Dakota is planning a pilot plant biomass gasification based BECCS to demonstrate future technology for bio-energy in combination with storage of carbon dioxide [9].

In order to meet the mitigation scenarios proposed by IEA [5], we would need to achieve 2.4 billion tons of negative emissions of CO_2 from BECCS operations in 2050. The same report also suggests that a total BECCS capacity worldwide of 35 million tones will be needed in 2020. Based on the anticipated long duration of deployment, this implies that we need 50-100 BECCS projects to be initiated within the next 2 years, and several hundreds more shortly thereafter.

1.3 Biomass gasification with CO_2

Biomass gasification is one of the favorable pathways of biomass utilization since the technology is relatively mature, acceptable for various kind of biomass and can produce various products. Gasification is partial oxidation of biomass with oxidizer and gasifying agent that resulting in the mixture of combustible gases consisting of carbon monoxide (CO), hydrogen (H_2) and traces of methane (CH_4), called as a producer gas. The producer gas can be used to run internal combustion engines , can be used as substitute for furnace oil in direct heat applications and can be used to produce some chemical products such as methanol, DME, etc. The common operating temperature is around 700-1300°C, while wide range of pressure, 1 -35 atm, can be applied.

Biomass gasification process occurs in three interrelated stages: devolatilization to produce volatile matter and char (eq.1.1), combustion and gasification of in situ formed char with reactive gases (eqs.1.2-1.6), and secondary reactions of primary gases and tars (eqs.1.7-1.16).

Biomass → CO, CO_2, CH_4, C_2H_4, H_2O + Primary tar (CH_xO_y) + Carbon		[eq.1.1]
C + O_2 → CO_2	-393.5 kJ/mol	[eq.1.2]
C + 0.5 O_2 → CO	-123.1 kJ/mol	[eq.1.3]
C + CO_2 → 2 CO	+159.9 kJ/mol	[eq.1.4]

$C + H_2O \rightarrow CO + H_2$	+118.5 kJ/mol	[eq.1.5]
$C + 2\ H_2 \rightarrow CH_4$	-87.5 kJ/mol	[eq.1.6]
Primary tar $\rightarrow$ CO, CO_2, CH_4, C_2H_4, H_2 + Secondary tar		[eq.1.7]
Secondary tars $\rightarrow$ C, CO, H_2		[eq.1.8]
Tar + $vH_2O \rightarrow xCO + yH_2$		[eq.1.9]
Tar + $vCO_2 \rightarrow xCO + yH_2$		[eq.1.10]
$H2 + 0.5\ O_2 \rightarrow H_2O$	-242 kJ/mol	[eq.1.11]
$CO + 0.5\ O_2 \rightarrow CO_2$	-283 kJ/mol	[eq.1.12]
$CH_4 + 0.5\ O_2 \rightarrow CO + 2\ H_2$	-110 kJ/mol	[eq.1.13]
$CH_4 + CO_2 \rightarrow 2\ CO + 2\ H_2$	+247 kJ/mol	[eq.1.14]
$CH_4 + H_2O \rightarrow CO + 3\ H_2$	+206 kJ/mol	[eq.1.15]
$CO + H_2O \rightarrow CO_2 + H_2$	-40.9 kJ/mol	[eq.1.16]

The slowest reaction is occur in heterogeneous reactions (eqs.1.4-1.6), thus they become the rate controlling steps of the overall process. Those steps are also importantly determining the energy intensity of the process which eventually determine the overall efficiency of the gasification system. The char reaction with oxygen, dominant in air gasification or oxygen gasification, is fast and energy extensive however it resulted in low energy recovery in producer gas. The char reaction with steam and with CO_2, dominant in steam gasification and CO_2 gasification, is slow and energy intensive but produce high energy yield in the producer gas. The char reaction with hydrogen is fast, energy extensive and resulted in high energy yield producer gas; however hydrogen itself is a precious gas that might be highly energy intensive in its production. The commonly utilized gasifying agent is air, oxygen, steam, or their mixture. The feature of each process is summarized in Table.1.1 [13].

Table 1.1 Modes of thermal gasification [13]

Partial oxidation with air	Main products are CO, CO_2, H_2, CH_4, N_2, tar. This gives a low heating value gas of ~5 MJ/m^3. Utilization problems can arise in combustion, particularly in gas turbines
Partial oxidation with oxygen	The main products are CO, CO_2, H_2, CH_4, tar (no N_2). This gives a medium heating value gas of ~10–12 MJ/m^3. The cost for providing and using oxygen is compensated by a better quality fuel gas. The trade-off is finely balanced
Steam (pyrolytic) gasification	The main products are CO, CO_2, H_2, CH_4, tar. This gives a medium heating value gas of ~15–20 MJ/m^3. The process has two stages with a primary reactor producing gas and char, and a second reactor for char combustion to reheat sand which is recirculated. The gas heating value is maximized due to a higher methane and higher hydrocarbon gas contents, but at the expense of lower overall efficiency due to loss of carbon in the secondary reactor

Compared to the abovementioned gasifying agent, CO_2 utilization in gasification is scarce. So far CO_2 gasification application is only limited for lab scale research work while the report about commercial operation of CO_2 gasifier is hardly found. These might be related to the difficulty of getting high concentration CO_2 stream in atmosphere and moreover the reaction of CO_2 with carbon, Eq. 1.4, is highly energy intensive. However, the increased concern on global warming might positively affect the development of this technology: the deployment of CCS in the coming years will provide a large number of high concentration CO_2 stream; in addition, CO_2 utilization to useful product in gasification is beneficial since it resulted in the carbon-negative intensity [14]. Moreover, in this study we recognize the potential utilization of biomass CO_2 gasification as a compatible method for BECCS concept since the producer gas will be mainly consisted of CO and CO_2. Combustion of the producer gas will result in a high purity CO_2 stream that can be sequestrated in a simple process and/or recycled back to gasifier.

The researches on CO_2 gasification can be roughly classified into three categories. The first category of studies focuses on the kinetics of char gasification in CO_2 atmosphere. It is the subject on which the most researches about of CO_2 gasification were performed. The second is engineering studies of utilizing CO_2 in a gasifier and study its performance characteristics. The third category is proposing a new system of feedstock conversion process that implemented CO_2 gasification within.

1.3.1 Kinetics of CO_2 gasification

Most of the research on this subject was performed using char in a chemically controlled reactor. A comprehensive review, more than 230 papers, of this subject on coal has been made by Irfan et al. [15]. It is summarized that CO_2 gasification was more reactive with low-rank coal due the presence of high concentration of oxygen-containing functional group, high proportion of transitional and macro pores, and high dispersion of catalytic inorganic matter. The gasification rate was decreased by the pressure increase due to the inhibition effect of CO but it is enhanced by the temperature increase below the ash melting temperature. The suitable kinetic models are simple power rate law for the low operating pressure and Langmuir-Hinshelwood for the high pressure. The activation energy (Ea) is highly dependent on coal and char properties and measured in the range of 32-247 kJ/mol. The best fit diffusion model is the random pore model and it's modified one (quantize solution method).

The research works on biomass roughly showed similar results. Ollero [16] found the kinetic parameters of nth order model where the activation energy (Ea) is 133 kJ/mol and the reaction order (n) is 0.43 for olive residue under pure CO_2 stream. Langmuir Hinshelwood well described the process when CO inhibition effect existed. Mani [17] found the parameters of Ea=156 kJ/mol and n=0.9 for wheat straw char. His results also showed the enhancement of the reaction rate as the temperature increased and the particle size reduced. The effective diffusivity increased rapidly with the reduction of the particle size and moderately with the increase of the temperature. Surface reactions might also play role in the

particle diameter of 925 µm. Zong [18] found that gasification can be divided into the chemisorption stage and the chemisorption negligible stage which were occurred at a low level (below 0.6) and a high level of conversion, respectively. The activation energy from DSC data is in good agreement with the calculated data from TG only in the later stage. For the diffusion controlled model, Sircar [19] found that the random pore model fitted the data better than those of the volumetric model and the non-reactive core model for pinewood char gasification. The calculated activation energy was Ea=125+30 kJ/mol. Apparent gasification rate parameters for large particles are comparable with those for much smaller particles. The pore structure parameter is increased from 0-16.5 within 1000-1170 K range. Regarding the three steps of C-CO_2 reaction: CO_2 chemisorption, endothermic reaction, and CO desorption, he found that the desorption step is the rate limiting step. The same conclusion regarding the model and the rate limiting step is also previously found in other researches [20,21,22]

Some works also focused the performance comparison of CO_2 gasification with steam gasification, which has been a more common method. Marquesz-Montesinos [23] found that Ea for CO_2 gasification is in the range of 200-250 kJ/mol, while that for steam gasification is 130-170 kJ/mol. Similarly, Ahmed [20] found the reaction rate of char with CO_2 was almost half of that with steam. The peak of the reaction rate of char with CO_2 was observed at 0.1 conversion degree while that with steam was observed at 0.3. For the mixed atmosphere, Guizani [24] and Nilsson [25] found that char reactivity in the mixed atmosphere can be expressed as the sum of the individual reactivity obtained in each single atmosphere experiment and CO_2 does not affect the char-steam reaction. These results were different from those of coal char with mixed atmosphere that showed the interference of char-H_2O and char-CO_2 reactions. The interference was resulted either in the inhibition effect [26, 27] or in the synergistic effect [27] depending on the mineral contents in their ash.

Since CO_2 gasification is slow, the other focus on the kinetic works is to add the catalyst for the reaction. Iwaki [28] used mixture of lithium sodium and potassium carbonates as a catalyst for wastepaper gasification at 923-1023 K. The reaction was approximately first order with Ea around 122-106 kJ/ mol and lithium played the most catalytic activity. Huang [29] found the activity order of metal catalyst as K>Na>Ca>Fe>Mg which also agreed with the result of other work [30]. He also found the de-activation of Ca catalyst at the temperature over 890°C due to the agglomeration. Different result was obtained in other research [28], that showed the activity order of metal catalyst as Na>Ca>Fe>K>Mg. The low activity of K-char was because of the increased sintering tendency of ash as high concentration of K was presented at high temperature (875°C) through the formation of potassium silicate eutectics. Lahijani [21] found the activity order of iron species as $Fe(NO_3)_3$>$FeCl_3$>$Fe_2(SO_4)_3$ and optimum at 5% loading. Ea of catalyzed reaction is 253.9 kJ/mol, a 50 kJ/mol decrease from that of raw char reaction. In other work, Lahijani [22] used palm empty fruit bunch ash which is rich in potassium as a natural

catalyst or palm shell char-CO_2 reaction. The activation energy of the catalyzed reaction found to be 158.75 kJ/mol while that of un-catalyzed is 268.11 kJ/mol

1.3.2 Performance characteristic of CO_2 gasification

This study focused on the performance of the overall reaction in the gasification process which indicated by the producer gas behavior. Garcia [31] investigated the pine sawdust CO_2 gasification catalyzed by Ni/Al at 700°C. He found that CO_2 is converted into valuable gas so that more CO and less H_2 than those of under steam gasification were observed under CO_2 gasification. Agreement of the initial gas yield to the equilibrium model prediction was observed at catalyst loading= 0.3 g-catalyst/g-biomass/h. Without catalyst, Ahmed [32] also found the consumption of CO_2 supply in the cardboard and paper gasification at 800-1000 °C. CO_2 to CO conversion was enhanced by the temperature increase. Kwon examined the possibility of CO_2 gasification with unconventional biomasses: macro-algae [33], municipal solid waste [34] and sewage sludge [35]. Beside increased the conversion, CO_2 injection resulted in 24.3 % and 30 % lower tar content than pyrolysis in the processing of algae and sewage sludge, respectively. Hanaoka [36] investigated the dried Gulfweed gasification with CO_2-O_2 mixture at 900°C. He found that solid conversion to gas under CO_2/O_2 atmosphere was higher than that of under He/O_2 due to the char-CO_2 reaction and decomposition of tarry component with 3-5 aromatic rings. CO increased and H_2 decreased as CO_2 concentration was increased. Renganathan [37] performed the thermodynamic analysis using Gibbs Minimization approach by using Aspen Plus software. The cold gas efficiency (CGE) over 100% was observed in the result due to the partial conversion of CO_2 to CO. Temperature brought positive impact to CO_2 gasification while, pressure brought negative impact. 850°C was found to be the optimum temperature to reach 100% carbon conversion with minimum energy supply for any fuel.

1.3.3 Proposal and performance analysis of CO_2 gasification system

Despite the abovementioned potential of CO_2 to be utilized as a gasifying agent, only limited number of research works examined the comprehensive system including the CO_2 supply and mostly performed with coal feedstock. Bermudez [38] performed the microwave –induced charcoal gasification with CO_2. They utilized the endothermic charcoal-CO_2 reaction as a storage of microwave heating energy produced by the other renewable energy source which have intermittency problem. 45% energy recovery can be achieved that is comparable to H_2-based fuel cell.

Castaldi [39] designed a special type of indirect gasifier which has dual chamber used for CO catalytic combustion and for coal gasification with steam and recycled CO_2. By using the thermodynamic model in Aspen Plus software, they found the efficiency of the system was achieving 79% in the energy form of hydrogen, heat from CO combustion and power from SOFC. The optimum condition was under 25 % CO_2 recycle and 1.5 steam to carbon ratio. With the same software, Walker [40] developed the dry

gasification oxy-combustion power cycle. The recycled flue gas (61% CO_2 and 32% H_2O) was utilized in a high pressure (6 atm.) O_2 blown gasification and boiler. 34.2 % system efficiency after CCS was obtained in DGOC that is 4.9% higher than the oxy-combustion based CCS technology. Oki [41] recently investigated the CO_2 recycle in the pressurized coal oxy-IGCC and successfully proposed a system with more than 40 % efficiency even after CO_2 sequestration.

Paphonwit [42] analyzed the performance of biomass gasification system with CO_2 recycle for the syngas production with H_2/CO of 1.5, which is suitable for dimethyl ether production. The thermodynamic model using Aspen Plus was also employed. Since the demand of steam was increased in most operating conditions, CO_2 recycle was resulted in the lower system efficiency and only beneficial for reducing CO_2 emission at CO_2/carbon around 0.1-0.2 in low temperature pressurized gasification (T=800°C, P>10 bar). This study revealed that CO_2 gasification is merely not suitable for producing syngas for chemical feedstock which requires high ratio of H_2/CO.

Despite the abovementioned prospective of CO_2 to be utilized as a gasifying agent, none of them examined the potential utilization of CO_2 gasification for implementing a simple and high efficiency BECCS. As previously mentioned, to create a simple and high efficiency biomass gasification system might be a key to successfully implement BECCS in the future while CO_2 gasification might contribute on this issue. Therefore a comprehensive study of the implementation of biomass CO_2 gasification for high efficiency and carbon-negative power generation is essential.

1.4 Objectives and structure of this thesis

General objective of this thesis is to propose a biomass CO_2 gasification based technology that can implement a simple and highly efficient BECCS system. In more detail the present study is divided into three parts: first we studied the basic biomass CO_2 gasification characteristics in lab scale experiment, then we examined the operability and performance of biomass CO_2 gasification in a pilot scale downdraft gasifier, and finally we proposed the CO_2-recycled biomass gasification system for high efficiency and carbon-negative power generation. This thesis will be presented in 5 chapters as follows:

In the current Chapter 1, the opportunity of biomass CO_2 gasification in giving positive contribution to the energy and environmental problems was discussed. The recent development and research works of this technology as well the challenge for implementation are also explained.

In Chapter 2, the performance study of CO_2 gasification that were performed in a lab-scale downdraft gasifier is presented. The effect of the temperature and the gasifying agent mixing with steam and/or O_2 on gas evolution and the thermal efficiency were investigated to obtain the knowledge of the reaction behavior and find the optimum operating condition.

Chapter 3 examined the scalability and performance of CO_2 gasification in a pilot scale downdraft gasifier. Findings in Chapter 2 was used as basic conditions while further examination was performed to investigate the effect of the CO_2 flow rate on the reactor temperature, the producer gas yield and the energy yield.

Chapter 4 presented the proposed CO_2-recycled biomass gasification system for high efficiency and carbon-negative power generation. The performance of the power system was analyzed using the thermal equilibrium model. Validation and adjustment of the model was performed on the gasifier component based on the result of Chapter 3. The parameter of CO_2 recycle ratio was examined under various gasifier target temperatures and turbine inlet temperatures to find the optimum operating condition.

Chapter 5 summarized the overall results along with some recommendations for further improvement of the biomass CO_2 gasification system as a valuable method for efficient and environmentally friendly utilization of biomass.

References

1. Grübler Arnulf, Transitions in Energy Use, In Encyclopedia of Energy, edited by Cutler J. Cleveland, Elsevier, New York, 2004, Pages 163-177
2. Looking to 2060: Long-term global growth prospects. OECD economic policy paper no.03, November 2102
3. International Energy Outlook 2013, U.S. Energy Information Administration. July 2013
4. Shahriar Shafiee, Erkan Topal, When will fossil fuel reserves be diminished?, Energy Policy, Volume 37, Issue 1, January 2009, Pages 181-189
5. World Energy Outlook Special Report: Redrawing the energy-climate map, U.S. Energy Information Administration , 10 June 2013
6. IPCC Fourth Assessment Report: Climate Change 2007, IPCC, 20017
7. Potential Contribution of Bioenergy to the World's Future Energy Demand. International Energy Agency Bioenergy, 2007
8. IPCC Special Report on Renewable Energy Sources and Climate Change Mitigation, IPCC, 2011
9. Global Status of BECCS Projects 2010, Global CCS Institute, 2010
10. Biomass with CO_2 Capture and Storage (Bio-CCS), European Technology Platform for Zero Emission Fossil Fuel Power Plants and European Biofuels Technology Platform, 2012
11. Michael Obersteiner Henrik Karlsson, Prestudy of BECCS Bio-Energy with Carbon Capture and Storage. MISTRA, 2011

12. Roger Ruan, Paul Chen, Richard Hemmingsen, Vance Morey, Doug Tiffany. Size matters: small distributed biomass energy production systems for economic viability, International Journal of agricultural and biological Engineering, 2008;1(1): 64
13. A.V Bridgwater, Renewable fuels and chemicals by thermal processing of biomass, Chemical Engineering Journal, Volume 91, Issues 2–3, 15 March 2003, Pages 87-10
14. Wojciech M. Budzianowski, Negative carbon intensity of renewable energy technologies involving biomass or carbon dioxide as inputs, Renewable and Sustainable Energy Reviews, Volume 16, Issue 9, December 2012
15. Muhammad F. Irfan, Muhammad R. Usman, K. Kusakabe, Coal gasification in CO_2 atmosphere and its kinetics since 1948: A brief review, Energy, Volume 36, Issue 1, January 2011, Pages 12-40
16. P. Ollero, A. Serrera, R. Arjona, S. Alcantarilla, The CO_2 gasification kinetics of olive residue, Biomass and Bioenergy, Volume 24, Issue 2, February 2003, Pages 151-161
17. Thilakavathi Mani, Nader Mahinpey, Pulikesi Murugan, Reaction kinetics and mass transfer studies of biomass char gasification with CO_2, Chemical Engineering Science, Volume 66, Issue 1, 1 January 2011, Pages 36-41
18. Nanfu Zong, Yang Liu, Learning about the mechanism of carbon gasification by CO_2 from DSC and TG data, Thermochimica Acta, Volume 527, 10 January 2012, Pages 22-26
19. Indraneel Sircar, Anup Sane, Weichao Wang, Jay P. Gore, Experimental and modeling study of pinewood char gasification with CO_2, Fuel, Volume 119, 1 March 2014, Pages 38-46
20. I.I. Ahmed, A.K. Gupta, Kinetics of woodchips char gasification with steam and carbon dioxide, Applied Energy, Volume 88, Issue 5, May 2011, Pages 1613-1619
21. Pooya Lahijani, Zainal Alimuddin Zainal, Abdul Rahman Mohamed, Maedeh Mohammadi, Ash of palm empty fruit bunch as a natural catalyst for promoting the CO_2 gasification reactivity of biomass char, Bioresource Technology, Volume 132, March 2013, Pages 351-355
22. Pooya Lahijani, Zainal Alimuddin Zainal, Abdul Rahman Mohamed, Catalytic effect of iron species on CO_2 gasification reactivity of oil palm shell char, Thermochimica Acta, Volume 546, 20 October 2012, Pages 24-31
23. F. Marquez-Montesinos, T. Cordero, J. Rodríguez-Mirasol, J.J. Rodríguez, CO_2 and steam gasification of a grapefruit skin char, Fuel, Volume 81, Issue 4, March 2002, Pages 423-429
24. C. Guizani, F.J. Escudero Sanz, S. Salvador, The gasification reactivity of high-heating-rate chars in single and mixed atmospheres of H_2O and CO_2, Fuel, Volume 108, June 2013, Pages 812-823
25. Susanna Nilsson, Alberto Gómez-Barea, Pedro Ollero, Gasification of char from dried sewage sludge in fluidized bed: Reaction rate in mixtures of CO_2 and H_2O, Fuel, Volume 105, March 2013, Pages 764-768

26. D.G. Roberts, D.J. Harris, Char gasification in mixtures of CO_2 and H_2O: Competition and inhibition, Fuel, Volume 86, Issues 17–18, December 2007, Pages 2672-2678
27. Yonghui Bai, Yulong Wang, Shenghua Zhu, Lunjing Yan, Fan Li, Kechang Xie, Synergistic effect between CO_2 and H_2O on reactivity during coal chars gasification, Fuel, Volume 126, 15 June 2014, Pages 1-7
28. Hiroyuki Iwaki, Shufeng Ye, Haruo Katagiri, Kuniyuki Kitagawa, Wastepaper gasification with CO_2 or steam using catalysts of molten carbonates, Applied Catalysis A: General, Volume 270, Issues 1–2, 30 August 2004, Pages 237-243
29. Yanqin Huang, Xiuli Yin, Chuangzhi Wu, Congwei Wang, Jianjun Xie, Zhaoqiu Zhou, Longlong Ma, Haibin Li, Effects of metal catalysts on CO_2 gasification reactivity of biomass char, Biotechnology Advances, Volume 27, Issue 5, September–October 2009, Pages 568-572
30. Keiichirou Mitsuoka, Shigeya Hayashi, Hiroshi Amano, Kenji Kayahara, Eiji Sasaoaka, Md. Azhar Uddin, Gasification of woody biomass char with CO_2: The catalytic effects of K and Ca species on char gasification reactivity, Fuel Processing Technology, Volume 92, Issue 1, January 2011, Pages 26-31
31. Pooya Lahijani, Zainal Alimuddin Zainal, Abdul Rahman Mohamed, Maedeh Mohammadi, CO_2 gasification reactivity of biomass char: Catalytic influence of alkali, alkaline earth and transition metal salts, Bioresource Technology, Volume 144, September 2013, Pages 288-295
32. L Garcia, M.L Salvador, J Arauzo, R Bilbao, CO_2 as a gasifying agent for gas production from pine sawdust at low temperatures using a Ni/Al coprecipitated catalyst, Fuel Processing Technology, Volume 69, Issue 2, February 2001, Pages 157-174
33. I. Ahmed, A.K. Gupta, Characteristics of cardboard and paper gasification with CO_2, Applied Energy, Volume 86, Issue 12, December 2009, Pages 2626-2634, ISSN 0306-2619
34. Eilhann E. Kwon, Haakrho Yi, Hyun-Han Kwon, Thermo-chemical process with sewage sludge by using CO_2, Journal of Environmental Management, Volume 128, 15 October 2013, Pages 435-440,
35. Toshiaki Hanaoka, Shou Hiasa, Yusuke Edashige, Syngas production by CO_2/O_2 gasification of aquatic biomass, Fuel Processing Technology, Volume 116, December 2013, Pages 9-15
36. Eilhann E. Kwon, Marco J. Castaldi, Urban energy mining from municipal solid waste (MSW) via the enhanced thermo–chemical process by carbon dioxide (CO_2) as a reaction medium, Bioresource Technology, Volume 125, December 2012, Pages 23-29,
37. Eilhann E. Kwon, Young Jae Jeon, Haakrho Yi, New candidate for biofuel feedstock beyond terrestrial biomass for thermo-chemical process (pyrolysis/gasification) enhanced by carbon dioxide (CO_2), Bioresource Technology, Volume 123, November 2012, Pages 673-677,
38. T. Renganathan, M.V. Yadav, S. Pushpavanam, R.K. Voolapalli, Y.S. Cho, CO2 utilization for gasification of carbonaceous feedstocks: A thermodynamic analysis, Chemical Engineering Science, Volume 83, 3 December 2012, Pages 159-170

39. J.M. Bermúdez, E. Ruisánchez, A. Arenillas, A.H. Moreno, J.A. Menéndez, New concept for energy storage: Microwave-induced carbon gasification with CO_2, Energy Conversion and Management, Volume 78, February 2014, Pages 559-564
40. Marco J. Castaldi, John P. Dooher, Investigation into a catalytically controlled reaction gasifier (CCRG) for coal to hydrogen, International Journal of Hydrogen Energy, Volume 32, Issue 17, December 2007, Pages 4170-4179
41. Paphonwit Chaiwatanodom, Supawat Vivanpatarakij, Suttichai Assabumrungrat, Thermodynamic analysis of biomass gasification with CO_2 recycle for synthesis gas production, Applied Energy, Volume 114, February 2014, Pages 10-17
42. Michael E. Walker, Javad Abbasian, Donald J. Chmielewski, and Marco J. Castaldi, Dry Gasification Oxy-combustion Power Cycle, Energy & Fuels, 2011, *25* (5), pp 2258–2266
43. Yuso Oki, Jun Inumaru, Saburo Hara, Makoto Kobayashi, Hiroaki Watanabe, Satoshi Umemoto, Hisao Makino, Development of oxy-fuel IGCC system with CO_2 recirculation for CO_2 capture, Energy Procedia, Volume 4, 2011, Pages 1066-1073

Chapter II

CO_2-steam mixture for direct and indirect gasification of rice straw in a downdraft gasifier: laboratory-scale experiments and performance prediction

2.1 Introduction

One of the desirable feature for applying the carbon capturing and storage (CCS) in biomass gasification system is the production of syngas without nitrogen content. Combined with oxy-fuel combustion techniques, combustion of nitrogen-free producer gas results in high CO_2 concentration stream that is suitable for the sequestration process [1]. Furthermore, the nitrogen-free producer gas is also favorable for the NO_X reduction [2] and for another conversion processes such as synthesis of liquid fuels and chemicals [3].

There are two existing methods to produce nitrogen free syngas. One method is direct (or autothermal) gasification, which supplies the mixture of oxygen and steam as an oxidant [4]. The other is indirect (or allothermal) gasification with two reactors: gasifier with steam supply and char/biomass combustor with air supply [5,6]. Char combustion provides necessary heat for gasification, which is transported to the gasifier by means of solid fluidized materials or sensible heat of steam.

The sensible heat of unreacted steam makes the overall thermal efficiency of such gasification processes lower, especially when we need to vaporize water to generate steam. Previous researches have noted that steam conversion in the gasifier was less than 10 %, either in fix bed gasifiers or in fluidized bed gasifiers [6-8]. CO_2 has a similar function as a gasifying agent with steam through the Bouduard's reaction [9] and the dry reforming [10]. In addition, CO_2 is in gas-phase at ambient condition, and often separated from final product (SNG, DME, FT-diesel, etc.) during product refining or syngas conditioning [11-13]. Therefore, it is worth investigating the feasibility of nitrogen-free syngas production via autothermal and allothermal gasification with CO_2 as a gasifying agent. In fact, recent studies have investigated oxy-CO_2 gasification of coal integrated with an oxy-fuel combustion boiler [14] or gas turbine [15].

Despite the potential of CO_2 to replace steam, no study was found that is comparing gasification performance under the atmospheres of CO_2, steam, and their mixtures in term of the thermal efficiency. Some studies showed the effect of steam [16, 17] or CO_2 [18-20] on the gasification characteristics of biomass using chemically controlled laboratory-scale reactors. The kinetics behavior of gasification under CO_2 compared with that of under steam has been well studied in some researches conducted with

char samples [21-23]. However, to bridge the implementation of this technology, a study about the effect of steam replacement by CO_2 on the performance of gasification process is required as a feasibility study. This chapter first presents the gas evolution behavior of rice straw sample under the flow of various gas mixtures (steam, CO_2 and their mixture). The reaction temperature and the presence of O_2 were also taken into account. Pyrolysis experiment was also performed and used as a base data for the comparison with the examined gasifying agents. Thermal efficiencies of rice straw gasification under the examined reaction conditions were then calculated and compared to investigate the feasibility of CO_2 gasification for high quality syngas production.

2.2 Experimental

2.1.1 Experimental set up

Fig. 2.1 shows the fixed bed downdraft gasifier used in this study. It consists of a 900 mm long, 23 mm outside diameter, and 20 mm inner diameter quartz tube; a 250 mm long electrical heater; a gas cleaning system; and a micro gas chromatograph. Stainless steel wire mesh was set as a grate inside the tube reactor. Two isopropanol (IPA) impinger bottles, a carbon filter, a cotton filter, and a silica gel tube were installed for cleaning the producer gas against tar and moisture. The quartz tube is vertically adjustable in accordance with the position of the reaction frontier in the sample bed. The electrical heater was connected to a temperature controller and the controller was equipped with a K-type thermocouple to detect the temperature of the outer surface of the reactor column.

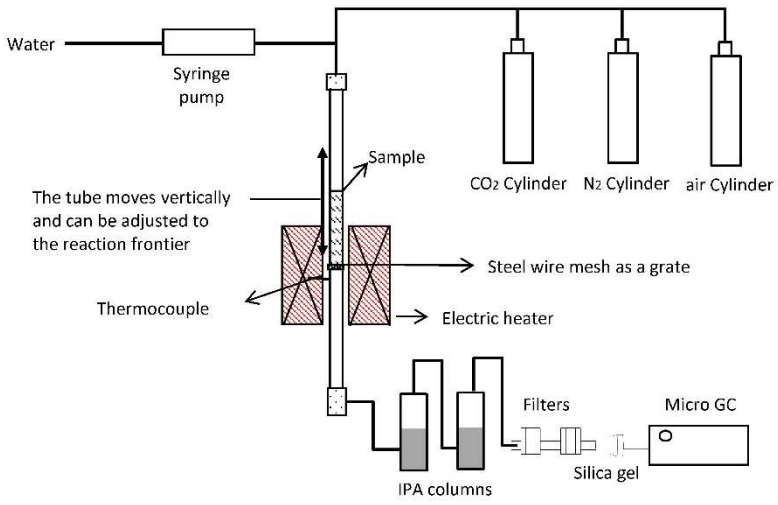

Figure 2.1 Experiment apparatus: downdraft fix bed gasifier

2.1.2 Materials

We used rice straw grown in farmlands in southern part of Japan since it is one of the most abundant biomass resources wasted in Asian countries. It was cut to the size of 15 - 20 mm in longitudinal direction. The proximate and ultimate analyses of the sample, shown in Table 2.1, were taken from previous experiments with the same sample [16]. The moisture content of the sample was 5.59 ±0.9 %.

Table 2.1 Proximate and ultimate analysis of rice straw sample [16]

Proximate analysis	Volatile matter	Fix carbon	Ash	
(wt% d.b.)	80,4	4,6	15	
Ultimate analysis	**C**	**H**	**N**	**O(diff.)**
(wt% daf)	43,8	6,4	0,9	48,9

2.1.3 Experimental Procedures

The gasification tests were carried out in a batch operation by feeding 3.5 gram of sample (approximately 150 mm height of the sample bed). Initially, the tube reactor was located at upper position so that the grate was kept in the cold zone. Sample was then loaded and reactor was purged with adjusted gasifying agent. After the heater reached the desired temperature, the reactor tube was shifted down so that 50 mm of the sample bed was located in the heated zone. Steam was injected just before the reactor tube was shifted down. The term of the reactor temperature hereafter in this paper is referred to the temperature that was set in the temperature controller. The setting temperature itself represented the overall working temperature of the experiments in spite of the occurrence of a relative small fluctuation at initial stage of experiment (50°C decreases for less than 5 minutes). The producer gas was analyzed for 90 minutes after the sample was inserted to the heated zone. Experiments were carried out by varying the mixing ratio of CO_2, steam, N_2, and O_2. CO_2, steam and O_2 were supplied as the examined gasifying agent while N_2 was supplied as an inert gas for the purpose of the flow rate quantification of each gas specie. The total flow rate of the gas supply during O_2 free experiments (simulating indirect gasification and pyrolysis conditions) was 590 ml/min at the standard state, with 60vol.% of gasifying agents (steam and CO_2) and 40vol.% of N_2 for gasification and 100vol.% of N_2 for pyrolysis. The total flow rate of gas during the experiments with the presence of O_2 (simulating direct gasification conditions) was 660 ml/min at the standard state, with 60vol.% of gasifying agents (mixture of steam and CO_2 with various mixing ratios), 8.3vol.% of O_2 and 31.7vol.% of N_2. All the experimental conditions were repeated twice and the presented data is the average of the results. The shown error bar is the standard deviation between the two experiment results.

2.1.4 Analytical method and devices

The producer gas composition was analyzed by a micro gas chromatograph (VARIAN CP-900, GL Sciences Inc.) equipped with two columns (MS 5A and PlotQ) and thermal conductivity detectors (TCD). H_2, O_2, N_2, CH_4, and CO were separated with the MS 5A column and CO_2, C_2H_4, and C_2H_6 were separated using the PlotQ column. Calibration of the peak area to determine the volume fraction of each gas specie was performed prior to the experimental run by analyzing the fixed composition gas and set it as a standard. The gas evolution rate (Y_i) and the gas yield (y_i) was calculated on the basis of the nitrogen flow rate (F_{N_2}), as shown in Eqs. 2.1 and 2.2. X_{pi} is the volume fraction of the gas specie i in the producer gas detected with the micro GC, while X_{pN_2} is that of N_2. Δt is the time interval between two micro GC analysis and m_{bm} is the mass of the sample. CO_2 yield was calculated at the net basis by subtracting the flow rate of CO_2 at the inlet from that of CO_2 at the outlet as shown in Eq. 2.2.

$$Y_i = \frac{F_{N_2} X_{pi}}{X_{pN_2}} \qquad (2.1)$$

$$y_i = \frac{\Sigma Y_i \Delta t}{m_{bm}} \qquad (2.2)$$

2.3 Results and discussion

2.3.1 Effects of the mixing ratio of CO_2 and H_2O on producer gas evolution without the presence of O_2

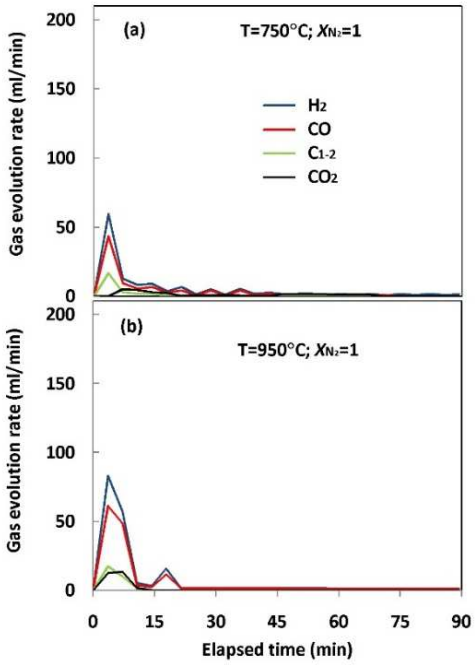

Figure 2.2 Gas evolution profiles during pyrolysis at the reaction temperatures of: (a) 750°C and (b) 950°C

Fig. 2.2 shows the gas evolution during the pyrolysis experiments under 100vol.% of N_2. Figs. 2.3 and 2.4 show the gas evolution profiles during the gasification experiments without the presence of oxygen at the reaction temperature of 750°C (Fig. 2.3) and 950°C (Fig. 2.4). In gasification experiments, the composition of the gasifying agent was varied among three different ratios: (a) N_2-40vol.%, H_2O-60vol.%, CO_2-0vol.%; (b) N_2-40vol.%, H_2O-30vol.%, CO_2-30vol.%; and (c) N_2-40vol.%, H_2O-0vol.%, CO_2-60vol.%. Either in pyrolysis or in gasification under every reaction conditions, major gas evolution was observed at the beginning of the experiments until 10-20 minutes of the elapsed time mainly due to the devolatilization of biomass. Then unlike those in pyrolysis, relatively low gas evolution of CO, CO_2 and H_2 was observed in the gasification until the end of the experiments due to the reaction of char with H_2O and/or CO_2. The H_2O-char reaction (Eq. 3) is known as the water gas reaction and the CO_2-char reaction (Eq. 5) is known as the Bouduard`s reaction. For easier interpretation, terminologies of the H_2O-char reaction and the CO_2-char reaction are used in this thesis.

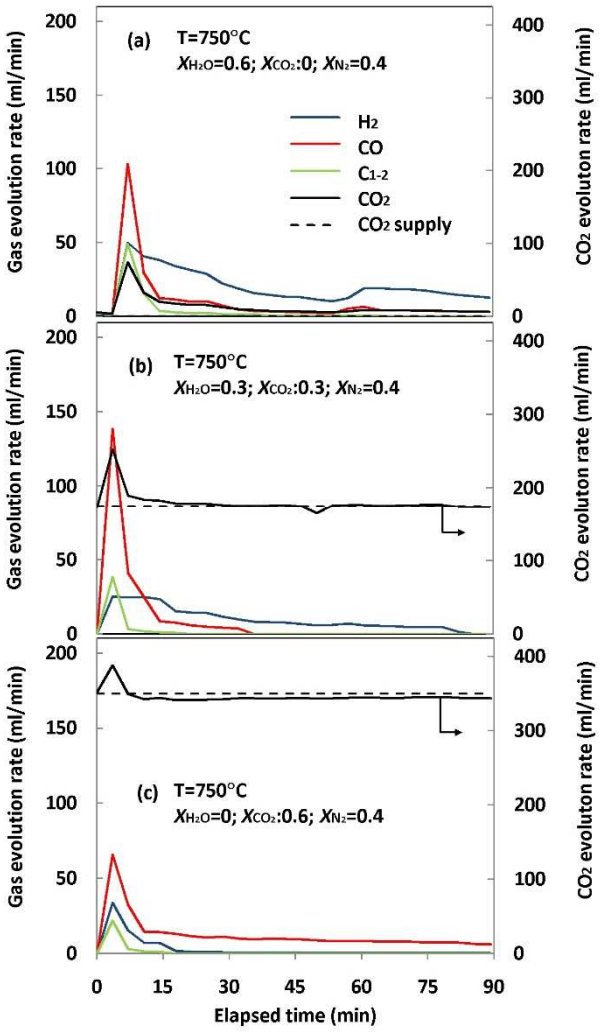

Figure 2.3 Gas evolution profiles at the reaction temperature of 750°C under CO_2:H_2O fractions of: (a) 0:0.6, (b) 0.3:0.3 and (c) 0.6:0 with the N_2 fraction of 0.4

$C + H_2O \rightarrow CO + H_2$ $\Delta H = 131.3$ kJ/mol (2.3)

$CO + H_2O \leftrightarrow CO_2 + H_2$ $\Delta H = -41.1$ kJ/mol (2.4)

$C + CO_2 \rightarrow 2CO$ $\Delta H = 171.1$ kJ/mol (2.5)

At the reactor temperature of 750°C, dissimilar to that of in pyrolysis (Fig. 2(a)), H_2 evolution rate during devolatilization under H_2O-N_2 atmosphere (Fig. 3(a) (0-20 minutes of elapsed time)) occurred in a broad peak which is gradually decreased until the end of the experiment. The evolutions of CO, CO_2, and hydrocarbon gas (C_{1-2}), which mainly consisted of CH_4, were also relatively high under the steam presented atmosphere. These occurrences implied the role of steam in yielding the gases through the H_2O-char reaction (the water gas reaction, Eq. 2.3), the water gas shift reaction (Eq. 2.4) and the methanations (Eqs. 2.6 and 2.7) simultaneous with devolatilization. Furthermore as shown in Fig. 2.3 (0-20 minutes of the elapsed time), the H_2 evolution rate during devolatilization decreased along with the increase of the CO_2 fraction in the gasifying agent. It was resulted from the lessen role of the water gas shift reaction and H_2 consumption by the presented CO_2 through the backward water gas shift reaction. The CO evolution rate showed the maximum peak value under the mixed atmosphere (30vol.% for both H_2O and CO_2 fractions) that might have come from the combination of CO evolution by the H_2O-char reaction and the backward water gas shift reaction. A decrease of hydrocarbon gas evolution was also observed as the CO_2 fraction increased. Hydrocarbon decrease was observed in parallel with the H_2 decrease, thus it probably came from the lessen methanation reactions. Similar trend of methane in gasification under H_2O and CO_2 was reported in the previous study [24]. The dry reforming reaction (Eq. 2.8) might also occur under the CO_2-N_2 atmosphere since its yield of hydrocarbon was lower than that of under N_2-only atmosphere (pyrolysis).

$CO_2 + 4H_2 \rightarrow CH_4 + 2H_2O$ $\Delta H = -165.0$ kJ/mol (2.6)

$CO + H_2 \leftrightarrow CH_4 + H_2O$ $\Delta H = -205.8$ kJ/mol (2.7)

$C_nH_m + nCO_2 \rightarrow {}^{m}/_{2}\, H_2 + 2n\, CO$ (2.8)

During char gasification under the H_2O-N_2 atmosphere, as shown in Fig. 2.3(a) (20-90 minutes of the elapsed time), continuous evolutions of H_2, CO_2 and CO were observed. It means that the H_2O-char and the water gas shift reactions were dominant. Under the mixed atmosphere, as shown in Fig. 2.3(b), H_2 evolution was continuously observed and CO evolution was only visible up to 40 minutes of the elapsed time. CO_2 slightly evolved although it is hardly observable from the figure. The continuous evolution

of H_2 and CO_2 but no CO means that CO evolved from the H_2O-char reaction and the CO_2-char reaction was suppressed by the water gas shift reaction. During char gasification under the CO_2-N_2 atmosphere, as shown in Fig. 2.3(c), CO evolution was observed together with CO_2 whose flow rate was below the supply rate. It means that the dominant reaction under this atmosphere was the CO_2-char reaction.

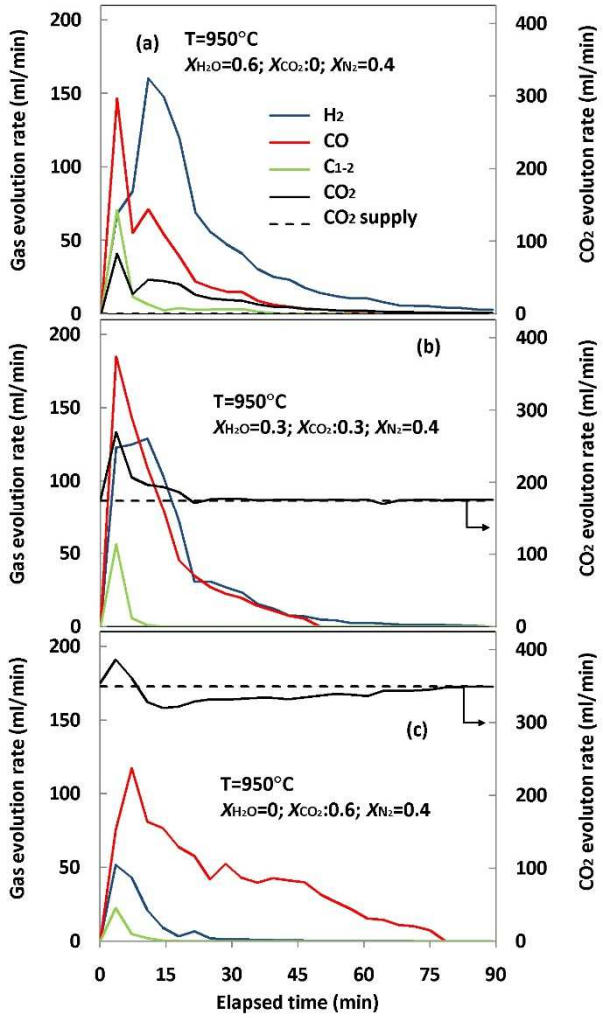

Figure 2.4 Gas evolution profiles at the reaction temperature of 950°C under CO_2:H_2O fractions of: (a) 0:0.6, (b) 0.3:0.3 and (c) 0.6:0 with the N_2 fraction of 0.4

In gasification experiments at the reactor temperature of 950°C, as shown in Fig. 2.4, similar evolution profiles of H_2 and CO to those at 750°C was observed during devolatilization (0-20 minutes of the elapsed time) but with much higher evolution rate of the most gases than those in pyrolysis, as shown in Fig. 2.2(b). Unlike char gasification at 750°C, CO showed approximately the same gas evolution rate as H_2 during the char gasification period (20-50 minutes of the elapsed time) under the mixed atmosphere, as shown in Fig. 2.4(b). CO evolution that came without the evidence of CO_2 consumption implied that the CO_2-char reaction occurred together with the forward water gas shift reaction. CO_2

consumption by the CO_2-char reaction was coincidentally balanced by CO_2 generation by the water gas shift reaction. Under the CO_2-N_2 atmosphere, as shown in Fig. 2.4(c), CO_2 consumption was more apparently observed during the char gasification. It is the evidence that CO_2 engaged in the gasification reactions. Gas evolution profiles at the reactor temperature of 850°C showed similar trends to those at 950°C (supplement material).

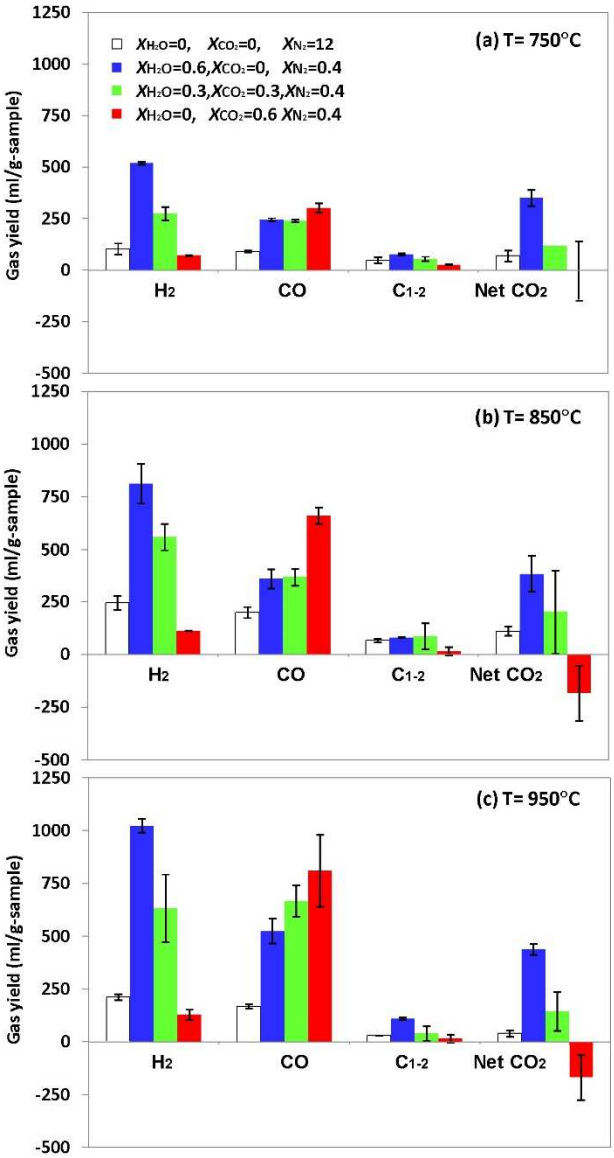

Figure 2.5 Effect of the CO_2 and H_2O mixing ratio on the gas yield at the reaction temperatures of: (a) 750°C, (b) 850°C, and (c) 950°C

The effect of the mixing ratio of the gasifying agent on the overall gas evolution at each reaction temperature and its comparison with the result of pyrolysis is shown in Fig. 2.5. The presented error bars shows the standard deviation of the repeated experimental results. In the experiment under the

presence of steam, the entire gas yield showed higher value than that of under N_2-only atmospehere in pyrolysis. While under the CO_2-N_2 experiment, slight lower yields of H_2 and hydrocarbons than those in pyrolysis, were shown together with significantly higher CO and lower net CO_2 evolution. These showed the important role of steam and CO_2 as a gasifying agent in yielding the producer gas, especially the combustible species.

In gasification experiment at the reactor temperature of 750 °C, as shown in Fig. 2.5(a), the H_2 yield constantly decreased around 225 ml/g-sample for every 0.3 CO_2 increase (which also means 0.3 H_2O fraction decrease). The CO yield remained unchanged and the CO_2 yield significantly decreased when the CO_2 fraction increased from 0 to 0.3. These changes implied less role of the H_2O-char reaction and the forward water gas shift by 0.3 H_2O fraction reduction. The expected CO yield increase was not observed because the progress of the CO_2-char reaction was not observable under the mixed atmosphere. Thus, the partial H_2O to CO_2 substitution was disadvantageous for combustible gas evolution. As the CO_2 fraction increased from 0.3 to 0.6, the CO yield increased along with the further decrease of the CO_2 yield down to zero. The occurrence of the CO_2-char reaction played important role for this change, as also shown in Fig. 2.3(c). The fact that the CO_2-char reaction was inconstantly affected by the CO_2 fraction while the H_2O-char reaction was constantly affected by the CO_2 fraction can be explained by inhibition effects between H_2O and CO_2 during the char gasification. Previous study [25] showed that the CO_2-char reaction is inhibited by H_2O while the H_2O-char reaction was not affected by CO_2. The hydrocarbon gas (C_{1-2}) yield also suppressed by the increase of the CO_2 mixing ratio due to the occurrence of gas phase reactions in the initial stage of experiment as was discussed earlier in this chapter.

At the reaction temperature of 850°C, as shown in Fig. 2.5(b), the increase of the CO yield were consistently observed as the CO_2 fraction increased in the gasifying agent. However, the inhibition effect of H_2O on the CO_2–char reaction was still seen as the CO yield showed a convex function against the CO_2 fraction. The net CO_2 yield showed negative value at the CO_2 fraction of 0.6. It is the evidence that CO_2 engaged in the gasification reactions, as also shown in Fig. 2.4(c). The H_2 yield declined linearly as the CO_2 fraction increased, but with a greater severity than those at a lower temperature.

At the reaction temperature of 950°C, as shown in Fig. 2.5(c), the inhibition effect of H_2O was not seen since the CO yield increased continuously by the increase of the CO_2 fraction. The continuous increase of CO and decrease of CO_2 implied the strong activity of the CO_2-char reaction that might be related to the enhanced catalytic property of the char by the CO_2 presence in high temperature. Previous research [26] about the catalytic properties of char during gasification with CO_2 at around 720°C -1000°C showed the positive trend toward the temperature rise on the formation of micropore network in char without any tendency of metal sintering on its surface. The micropore provided access for gasifying agent to reach the active sites thus enhanced the catalytic property of the char.

2.3.2 Effects of the mixing ratio of CO_2 and H_2O on the producer gas evolution with the presence of O_2

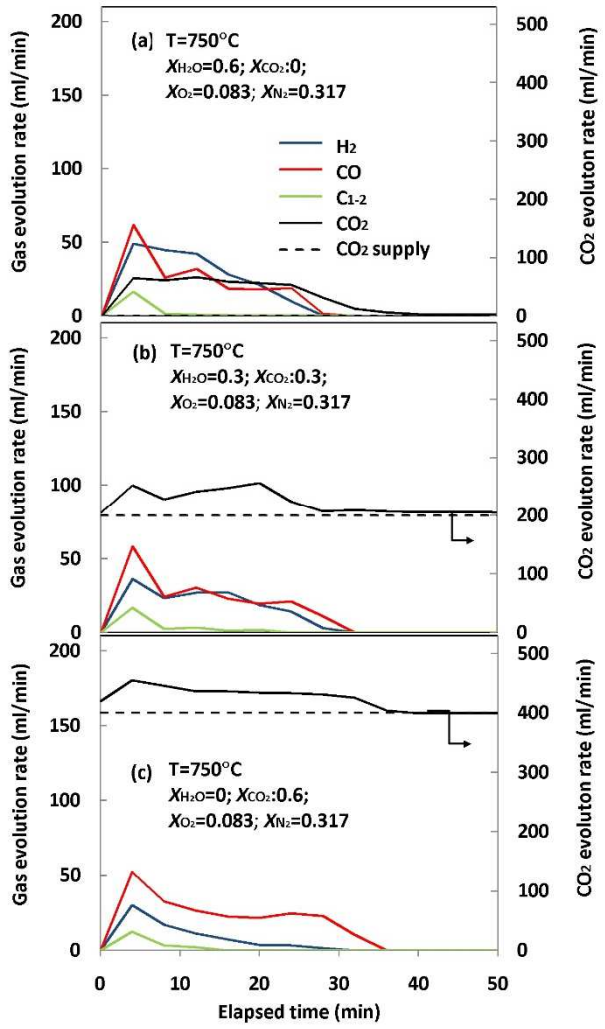

Figure 2.6 Gas evolution profiles at the reaction temperature of 750°C under CO_2:H_2O fractions of: (a) 0; 0.6, (b) 0.3; 0.3 and (c) 0.6; 0 with the N_2 fraction of 0.317 and O_2 fraction of 0.083

To simulate the reaction conditions in autothermal/direct gasification, O_2 was introduced into the reactor with the molar fraction of 8.3vol.%. Figs. 2.6 and 2.7 show the gas evolution profiles at the reaction temperatures of 750°C and 950°C under the presence of O_2. Gas evolutions of gasification under the presence of O_2 completed at around 40 minutes, earlier than those under O_2 absence atmosphere, at around 90 minutes. The reaction rate of the char combustion (Eq. 2.9) is higher than those of the char gasification with steam and carbon monoxide [9]. The border between devolatilization and char gasification stages was not as clear as the one observed without the presence of O_2. In this section, we define the devolatilization stage when hydrocarbon gases evolved, and the rest is called as the char gasification stage although there might be an overlap between them.

$$C+\gamma \cdot O_2 \rightarrow 2(1-\gamma)\ CO+(2\gamma-1)\cdot CO_2 \qquad (2.9)$$

At the reaction temperature of 750°C, H_2 evolution was observed during the char gasification stage under H_2O presence atmosphere. It means that the H_2O-char reaction engaged in gasification reactions. In addition, significant CO evolution was also observed during the char gasification under all reaction conditions. CO evolution might have come from partial combustion of char, especially in steam-injected atmospheres, since those were not significantly observed in the experiment without O_2 presence.

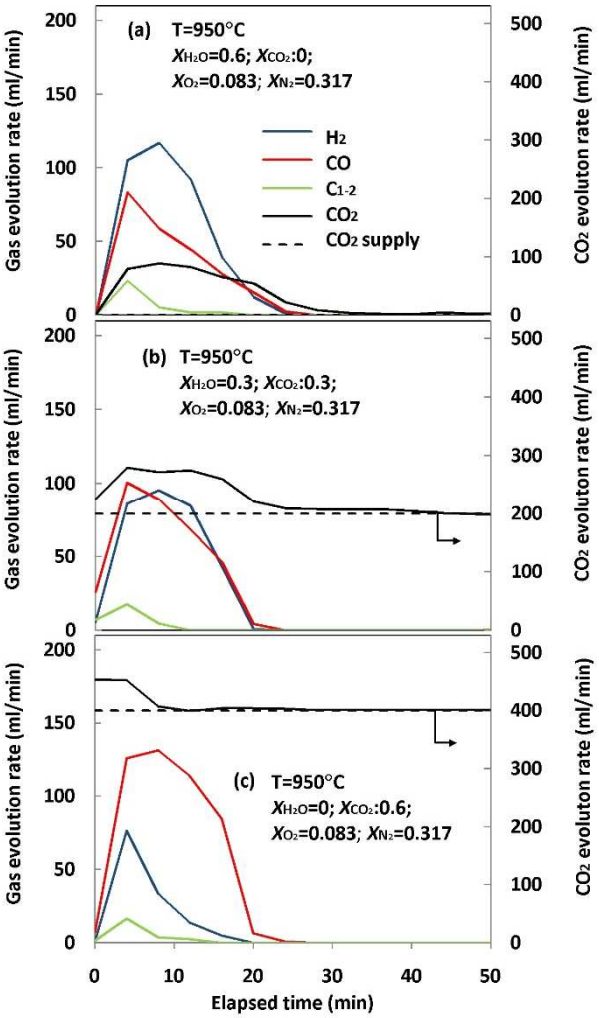

Figure 2.7 Gas evolution profiles at the reaction temperature of 950^{0}C under CO_2:H_2O fractions of: (a) 0; 0.6, (b) 0.3; 0.3 and (c) 0.6; 0 with the N_2 fraction of 0.317 and O_2 fraction of 0.083

At the reaction temperature of 950^{0}C, the highest CO peak was observed under the CO_2-O_2-N_2 atmosphere. It means that the CO_2-char reaction played an important role in gasification reactions. Under this experimental condition (Fig. 2.7(c)), there was no net evolution or consumption of CO_2 at the elapsed time of 10 minutes to 20 minutes although the evolutions of other gases showed their peak

values at around 10 minutes after the experiments started. It implies that the generation rate of CO_2 by devolatilization and char combustion was the same as the consumption rate of CO_2 by the CO_2-char reaction coincidentally.

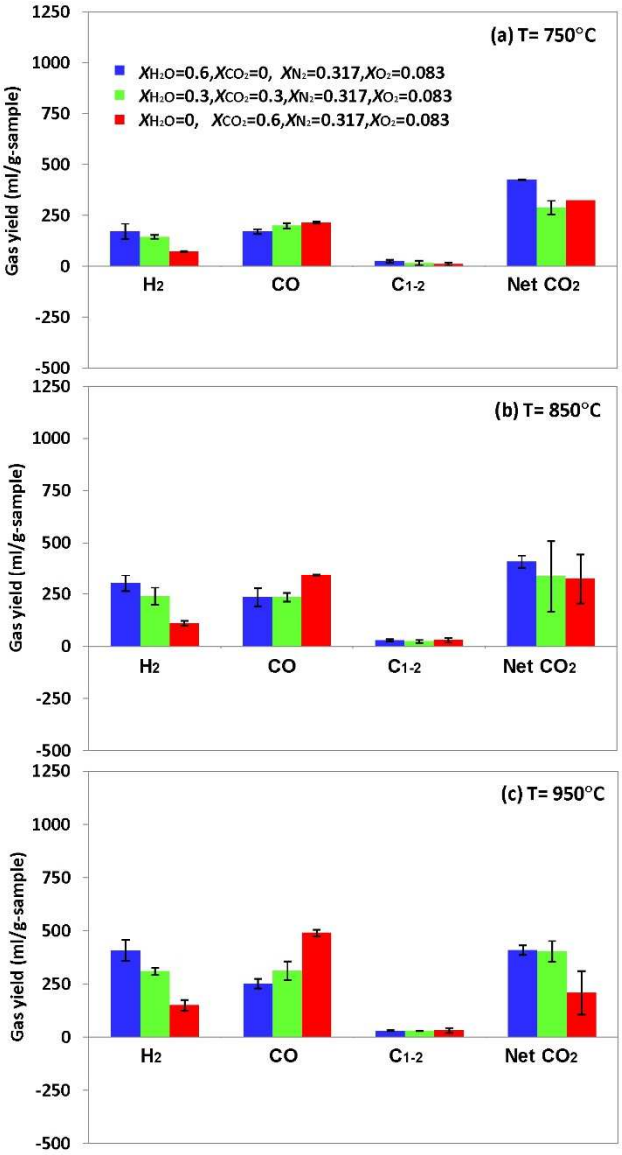

Figure 2.8 Effect of the CO_2 and H_2O mixing ratio on the gas yield at the reaction temperatures of: (a) 750°C, (b) 850°C, and(c) 950°C under the presence of O_2

Fig. 2.8 shows the effect of the mixing ratio of the gasifying agent on the overall gas evolution in gasification experiments with the presence of O_2 at each reaction temperature. Continuous decrease of H_2, which indicated less role of the H_2O-char reaction, was observed with the increase of the CO_2 fraction at all temperatures examined. Meanwhile, the convex increase of CO against the CO_2 mixing ratio implies inhibition of the CO_2-char reaction by steam at the reaction temperature of 850°C and 950 °C (Figs. 2.8(b) and 2.8(c)). In general, the net CO_2 yield decreased as the H_2O fraction in the gasifying

agent was substituted by CO_2. It might show the domination of the CO_2-char reaction over the CO_2 evolving reaction with the increase of the CO_2 mixing ratio. The hydrocarbon gas yields showed no significant difference at different CO_2 mixing ratios.

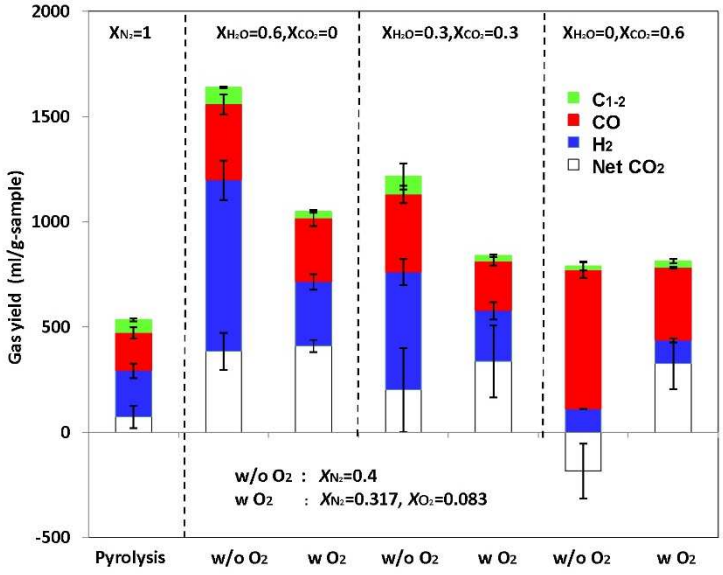

Figure 2.9 Comparison between gases yield of the experiment without and with the presence of O_2 at the reaction temperature of 850°C

Fig. 2.9 shows the gas yield of the experiment carried without and with the presence of O_2 at the reaction temperature of 850°C. Although not as significant as those without the presence of O_2, the role of steam and CO_2 with the presence of O_2 in yielding the producer gas compared to the N_2 atmosphere in pyrolysis is also remarkable. Higher yield of H_2 and CO than those of pyrolysis was shown in the gasification under steam presented atmospheres, while slight lower H_2 yield and much higher CO yield than those of pyrolysis observed in the gasification under the CO_2-O_2-N_2 atmosphere. Compared with the gasification experiments without O_2 injection, the combustible gas yield under the presence of O_2 showed low values at all the reaction temperatures examined. Under the H_2O-N_2 atmosphere, O_2 injection decreased the H_2 yield the most and then the CO yield. Under the H_2O-CO_2-N_2 atmosphere, the decreases of H_2 and CO were more comparable. Meanwhile, a significant decrease as a result of O_2 injection was only observed for the CO yield under the CO_2-N_2 atmosphere. Hydrocarbon yields under all atmospheres with the injection of O_2 were lower than the yields of pyrolysis and gasification without the injection of O_2. Combustion of each combustible gas seems to be responsible for those decreases. The net CO_2 yield increased with the O_2 injection in all atmospheres. These increments were proportional to the CO_2 mixing ratio and furthermore to the CO yield decrease in each atmosphere. It showed that the most of the CO_2 yield in the experiment with the presence of O_2 came from CO combustion.

2.3.3 Expected thermal efficiency of direct and indirect gasifiers using the mixture of CO_2 and H_2O as a gasifying agent

As also shown in Fig. 2.9, the substitution of steam by CO_2 mostly resulted in lowering combustible gas yields in all examined conditions. Nevertheless, since steam has higher enthalpy than CO_2 owing to the latent heat, the replacement of steam by CO_2 would potentially increase the thermal efficiency of the system. Further examination was then performed by calculating the thermal efficiency of a gasifier. It was calculated as the ratio of chemical energy output of the producer gas to the sum of energy input considered from the energy of feedstock, gasifying agent preheating, and O_2 production (Eq. 2.10).

$$\text{Thermal efficiency of gasifier} = \frac{LHV_p(J/ml - producer\ gas) \times y_p(ml/g - wet\ biomass)}{(LHV_{\text{b}} + E_{\text{Gasifying agent preheating}} + E_{O_2\ production})(J/g - wet\ biomass)} \quad (2.10)$$

Higher heating value (HHV) and lower heating value (LHV) of biomass was calculated from the dry base mass percentage of the biomass components using a unified formula suggested in previous research [27] (Eqs. 2.11 and 2.12, respectively). C, H, O, N, S and A are the mass percentage of carbon, hydrogen, oxygen, nitrogen, sulphur and ash. w_H is the hydrogen mass fraction and L_{H_2O} is the latent heat of water vaporization. The calculated dry based heating values were then adapted to wet based and applied in Eqs. 2.10 and 2.13

$$HHV_b(J/g - dry\ biomass) = (0.3491\text{C} + 1{,}1783\text{H} + 0.1005\text{S} - 0.0151\text{N} - 0.0211\text{A}) \times 1000 \quad (2.11)$$

$$LHV_b(J/g - dry\ biomass) = HHV_b - 9w_H \times L_{H_2O} \quad (2.12)$$

$$m_g\left(\sum_i \int_{T_o}^{T_g} w_{gi}C_{p,gi}dT + w_{gH_2O}L_{H_2O} + \frac{w_{gO_2}}{\alpha}HHV_b\right)(1 - \eta_{loss}) = m_g\left(\sum_i \int_{T_o}^{T_r} w_{gi}c_{p,gi}dT + w_{gH_2O}L_{H_2O}\right) + m_b \int_{T_o}^{T_r} c_{p,b}dT \quad (2.13)$$

The energy input of the gasifying agent was calculated so that the gasifying agent should be preheated to the target reaction temperature according to a simple energy balance (Eq. 2.13). As shown in Fig. 2.10, the sensible heat source is the combustion of biomass and/or residual char. The preheated temperature of the gasifying agent was assumed to be 1050ºC, which was the highest temperature achieved at pilot scale experiments of high temperature steam gasification [7]. For the O_2 injected process, the heat for gasification reactions was supplied not only by the sensible heat of the preheated

gasifying agent, but also by the heat of biomass partial combustion. 5% of the total thermal energy input was assumed to be lost from the system. For the gasification experiment, N_2 fraction was not counted in this calculation since it only exist as a carrier gas and will not be supplied in the real gasification process. For the gasification experiments without O_2, the CO_2 fraction of 0.5 in the thermal efficiency calculation was corresponding to the experiments with the CO_2 fraction of 0.3 in previous sections, (i.e. the CO_2 fraction of 1 in the thermal efficiency calculation is equivalent to the CO_2 fraction of 0.6 in the experiments). The fraction of the gasifying agent for the experiments with O_2 was modified so that the O_2 fraction becomes 12vol.% and the fraction of the steam/CO_2 mixture becomes 88vol.%. The O_2 production energy, 576 J/g-O_2, was taken from the energy requirement of a commercial cryogenic air separation unit [28].

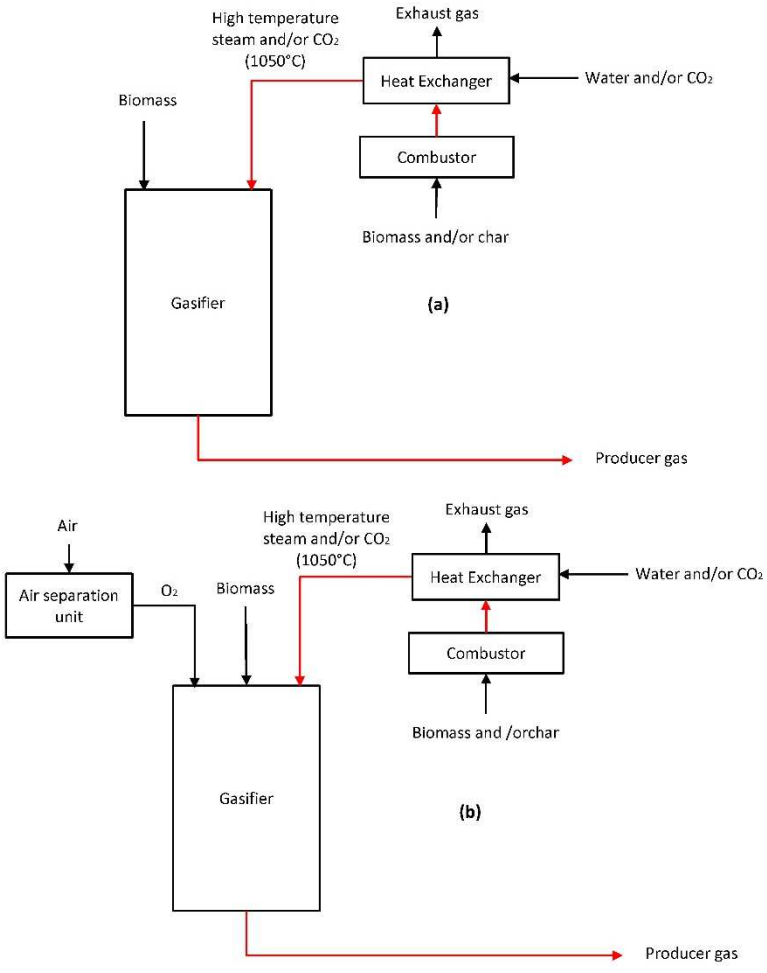

Figure 2.10 Concept of (a) indirect and (b) direct gasification system

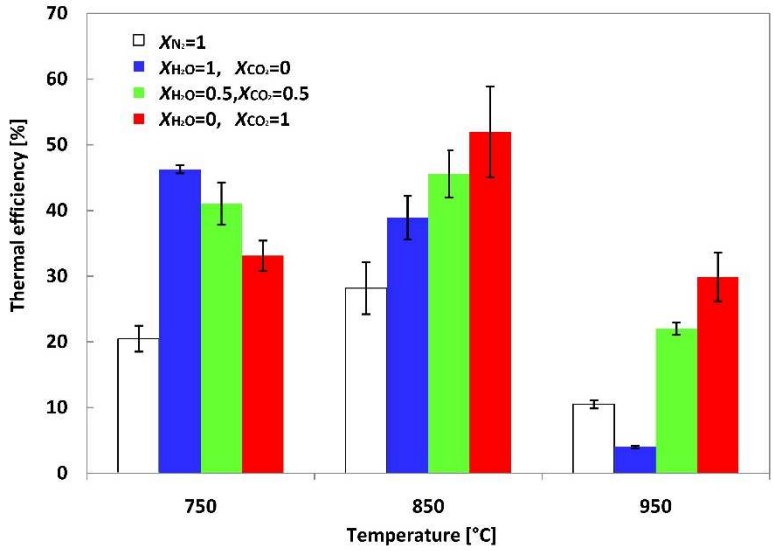

Figure 2.11 Thermal efficiency of the pyrolysis and the indirect gasification under various CO_2 and H_2O mixing ratio

Fig. 2.11 shows the effect of the CO_2 fraction on the expected thermal efficiency of the pyrolyzer and the indirect gasifier at various reaction temperatures. Due to the higher gas yield, most of the indirect gasifier had higher thermal efficiency than the pyrolyzer at each examined reaction temperatures. The lower thermal efficiency than that of the pyrolyzer was only produced in the gasifier with steam-only atmosphere at the reaction temperature of 950°C owing to its high energy requirement. The thermal efficiency of the gasifier decreased as the CO_2 fraction increased at the reaction temperature of 750ºC, while it increased at higher temperatures. At the reaction temperature of 750ºC, the energy yield dropped more than the energy input did by the replacement of steam by CO_2, which resulted in a low gasification thermal efficiency at a high CO_2 fraction. At the reaction temperatures of 850ºC and 950°C, the decrease in the chemical energy of the producer gas was less significant than the decrease in the energy input by the gasifying agent, which resulted in a higher efficiency at a high CO_2 fraction in the gasifying agent. At the reaction temperature of 950ºC, the thermal efficiency was lower than those at 850 ºC at all CO_2 fractions, and lower than those at 750ºC under steam involved conditions. It means that the increase in the chemical energy of the producer gas by increasing the reaction temperature from 850°C to 950ºC was less than the increase in the required energy input to reach the target reaction temperature. The highest thermal efficiency expected for the indirect gasification, 52%, was obtained under pure CO_2 atmosphere at 850 ºC.

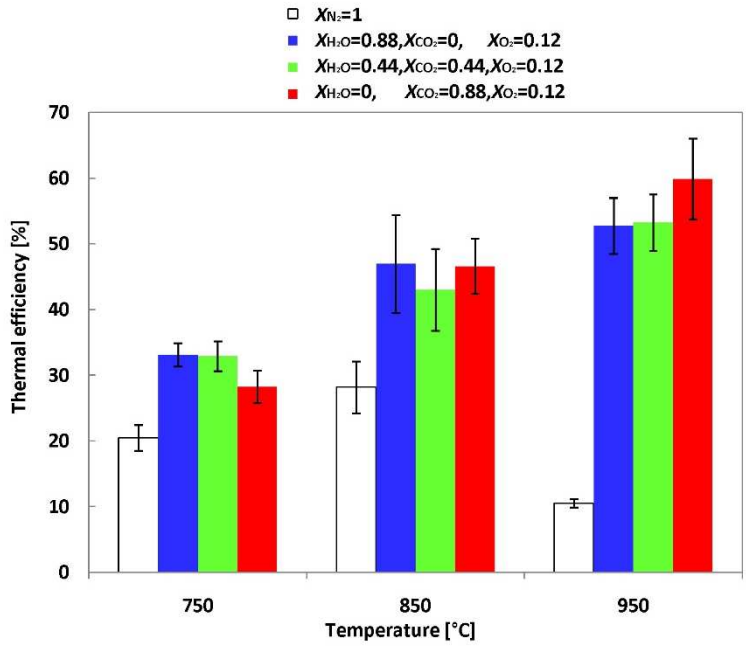

Figure 2.12 Thermal efficiency of the pyrolysis and the direct gasification under various CO_2 and H_2O mixing ratio

In the direct gasification process, the amount of gasifying agent required to supply the heat of reaction was significantly reduced by the biomass partial combustion. Thus, the producer gas energy affected the thermal efficiency greater in the direct gasifier than in the indirect gasifier. Fig. 2.12 shows the effect of the CO_2 fraction on the expected thermal efficiency at various temperatures in the direct gasification and its comparison with pyrolysis. Due to the higher gas yield and lower heat input in the gasifying agent, the direct gasifier had a higher thermal efficiency than pyrolyzer at all examined reaction conditions. At the reaction temperatures of 750ºC and 850º C, the increase of the CO_2 fraction in the gasifying agent brought no positive effect on the thermal efficiency of the gasifier. As previously shown in Fig. 2.8, the decrease of H_2 yields which were more significant than CO increase at the reaction temperature below 850º C caused this trend. At the reaction temperature of 950 ºC, the thermal efficiency increased as the steam fraction fully substituted with CO_2. The high yield of CO was responsible for this occurrence. Suppression of CO due to the inhibition of CO_2-char reaction by steam lowered the thermal efficiency of gasification under the steam-CO_2-O_2atmosphere. At the reaction temperature of 850ºC, gasification under the mixed atmosphere has the lowest thermal efficiency among those of under the other atmospheres. While at the reaction temperature of 950ºC, no increase of the thermal efficiency was observed as the steam partially substituted by CO_2. The highest thermal efficiency expected for the direct gasification process was 60% under the CO_2–O_2 atmosphere at 950 ºC. Considering the required period for complete gas evolution, 24 minutes, the ratio between the gasifying agent and the feedstock in the experiment under CO_2–O_2 atmosphere at 950 ºC can be

approximately correlated to the condition of 3.6 CO_2/C ratio and 0.4 equivalence ratio (molar ratio between the supplied oxygen to the amount of oxygen required for stoichiometric combustion of the feedstock).

2.3.4 Comparison of the results of equilibrium calculation and experiment

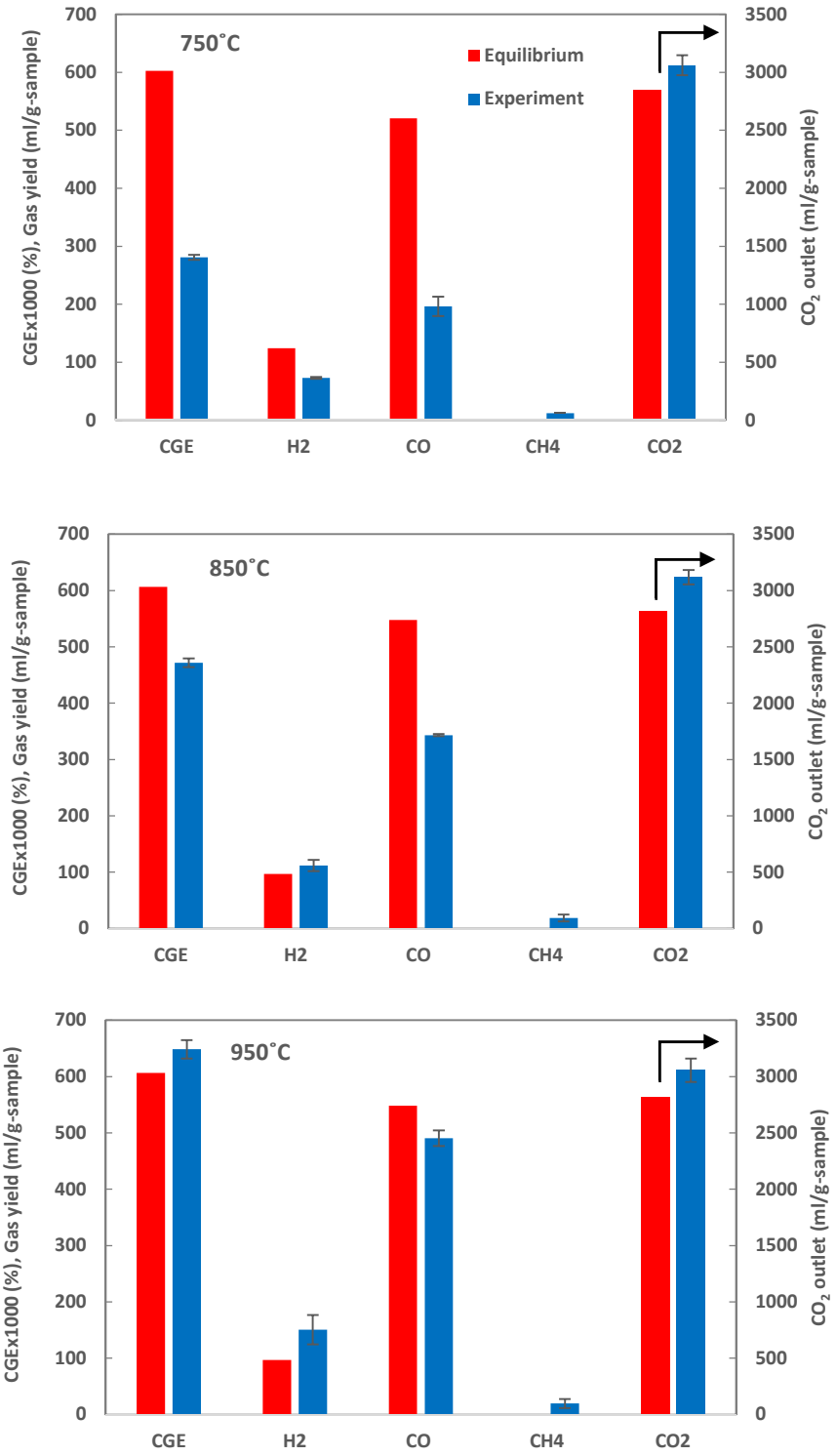

Figure 2.13 Comparison of the result of equilibrium calculation and experiment

In order to conduct the further study about the reaction performance of CO_2 gasifier and also the limitation occurred at each reaction temperature, comparison between the experiment results and the equilibrium calculation were analyzed. The equilibrium analysis was performed by treating the comparable amount of the reaction components involved during 0-24 minutes, correlated with 0.4 equivalence ratio, as one equilibrium system. The calculation was executed based on the mass and thermodynamic balances of three atomic components and two chemical reactions, respectively. Aspen Plus software was utilized in this analysis.

$$\text{Cold gas efficiency} = \frac{LHV_p(J/ml - producer\ gas) \times y_p(ml/g - wet\ biomass)}{LHV_b(J/g - wet\ biomass)} \quad (2.14)$$

Fig. 2.13 showed the comparison of the cold gas efficiency (CGE) and the gas yield between the equilibrium calculation and the experiment result under CO_2-O_2 atmosphere. CGE was calculated as a ratio of the energy output in the producer gas to the energy input in biomass, as shown in Eq. 2.14. At 750˚C, a large overestimation of the CO yield and underestimation of the CO_2 outlet compared to the experiment results were shown by the equilibrium calculation. These implied that CO_2-char reaction extent in the experiment was far from the ideal condition. The kinetics and diffusional limitations might play important role under this condition. The experimental CGE was roughly only a half of the ideal condition. At 850˚C, smaller gaps of the CO overestimation and CO_2 underestimation between the equilibrium prediction and the experiment result than those at 750˚C were observed. These implied that CO_2-char reaction was more highly activated at this temperature. The experimental CGE can reasonably represent the equilibrium predicted CGE. A better fit with the equilibrium prediction than those of at the lower reactor temperatures was shown by the experiment result at 950˚C. The kinetics and diffusional limitations on CO_2-char reaction might play less significant role at this temperature. The equilibrium under-prediction to the experiment results were observed for the H_2 yield at the reaction temperatures of 850˚C and 950˚C. These might be caused by the limited extent of the gas phase reaction especially the reverse water gas shift reaction.

2.4 Conclusion

A series of biomass pyrolysis and CO_2-steam gasification experiments without and with O_2 have been performed. Compared with pyrolysis, CO_2-steam gasification without and with O_2 yielded high amount of combustible gas. Both gasification conditions also showed similar effect of the CO_2 mixing ratio, while experiments with O_2 showed a lower combustible gas yield. The results showed that substitution of steam with CO_2 would generally lower the H_2 yield and enhance the CO yield. Inhibition of the CO_2-char reaction was observed under the presence of steam. It was confirmed by a significant CO evolution under pure CO_2 atmosphere.

A positive effect of CO_2 mixing ratio on the thermal efficiency of the gasifier was observed at the temperature of 850º C and above. For the indirect gasification (without O_2 supply), the highest thermal efficiency of the gasifier, 52%, was gained under CO_2-only atmosphere at 850 ºC. For the direct gasification (with O_2 supply), the highest thermal efficiency of 60% was gained under CO_2-O_2 atmosphere at 950º C. This calculation result shows that the gasification process with CO_2 as a gasifying agent and a heat carrier, especially in the direct gasification process, is more efficient than the pyrolysis with N_2 for syngas production. Furthermore, CO_2 is also potentially be more efficiently utilized in N_2-free syngas production than steam.

The kinetics and diffusional limitations of CO_2-reaction might be significant at the reaction temperature of 750ºC. These limitations caused the experimental CGE of CO_2-O_2 gasification to be much less than the equilibrium prediction. At the reaction temperature of 850ºC and above, the kinetics and diffusional limitations of CO_2-reaction were less significant than those of at 750ºC so that the experimental CGE of CO_2-O_2 gasification was closer to the equilibrium prediction.

Nomenclatures

Symbols

C_p specific heat [J/g °C]

E energy (J/g-sample)

F flow rate [ml/min]

HHV higher heating value [J/g]

L latent heat of water evaporation [J/g]

LHV lower heating value [J/g or J/ml]

m mass [g]

T temperature [°C]

t sampling time [minutes]

w weight fraction [dimensionless]

X volume fraction [dimensionless]

Y gas evolution rate [ml/min]

y gas yield per sample weight [ml/g]

Greek letters

α stoichiometric of oxygen amount [g-O_2/g-wet biomass]

η efficiency (%)

Subscript

0 initial condition

b biomass

g gasifying agent

i gas species

p producer gas

r targeted reaction condition

References

[1] Calin-Cristian Cormos, Anamaria Padurean, Paul Serban Agachi, Technical evaluations of carbon capture options for power generation from coal and biomass based on integrated gasification combined cycle scheme, Energy Procedia, Volume 4, 2011, Pages 1861-1868

[2] Kevin J. Whitty, Hongzhi R. Zhang, and Eric G. Eddings, Emissions from syngas combustion, Combustion Science and Technology 180, no. 6 2008, Pages 1117-1136..

[3] A.V Bridgwater, Renewable fuels and chemicals by thermal processing of biomass, Chemical Engineering Journal, Volume 91, Issues 2–3, 15 March 2003, Pages 87-102

[4] Jose Corella, Jose-Manuel Toledo, and Gregorio Molina, Biomass gasification with pure steam in fluidised bed: 12 variables that affect the effectiveness of the biomass gasifier, International Journal of Oil, Gas and Coal Technology 1, no. 1 2008, Pages 194-207.

[5] Marcin Siedlecki , Wiebren De Jong, and Adrian HM Verkooijen, Fluidized bed gasification as a mature and reliable technology for the production of bio-syngas and applied in the production of liquid transportation fuels—a review, Energies4, no. 3 2011, Pages 389-434.

[6] Jose Corella, Jose M. Toledo, and Gregorio Molina, A review on dual fluidized-bed biomass gasifiers. Industrial & Engineering Chemistry Research 46, no. 21 2007, Pages 6831-6839.

[7] Kentaro Umeki, Kouichi Yamamoto, Tomoaki Namioka, Kunio Yoshikawa, High temperature steam-only gasification of woody biomass, Applied Energy, Volume 87, Issue 3, March 2010, Pages 791-798

[8] Christoph Pfeifer, Reinhard Rauch, and Hermann Hofbauer, In-bed catalytic tar reduction in a dual fluidized bed biomass steam gasifier, Industrial & engineering chemistry research 43, no. 7 2004, Pages 1634-1640.

[9] Colomba Di Blasi, Combustion and gasification rates of lignocellulosic chars, Progress in Energy and Combustion Science, Volume 35, Issue 2, April 2009, Pages 121-140

[10] Chunshan Li, Kenzi Suzuki, Tar property, analysis, reforming mechanism and model for biomass gasification—An overview, Renewable and Sustainable Energy Reviews, Volume 13, Issue 3, April 2009, Pages 594-604

[11] Martin Gassner, François Maréchal, Thermo-economic process model for thermochemical production of Synthetic Natural Gas (SNG) from lignocellulosic biomass, Biomass and Bioenergy, Volume 33, Issue 11, November 2009, Pages 1587-1604

[12] Lasse R. Clausen, Brian Elmegaard, Niels Houbak, Technoeconomic analysis of a low CO_2 emission dimethyl ether (DME) plant based on gasification of torrefied biomass, Energy, Volume 35, Issue 12, December 2010, Pages 4831-4842

[13] Oscar P.R. van Vliet, André P.C. Faaij, Wim C. Turkenburg, Fischer–Tropsch diesel production in a well-to-wheel perspective: A carbon, energy flow and cost analysis, Energy Conversion and Management, Volume 50, Issue 4, April 2009, Pages 855-876

[14] Michael E. Walker, Javad Abbasian, Donald J. Chmielewski, and Marco J. Castaldi, Dry Gasification Oxy-combustion Power Cycle, Energy & Fuels, 2011, 25 (5), pp 2258–2266

[15] Yuso Oki, Jun Inumaru, Saburo Hara, Makoto Kobayashi, Hiroaki Watanabe, Satoshi Umemoto, Hisao Makino, Development of oxy-fuel IGCC system with CO_2 recirculation for CO_2 capture, Energy Procedia, Volume 4, 2011, Pages 1066-1073

[16] Kentaro Umeki, Tomoaki Namioka, Kunio Yoshikawa, The effect of steam on pyrolysis and char reactions behavior during rice straw gasification, Fuel Processing Technology, Volume 94, Issue 1, February 2012, Pages 53-60

[17] Ahmed, A.K. Gupta, Evolution of syngas from cardboard gasification, Applied Energy, Volume 86, Issue 9, September 2009, Pages 1732-1740

[18] I. Ahmed, A.K. Gupta, Characteristics of cardboard and paper gasification with CO_2, Applied Energy, Volume 86, Issue 12, December 2009, Pages 2626-2634

[19] Butterman, Heidi C., and Marco J. Castaldi, CO2 as a carbon neutral fuel source via enhanced biomass gasification, Environmental science & technology 43, no. 23 2009, Pages 9030-9037.

[20] Eilhann E. Kwon, Marco J. Castaldi, Urban energy mining from municipal solid waste (MSW) via the enhanced thermo–chemical process by carbon dioxide (CO_2) as a reaction medium, Bioresource Technology, Volume 125, December 2012, Pages 23-29

[21] I.I. Ahmed, A.K. Gupta, Kinetics of woodchips char gasification with steam and carbon dioxide, Applied Energy, Volume 88, Issue 5, May 2011, Pages 1613-1619

[22] Susanna Nilsson, Alberto Gómez-Barea, Pedro Ollero, Gasification of char from dried sewage sludge in fluidized bed: Reaction rate in mixtures of CO_2 and H_2O, Fuel, Volume 105, March 2013, Pages 764-768

[23] C. Guizani, F.J. Escudero Sanz, S. Salvador, The gasification reactivity of high-heating-rate chars in single and mixed atmospheres of H_2O and CO_2, Fuel, Volume 108, June 2013, Pages 812-823

[24] Wei-Hsin Chen, Bo-Jhih Lin, Hydrogen and synthesis gas production from activated carbon and steam via reusing carbon dioxide, Applied Energy, Volume 101, January 2013, Pages 551-559

[25] Chao Chen, Jing Wang, Wei Liu, Sen Zhang, Jingshu Yin, Guangqian Luo, Hong Yao, Effect of pyrolysis conditions on the char gasification with mixtures of CO_2 and H_2O, Proceedings of the Combustion Institute, Volume 34, Issue 2, 2013, Pages 2453-2460

[26] Naomi B. Klinghoffer, Marco J. Castaldi, and Ange Nzihou, Catalyst properties and catalytic performance of char from biomass gasification, Industrial & Engineering Chemistry Research 51, no. 40 (2012) Pages 13113-13122.

[27] Xiangmei Meng, Wiebren de Jong, Ningjie Fu, Adrian H.M. Verkooijen, Biomass gasification in a 100 kWth steam-oxygen blown circulating fluidized bed gasifier: Effects of operational conditions on product gas distribution and tar formation, Biomass and Bioenergy, Volume 35, Issue 7, July 2011, Pages 2910-2924

[28] Jean-Pierre Tranier, Richard Dubettier, Arthur Darde, Nicolas Perrin, Air separation, flue gas compression and purification units for oxy-coal combustion systems, Energy Procedia, Volume 4, 2011, Pages 966-971

\

Supplement Material

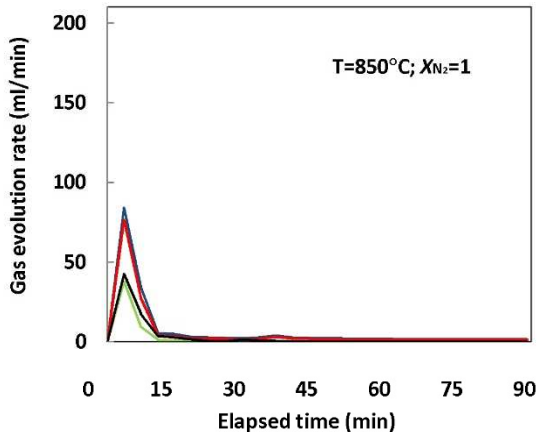

Supplement Figure 2.1 Gas evolution profiles during pyrolysis at the reaction temperature of 850°C.

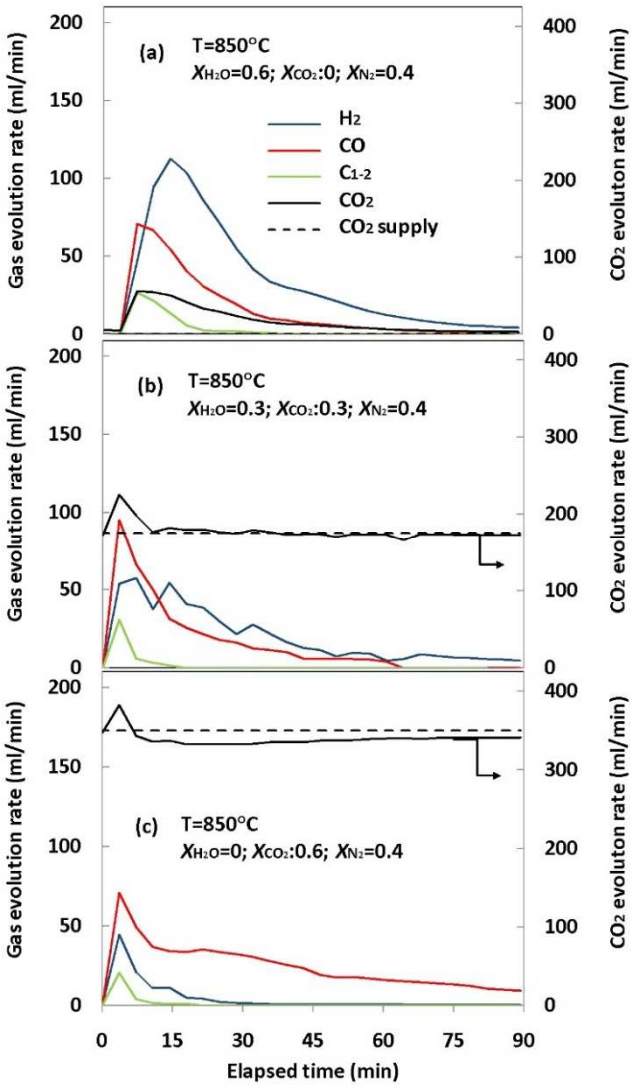

Supplement Figure 2.2 Gas evolution profiles at the reaction temperature of 850°C under CO_2:H_2O fractions of: (a) 0:0.6, (b) 0.3:0.3 and (c) 0.6:0 with the N_2 fraction of 0.4

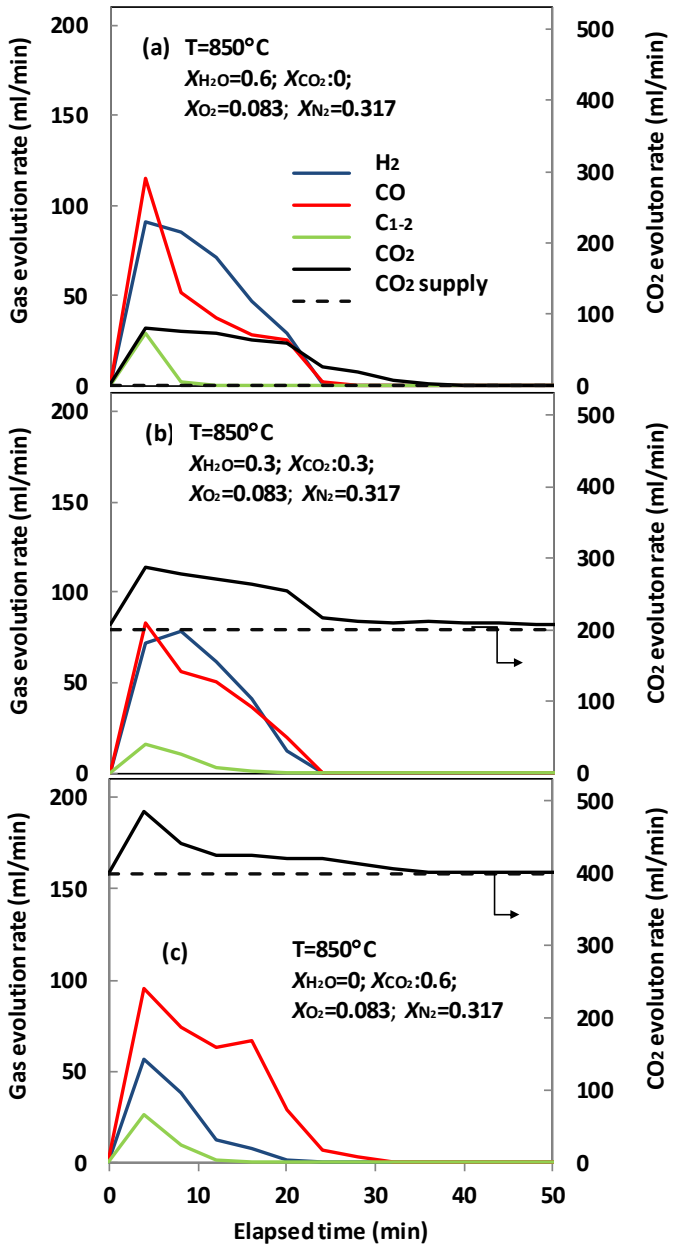

Supplement Figure 2.3 Gas evolution profiles at the reaction temperature of 850°C under CO_2:H_2O fractions of: (a) 0; 0.6, (b) 0.3; 0.3 and (c) 0.6; 0 with the N_2 fraction of 0.317 and O_2 fraction of 0.083

Chapter III

Pilot scale downdraft gasification of coconut shell with CO_2-O_2 mixture

3.1. Introduction

Despite of the investigated potentials of CO_2 gasification, only few studies were found reporting the performance of CO_2 gasification experimentally [1-3] and none was found performed in the pilot-scale gasifier. A preliminary pilot-scale experiment of gasification with CO_2-O_2 mixture was performed by Pettinau et.al [4], but no parametric study was carried out due to the difficulty of the process control. Thus, the examination of the operability and performance evaluation of CO_2 gasification using a pilot-scale plant still remains an important issue.

This chapter presents the gasification performance of coconut shell using a pilot-scale fixed bed downdraft gasifier under various CO_2 flow rates, 0.6 to 1.6 CO_2/C ratios, with the presence of fixed amount of O_2 with the equivalence ratio of around 0.4 – 0.6. The reactor temperature, the producer gas composition and the energy yield were examined to investigate the effect of the CO_2/C ratio and to find the optimum value of the CO_2/C ratio. The obtained results were also compared with those of air gasification

3.2. Experimental

3.2.1. Material

Coconut shell obtained from local area of Bandung, West Java, Indonesia, was used as a biomass feedstock. The sample was naturally dried for more than 24 hours and roughly ground to the size below 50 mm in the diameter. The ultimate and proximate analysis results of the sample are shown in Table 3.1. The moisture content of the feedstock was 11.0±1.1 %

Table 3.1 Proximate and ultimate analysis results of coconut shell

Proximate analysis (%wt.)[a]	
Volatile matter	83.9
Fix carbon	13.3
Ash	2.8
Ultimate analysis (%wt.)[b]	
C	49.3

H	5.5
O	45.0
N	0.2

[a]:d.b , [b]: d.a.f

3.2.2. Apparatus

A pilot scale downdraft gasification system was utilized in this experiment. The total scheme of the gasification system is shown in Fig. 3.1, while the detail drawing of the gasifier is shown in Fig.3.2. The gasification system consists of a downdraft gasifier, a gas supply system, a cyclone, a gas-cooling system, a tar-capturing system, and a suction blower. 30-40 kg of feedstock bunker with a stirrer is attached to the gasifier. The gasifier has a throat of 160 mm in diameter, covered by the castable refractory cement for the inner layer with a steel plate for the outer layer. Three K-type thermocouples are attached for monitoring the temperature inside the reactor (hereafter called as T1–T3 points) and a S-type thermocouple was attached for measuring the producer gas temperature (hereafter called as Tgas point) at the position of flow measurement. Three orifice-type gas flow meters were used for measuring the flow rate of supplied O_2, supplied CO_2 or air and the generated producer gas. O_2 and CO_2 (both are 99.5 vol.% purity) were supplied directly from gas cylinders and the flow rate was adjusted by the cylinder valve opening. The air supply was adjusted by the suction force of the blower. A GC-TCD (Shimadzu GC 14B) equipped with two columns (Molecular sieve and Porapack PlotQ) was used for gas composition analysis.

3.2.3. Experimental procedure

The gasification tests were carried out in semi-batch operation for 140 minutes. Each experimental run consists of two periods: the preheating period and the measurement period. First, the gasifier was preheated by partial combustion of the sample with 6.8 g/sec of air flow rate for 60 minutes. Then, 10-17 kg of the feedstock was supplied to the gasifier and the measurement period continued for about 70 minutes with the preset CO_2-O_2 flow rate. The CO_2 flow rate was varied from 3.6-9.2 g/sec that is corresponding to the CO_2/C ratio of 0.6 - 1.6. The O_2 flow rate was kept constant at 1.9 g/sec that is corresponding to the equivalence ratio (E/R) of around 0.4. CO_2/C ratio and E/R were calculated based on Eqs.1 and 2, respectively. The detail of experiment conditions in the measurement period is presented in table 3.2.

$$CO_2/C\ ratio = \frac{CO_2\ supply\ rate\ (mol/sec)}{C\ in\ biomass\left(\frac{mol}{kg}\right) X\ consumed\ biomass(g/sec)} \quad (3.1)$$

$$\text{Equivalence ratio } (E/R) = \frac{O_2 \ supply \ (mol)}{O_2 \ for \ stochiometric \ combustion \ (mol)} \qquad (3.2)$$

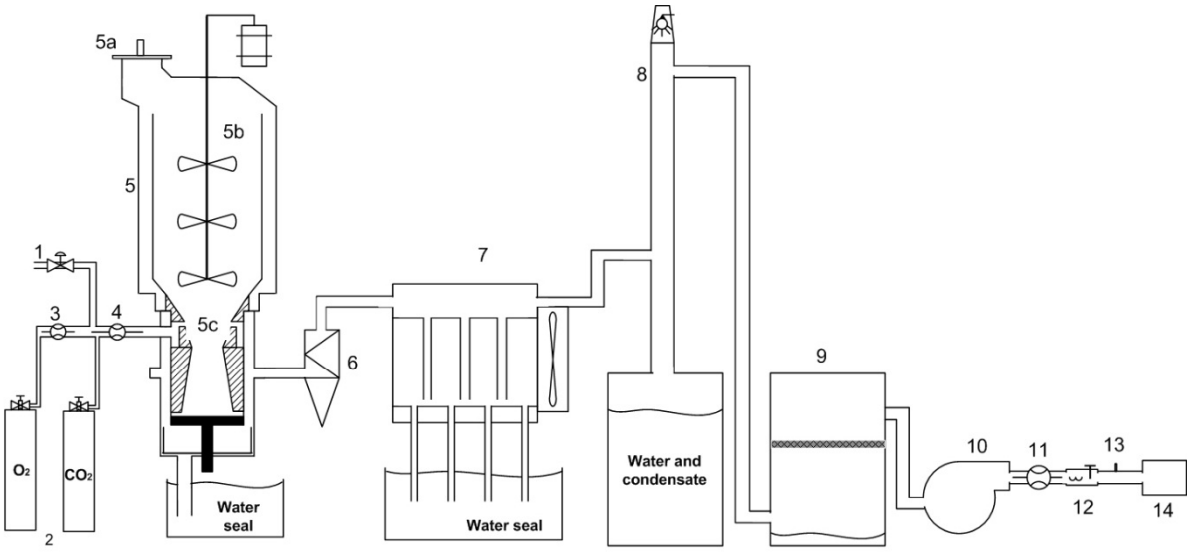

1. Air inlet port	5a. Feedstock hoper	7. Condenser	11. Producer gas flow meter
2. Gas cylinders	5b. Bunker with stirrer	8. Water scrubber	12. Thermometer
3. O_2 flow meter	5c. Reaction zone	9. Liquid collector	13. Gas sampling port
4. CO_2+O_2 or air flow meter	6. Cyclone	10. Suction blower	14. Burner
5. Gasifier			

Figure 3.1 Scheme of the gasification system

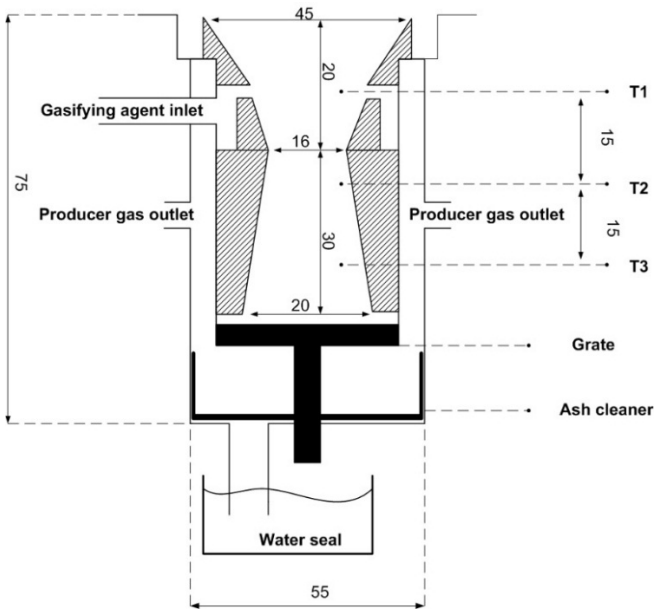

Figure 3.2 Detail of the gasifier (cm unit)

The feedstock was refilled prior to the measurement period to minimize the effect of the sample level on the reaction system behavior. The stirrer attached in the feedstock bunker was used every ten minutes to ensure a proper feedstock distribution and down-flow. The temperatures in the attached thermocouples were recorded at the interval of 2 minutes. Fig. 3.3 shows the typical data of temperature measurements over time at the zones of T1, T2, T3 (see Fig. 3.2 for the locations) and Tgas (No.12 in Fig.3.1). Temperature increase was observed during the pretreatment period (first 60 minutes) at all the measurement points. Stable condition in this study was defined when the temperature variance was less than 5°C/min. T1, which is highly affected by combustion, became stable about 90 minutes after the experiment had started. T2 and T3 (located at the lower part of the gasifier) and Tgas became stable earlier during the preheating period.

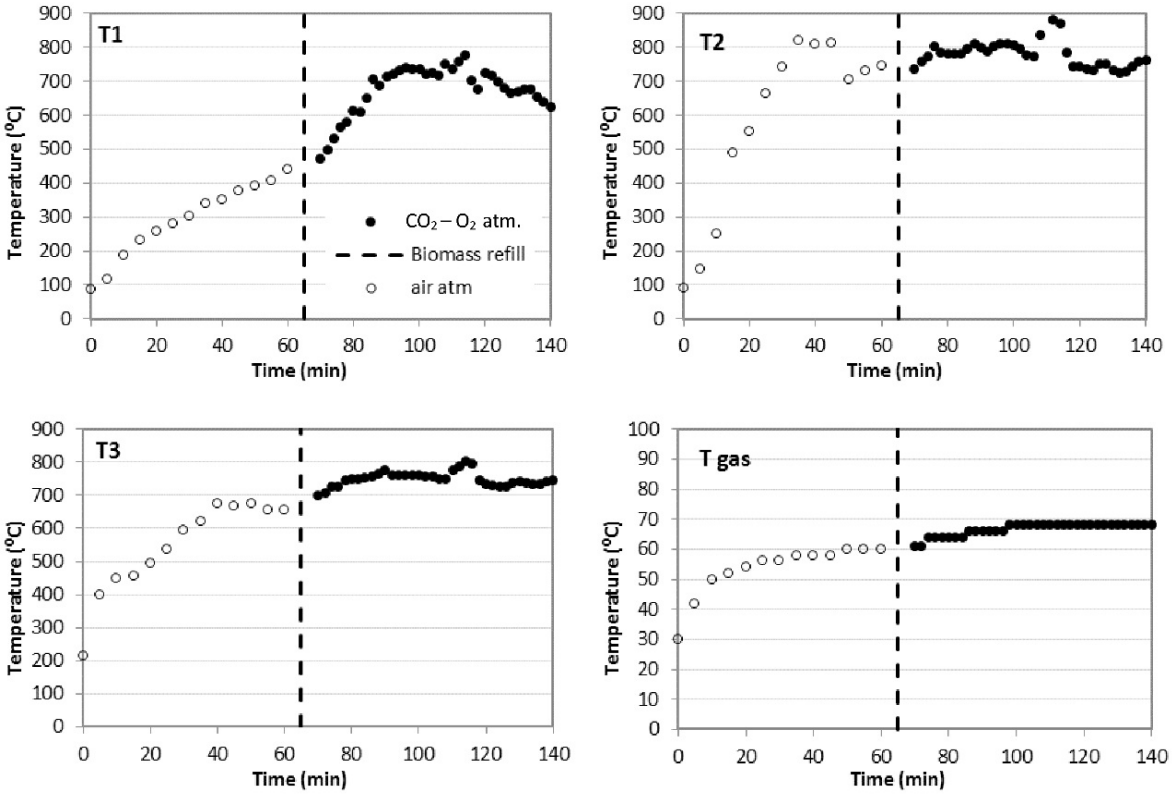

Figure 3.3 Temperature evolution during the experimental runs

The producer gas flow rate was measured by an orifice flow meter at the same time with the temperature measurement and the gas composition was analyzed by a GC-TCD every 7 minutes of the CO_2-O_2 injection period. Fig. 3.4 shows the typical data of the gas composition and the flow rate measurements over time for some experiment runs. For further analysis, the average value of the temperature and the gas data will be utilized and the fluctuation range will be shown in the standard deviation bar. Furthermore, the data shown in Fig.3.4 were then used to calculate the gas evolution rate, the gas yield,

and eventually the cold gas efficiency. The gas evolution rate was calculated by multiplying the volume percentage of the gas specy i (Xi) with the instantaneous producer gas flow rate (Fp [ml/sec]) at the correlated timing and then changed the results to mass base [kg/sec] using the ideal gas law. The gas yield (Yi [kg-gas/kg-dry biomass]) was calculated according to Eq. 3.3: dividing the sum of the product of the gas evolution rate and the time interval of the GC measurement (Δt[sec]) with the total mass of the biomass consumed during the examination period (m_b[kg]). The total biomass consumption during the measurement period was quantified by weighing up the required feedstock amount for refilling the bunker to the initial feedstock level just before the measurement period after the experiment.

$$Y_i = \sum Xi \cdot F_p \cdot \Delta t / m_b \qquad (3.3)$$

3.3. Results and Discussion

Despite of some fluctuations, stable operation under the CO_2-O_2 atmosphere can be generally judged from the relatively stable temperature and gas composition profile as shown in Figs.3.3 and 3.4 and also in the figures in supplement materials. Thus in this frame of study, it can be stated that CO_2-O_2 gasification can be operated in the pilot scale downdraft gasifier. However, highly fluctuated gas flow rate measurement was observed in most of the experiment runs as shown in Figs.3.4 and in supplement materials. The unsteady gas flow rate might not indicate the instability in the process but seems to be more caused by the alternated condition of the producer gas orifice flow meter due to the tar blocking during the experiment run. The constriction of orifice hole increased the sensitivity of the orifice meter and lead to the inaccurate flow measurement. Therefore, the calculated data involving the gas flow rate, i.e. the cold gas efficiency, can be used merely for qualitative analysis and not for investigating the absolute value.

Table 3.2 shows the summary of experimental conditions and the measurement results. Mass balance calculations were also performed based on those data for examining the accuracy of the measurement and calculation performed in this experiment. Table 3.3 shows the accumulated mass balance and atomic mass flow balance of C, H, O, and N where the input was counted from the feedstock and gas supply and the output was counted from the producer gas. Some signs of measurement inaccuracy were observable in the accumulated mass balance of experiment Nos. 1, 2 and especially No.3 that showed more output amount than the input. Further analysis by the atomic mass flow balance shows that the source of the inaccuracy of the experiment Nos. 1 and 3 was partially came from C balance. Since the possible source of C in this experiment only came from the supplied biomass and gasifying agent, these inaccuracy could indicate the imprecise measurement of the producer gas flow rate. Therefore, the quantitative efficiency analysis of run Nos. 1 and 3 were not taken into account. The source of mass

balance inaccuracy of experiment No.2 came from the N_2 balance. As also happen in all experiment runs, the N_2 balance showed more amounts in the output than in the input that indicated the unexpected N_2 entrainment to the system. The source of entrained N_2 is thought to be the air intake from the feedstock hopper due to negative pressure because no O_2 was detected in producer gas as shown in table 3.2. Since the entrained air that can act as an additional gasifying agent, the equivalence ratio (E/R) were recalculated by adding the additional O_2 from air based on the detected N_2 amount in the producer gas. However, since the N_2 amount calculation was involving the gas flow rate measurement, it should be noted that the air adjusted E/R shown in Table 3.2 were merely approximated values

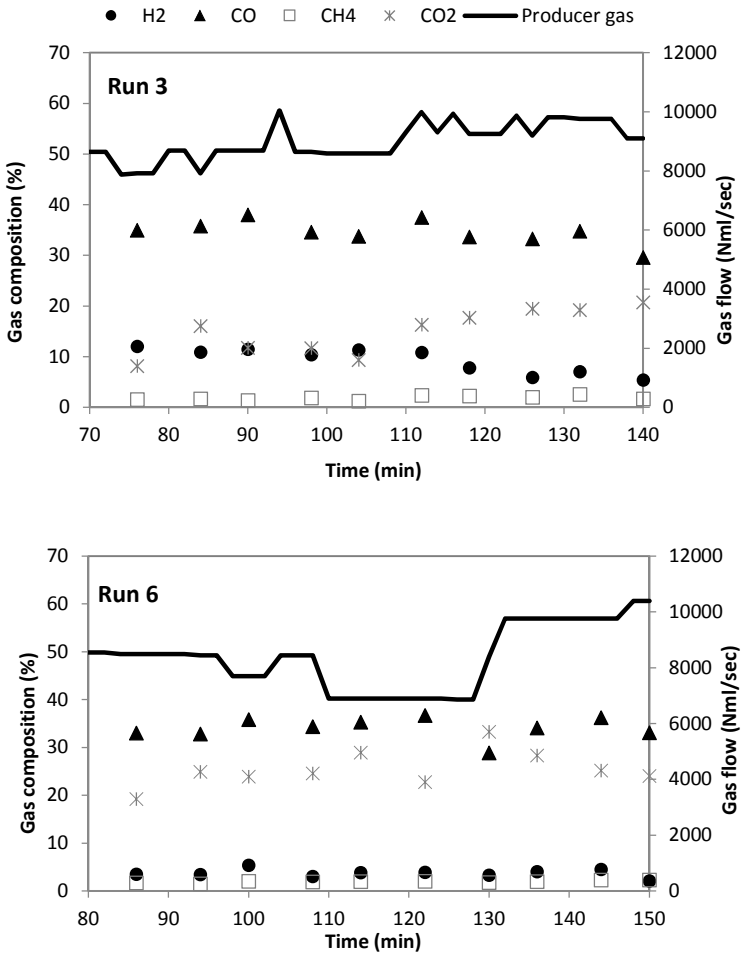

Figure 3.4 Producer gas evolution during the experimental runs

The accumulated mass balance of other run show 3- 7 % mass loss. As also indicated in the atomic mass flow balance of C and H, the loss can be explained from the unmeasured amount of those material in tar, condensed matter, ash bounded solid residue, and might also come from gas leakage. Related to solid residue, many researches [5-7] showed that the injection of CO_2 to the direct gasifier will be resulted in the higher carbon conversion than that of in O_2+inert atmosphere. However regarding tar

content, the effect of CO_2 injection may vary from positive to negative depend on the utilized sample. Some researcher found that CO_2 can decompose tarry compound [5], but the others found that CO_2 might inhibit the tar decomposition [6, 7]. The study of tar behavior under CO_2 atmosphere still hardly performed with obtained the data in this experiment and will be our foccus in the near future.

3.3.1. Effect of the CO_2/C ratio on the reactor temperature

Fig. 3.5 shows the effect of the CO_2/C ratio on the reactor temperature in the measurement zones of T1, T2 and T3. CO_2/C ratio was calculated as the ratio of the mole flow of CO_2 supplied to the mole flow of carbon in the consumed biomass. Analysis of temperature in all measurement zones was performed after 90 minutes to avoid the disturbance of the transient phase at the early period of CO_2-O_2 injection. The increase of the CO_2/C ratio generally decreased the temperature at T1. This implies the delay of combustion due to the effect of CO_2 dilution on O_2. The recorded T1 temperatures under the CO_2/C ratio of 0.9 and below were higher than those of under air combustion while the T1 temperatures under the CO_2/C ratio of 1.2 and above were around the same and lower than those of under air combustion, respectively.

The high temperature under low CO2/C values can be explained by a higher fraction of O2 in the gasifying agent (0.012-0.013 kmol/m3) than that of in air (0.009 kmol/m3). The high O2 fraction enhanced the combustion under those range of CO2 injection to occur at the closer distance to the gas inlet port than the combustion in air gasification. This condition might be beneficial for enhancing the endothermic reactions since they can be triggered at closer position to the gas inlet port and eventually had longer effective residence time in the reactor.

On the other hand, the T1 temperatures during the gasification tests with CO_2/C=1.2 were just around the temperature range of two air gasification runs despite the higher O_2 fraction (0.010 kmol/m3). The T1 temperatures during the gasification tests with CO_2/C=1.6 were lower than the temperature in air gasification runs despite the comparable O_2 fraction. Those implied the progress of CO_2-char (Eq.3.4) reaction which is an endothermic reaction. The low combustion rate of O_2 under CO_2 dilution compared to those of air might also play an important role. The low aggressiveness of O_2 in the CO_2-O_2 mixture which is related to the low diffusivity of O_2 under CO_2 dilution compared to those of O_2 under N_2 dilution has also been intensively reported in the oxy-fuel combustion researches [8, 9].

Table 3.2 Parameter settings, biomass consumption and gas measurement results

Run no.	Gasifying agent flow (g/sec)			Biomass consumption (kg)	CO_2/C ratio	E/R	Entrained air adjusted E/R	Producer gas					
								Composition (vol.%)					Flow (Nml/sec.)
	Air	O_2	CO_2					H_2	CO	CH_4	CO_2	N_2	
1	6.8	-	-	13.4	-	0.39	0.53	6.14	23.22	1.44	5.63	63.24	8784.80
2	6.8	-	-	14.4	-	0.36	0.55	5.53	21.43	1.14	4.66	67.25	8510.89
3	-	1.9	3.6	14.0	0.6	0.38	0.74	8.76	34.38	1.90	15.79	39.90	9257.85
4	-	1.9	5.6	15.2	0.8	0.35	0.59	10.85	33.97	1.62	17.87	35.46	7190.78
5	-	1.9	5.6	14.0	0.9	0.38	-	-	-	-	-	-	9741.57
6	-	1.9	8.2	16.0	1.2	0.34	0.59	3.73	34.28	2.00	26.35	34.60	8368.83
7	-	1.9	9.2	16.2	1.6	0.33	0.61	3.66	31.25	1.40	30.70	32.97	9921.13

Table 3.3 The accumulated mass balance and the atomic mass flow balance of C, H, O, and N

Run No.	Accumulated mass balance (kg)					Atomic mass flow balance (g/sec)											
	In			Out		C			H			O			N		
	Gasifying agent	Feedstock	Sum	Producer gas	Loss	In	Out	Δ	In	Out	Δ	In	Out	Δ	In	Out	Δ
1	25.27	14.38	39.65	41.71	-2.06	1.36	1.44	-0.08	0.19	0.07	0.12	2.96	2.19	0.76	4.93	6.22	-1.29
2	25.27	15.45	40.72	43.67	-2.95	1.46	1.34	0.12	0.21	0.06	0.14	3.07	2.02	1.05	4.96	6.97	-2.02
3	19.05	15.03	34.07	46.96	-12.89	2.24	2.48	-0.23	0.20	0.10	0.10	5.34	4.17	1.17	0.33	4.43	-4.10
4	24.83	16.31	41.14	38.13	3.01	2.74	2.10	0.64	0.22	0.09	0.13	6.48	3.65	2.83	0.36	3.25	-2.89
5	24.83	15.03	39.85	-	-	2.62	-	-	0.20	-	-	6.34	-	-	0.33	-	-
6	35.26	17.17	52.44	49.09	3.35	3.50	2.80	0.71	0.23	0.06	0.17	8.38	5.16	3.22	0.38	3.67	-3.29
7	44.97	17.39	62.36	60.38	1.98	4.15	3.52	0.64	0.23	0.06	0.17	10.08	6.82	3.26	0.38	3.98	-3.60

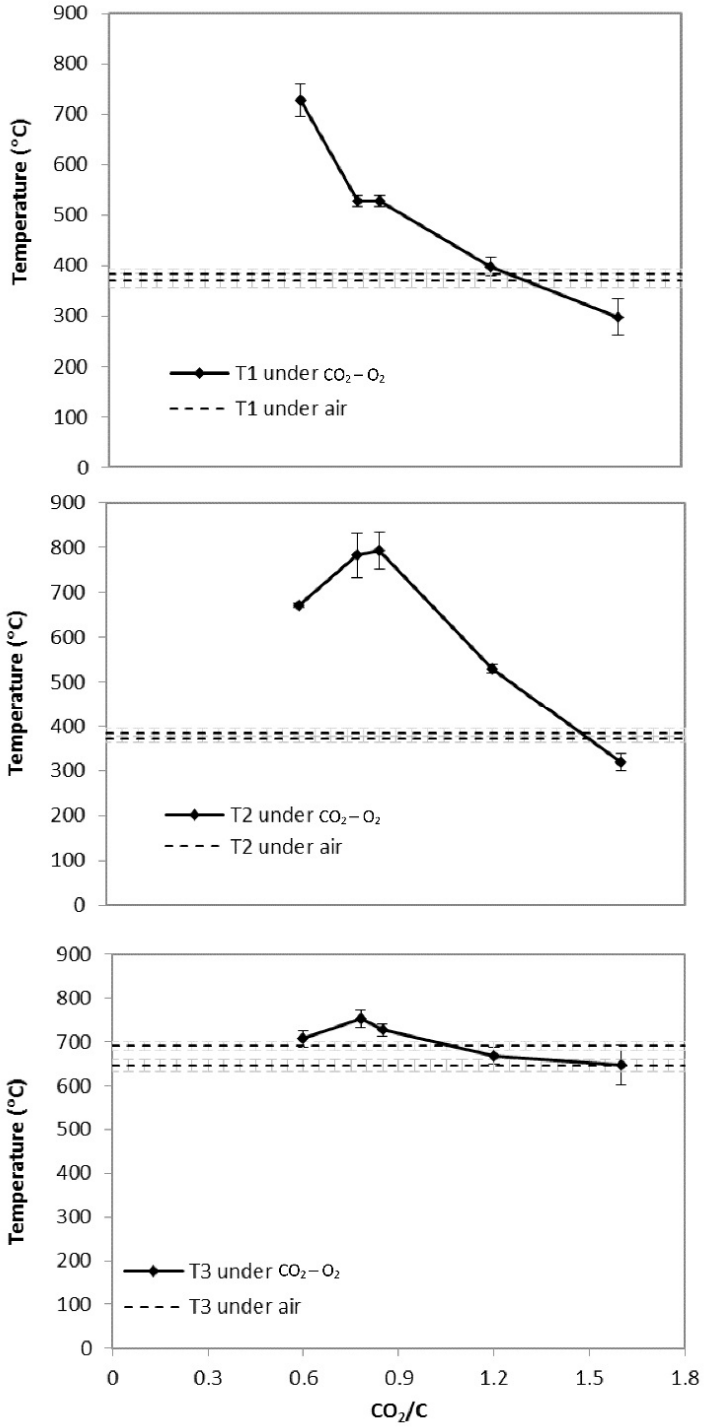

Figure 3.5 The effect of CO_2/C ratio on the reactor temperature at T1, T2 and T3 points

In the measurement zone of T2, the increase of the CO_2/C ratio from 0.6 to 0.9 resulted in the reactor temperature increase. Combined with the temperature profile in the T1 zone, it can be implied that the increase of the CO_2/C ratio in this range delayed the occurrence of the flame front from around the T1 zone to the T2 zone. Further CO_2/C ratio increase to 1.6 monotonically decreased the reactor

temperature. The T2 temperatures under the CO_2/C ratio of 1.2 and below were higher than those of under air gasification. It implied that the flame front under those range of CO_2 injection was closer to the gasifying agent inlet than the flame front in air gasification.

Compared with T1 and T2 zones, a stable temperature profile against the gasifying agent composition was observed in the T3 zone. The flame front under all tested conditions seems to be located upstream of the T3 zone and resulted in the similar measured temperature in the T3 zone. In general, compared with that of air gasification, the temperature profile of CO_2-O_2 gasification with the CO_2/C ratio of 1.2 and below indicated the occurrence of the long and uniformly distributed high temperature zone in the reactor. This condition might be favorable for assisting gasification reactions that are mostly the endothermic to occur in the higher extent.

3.3.2. Effect of the CO_2/C ratio on the producer gas composition

Fig.3.6 shows the effect of the CO_2/C ratio on the producer gas composition. Same as the temperature analysis, the analysis of gas composition was performed after 90 minutes to avoid the transient phase disturbance. In general, the increase of the dilution effect of unreacted CO_2 was observed as the CO_2/C ratio increased and resulted in the suppression of other gas fraction in the producer gas. Moreover, it is observable that the overall decrease of the CO fraction was less significant than the increase of the CO_2 fraction as the CO_2/C ratio increased. It implied the progress of CO_2 to CO conversion that might be occurred mainly through Eqs.3.4 and 3.5 and the reverse of Eq.3.6. The H_2 fraction was slightly increased as the CO_2/C ratio increased from 0.6 to 0.8 and then significantly suppressed under the CO_2/C ratio increase over 0.8.

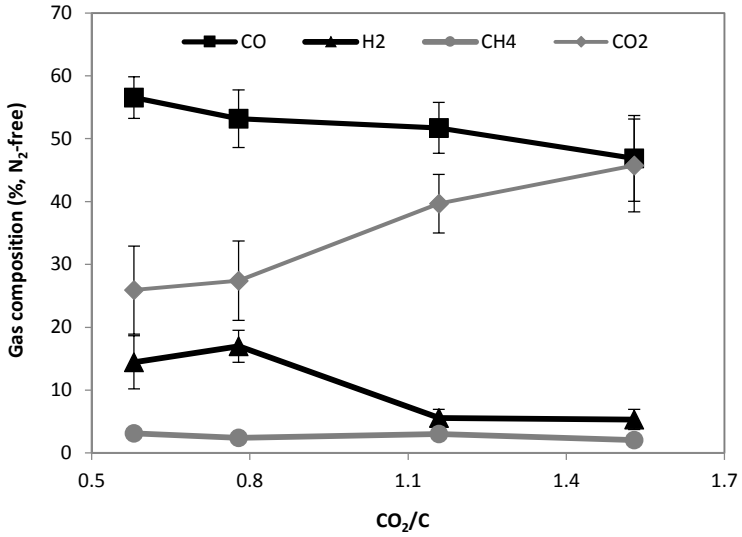

Figure 3.6 The effect of CO_2/C ratio on the producer gas composition

The H_2 fraction increase as the CO_2/C ratio increased from 0.6 to 0.8 might be related to the delayed occurrence of the high temperature zone in the reactor (discussed in previous section) which is therefore lessened the extent of the reverse water gas shift reaction (the reverse of Eq.3.6). The lessened extent of the reverse water gas shift reaction also made the CO fraction decrease as the C_{O2}/C ratio increase at this range was more significant than those as the CO_2/C ratio increase at the other range. In addition to the dilution effect, the suppressed H_2 fraction under the CO_2/C ratio of 0.8 and above might be related to the decrease of the reactor temperature by the CO_2 injection over that range which subsequently suppressed the H_2 evolution through devolatilization. The CH_4 fraction is trivially affected by CO_2 injection since the contradictory effect of the temperature on the CH_4 evolution through devolatilization and the dry reforming (Eq. 5) might occur simultaneously

$$C + CO_2 \rightarrow 2CO \qquad (3.4)$$

$$H_2 + CO_2 \leftrightarrow CO + H_2O \qquad (3.5)$$

$$C_nH_m + n\ CO_2 \rightarrow m/2\ H_2 + 2n\ CO \qquad (3.6)$$

3.3.3. Effect of the CO_2/C ratio on the gasifier performance

Fig.3.7 shows the effect of the CO_2/C ratio on the lower heating value (LHV) and the H_2/CO ratio of the producer gas. LHV and the H_2/CO ratio are the important parameters for judging the quality of the producer gas which determine its suitable utilization. The increase of the CO_2/C ratio decreased the producer gas LHV. This was related to the increased amount of unreacted CO_2 that diluted the combustible gases. However, the producer gas obtained in CO_2-O_2 gasification had a higher LHV, 4.6–5.8 MJ/Nm^3, than those obtained in air gasification, 3.5-3.8 MJ/Nm^3. The removal of N_2 by the oxidizer change from air to O_2 is one of the reason. In addition, the enhanced CO_2 to CO conversion as CO_2 was introduced into the gasifier might also play important role indicated by the higher producer gas LHV of CO_2-O_2 gasification than that of air gasification at the comparable amount of O_2 diluent in the gasifying agent (at CO_2/C=1.6). This occurrence also agreed the finding of the previous research [26].

As previously discussed, the measured gas compositions in CO_2-O_2 experiments were containing N_2 from air leakage due to the insufficient sealing of the gasification system. However, N_2 could be expected to be absent in the ideal CO_2-O_2 gasification since air is not involved in any part of the process. Analysis of the effect of the CO_2/C ratio on the expected N_2-free LHV is also shown in Fig.3.8. The N_2 free LHV were roughly 1.5 times higher than that with N_2 presence, 6.9–9.3 MJ/Nm^3.

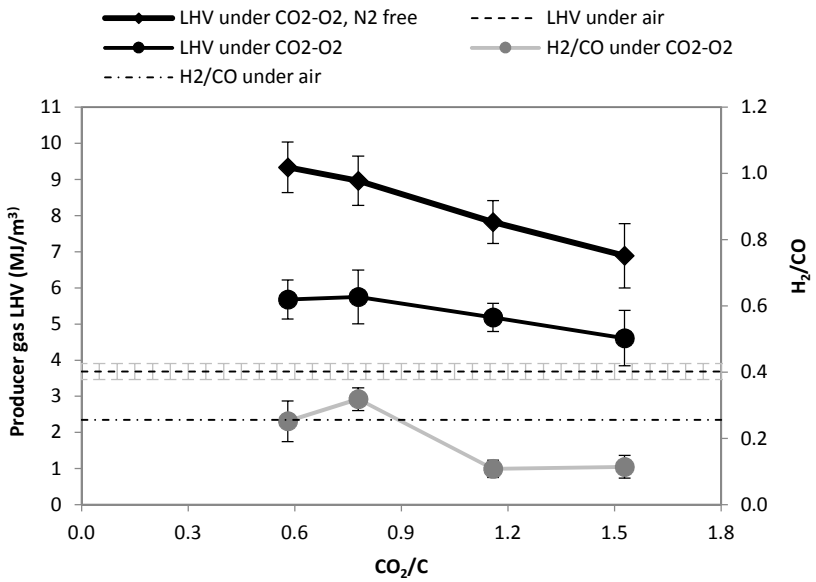

Figure 3.7 The effect of CO_2/C ratio on the producer gas LHV and H_2/CO ratio

CO_2-O_2 gasification did not bring significant improvement of the H_2/CO ratio compared with air gasification. The H_2/CO ratio of the producer gas of the experiment with the CO_2/C ratio equals to and below 0.8 were just about same as the value of air gasification. Related to the low H_2 evolution, the CO_2/C ratio equals to and above 1.2 produced the producer gas with a lower H_2/CO ratio than that of air gasification. Hence, the utilization the producer gas seems more suitable as a fuel gas in heat and power generation than for the feed gas of the chemical product synthesis which in most case requires higher H_2/CO ratio over 1.

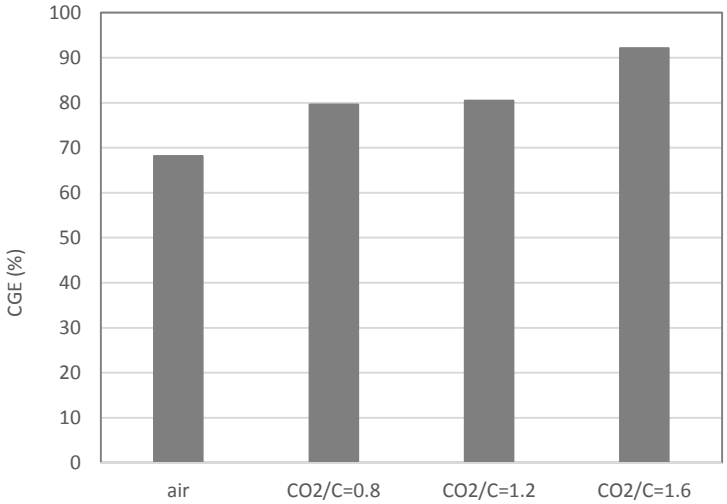

Figure 3.8 Cold gas efficiency of the air gasification and the CO_2-O_2 gasification

$$Cold\ gas\ efficiency\ \ (CGE)\ =\ \frac{\sum Y_i\left(\frac{\mathrm{kg}_{gas}}{\mathrm{kg}_{dry\ biomass}}\right)\ x\ LHV_i\left(\frac{MJ}{\mathrm{kg}_{gas}}\right)}{LHV_{dry\ biomass}\left(\frac{MJ}{\mathrm{kg}_{gas}}\right)}\ \ x\ 100\% \qquad (3.7)$$

Fig.3.8 shows the cold gas efficiency (CGE) of the air gasification and the CO_2-O_2 gasification under the various CO_2/C ratio. CGE was calculated as a ratio of the energy output of the producer to the lower heating value of dry biomass (Eq.3.7). CO_2-O_2 gasification under the examined CO_2/C range demonstrated higher cold gas efficiency than air gasification that might be correlated to the enhanced CO evolution. This finding shows that the implementation of CO_2-O_2 gasification is promising for realizing a high efficiency heat and power generation system. However, the significant effect of CO_2/C ratio on the efficiency profile is still unclear. Moreover as previously notified, the shown CGE values can be used merely for qualitative analysis and not for investigating the absolute value. Thus, further examination with more accurate gas flow measurement is required for more precisely examining the effect of CO_2 injection on the CGE.

3.4. Conclusion

The operability and the effect of the CO_2/C ratio in CO_2-O_2 gasification has been examined in this experimental campaign. CO_2-O_2 gasification was stably operated in a pilot scale downdraft gasifier under 0.6 - 1.6 CO_2/C ratios with the equivalence ratio of around 0.4-0.6.

Related to the O_2 concentration in the gasifying agent mixture, most of the recorded temperatures under the CO_2/C ratio of 0.6 and 0.9 were higher than those of under air gasification while the recorded temperatures under the CO_2/C ratio of 1.2 and 1.6 were mostly comparable with those under air gasification. Compared with that of air gasification, the temperature profile of CO_2-O_2 gasification with the CO_2/C ratio of 1.2 and below indicated the occurrence of the long and uniformly distributed high temperature zone in the reactor that might be favorable for the progress of endothermic reactions.

The dilution effect of unreacted CO_2 was increased as the CO_2/C ratio increased and suppressed the other gases fraction in producer gas. The decrease of the CO fraction was less significant than the increase of the CO_2 fraction that implied the progress of CO_2 to CO conversion.

Owing to the increase of the dilution by unreacted portion of CO_2, the producer gas LHV was decreased by the increase of the CO_2/C ratio. Nevertheless, the producer gas of CO_2-O_2 gasification still had higher LHV than those of air gasification even at the comparable amount of O_2 diluent in the gasifying agent. CO_2-O_2 gasification did not bring significant improvement of the H_2/CO ratio compared with air gasification. It implied the suitability of the producer gas for heat and power generation.

No significant effect of the CO_2/C ratio was observed on the cold gas efficiency of the gasifier. However, the cold gas efficiencies of CO_2-O_2 gasification were consistently higher than those of air gasification at the examined CO_2/C ratio range. These finding show that the implementation of CO_2-O_2 gasification is promising in replacing the conventional air gasification for a high efficiency heat and power generation system.

References

[1] L Garcia, M.L Salvador, J Arauzo, R Bilbao, CO_2 as a gasifying agent for gas production from pine sawdust at low temperatures using a Ni/Al coprecipitated catalyst, Fuel Processing Technology, Volume 69, Issue 2, February 2001, Pages 157-174

[2] Karel Svoboda, Michael Pohořelý, Michal Jeremiáš, Petra Kameníková, Miloslav Hartman, Siarhei Skoblja, Michal Šyc, Fluidized bed gasification of coal–oil and coal–water–oil slurries by oxygen–steam and oxygen–CO_2 mixtures, Fuel Processing Technology, Volume 95, March 2012, Pages 16-26

[3] Bayu Prabowo, Kentaro Umeki, Mi Yan, Masato R. Nakamura, Marco J. Castaldi, Kunio Yoshikawa, CO_2–steam mixture for direct and indirect gasification of rice straw in a downdraft gasifier: Laboratory-scale experiments and performance prediction, Applied Energy, Volume 113, January 2014, Pages 670-679

[4] Alberto Pettinau, Caterina Frau, Francesca Ferrara, Performance assessment of a fixed-bed gasification pilot plant for combined power generation and hydrogen production, Fuel Processing Technology, Volume 92, Issue 10, October 2011, Pages 1946-1953

[5] Toshiaki Hanaoka, Kinya Sakanishi, Yukihiko Okumura, The effect of N2/CO2/O2 content and pressure on characteristics and CO2 gasification behavior of biomass-derived char, Fuel Processing Technology, Volume 104, December 2012, Pages 287-294

[6] M. Pohořelý, M. Jeremiáš, K. Svoboda, P. Kameníková, S. Skoblia, Z. Beňo, CO2 as moderator for biomass gasification, Fuel, Volume 117, Part A, 30 January 2014, Pages 198-205

[7] M. Pohořelý, M. Jeremiáš, K. Svoboda, P. Kameníková, S. Skoblia, Z. Beňo, CO2 as moderator for biomass gasification, Fuel, Volume 117, Part A, 30 January 2014, Pages 198-205

[8] J. Riaza, M.V. Gil, L. Álvarez, C. Pevida, J.J. Pis, F. Rubiera, Oxy-fuel combustion of coal and biomass blends, Energy, Volume 41, Issue 1, May 2012, Pages 429-435

[9] Terry Wall, Yinghui Liu, Chris Spero, Liza Elliott, Sameer Khare, Renu Rathnam, Farida Zeenathal, Behdad Moghtaderi, Bart Buhre, Changdong Sheng, Raj Gupta, Toshihiko Yamada, Keiji Makino, Jianglong Yu, An overview on oxyfuel coal combustion—State of the art research and technology development, Chemical Engineering Research and Design, Volume 87, Issue 8, August 2009, Pages 1003-1016

Supplement Material

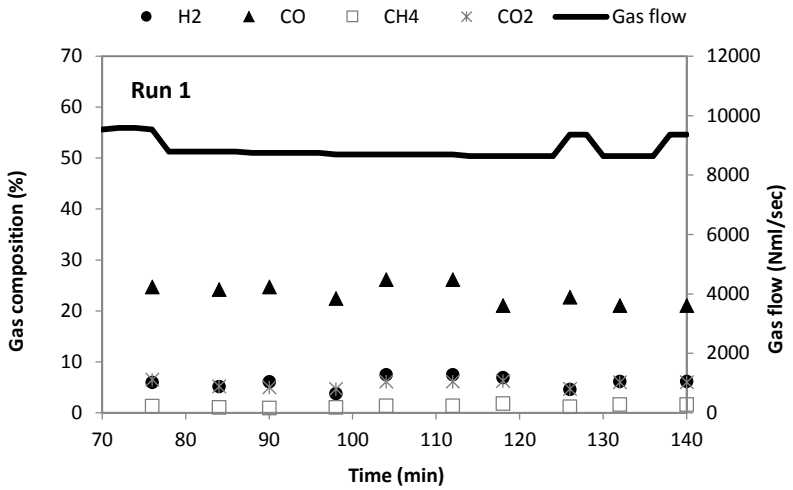

Supplement Figure 3.1 Producer gas evolution during the experimental run 1

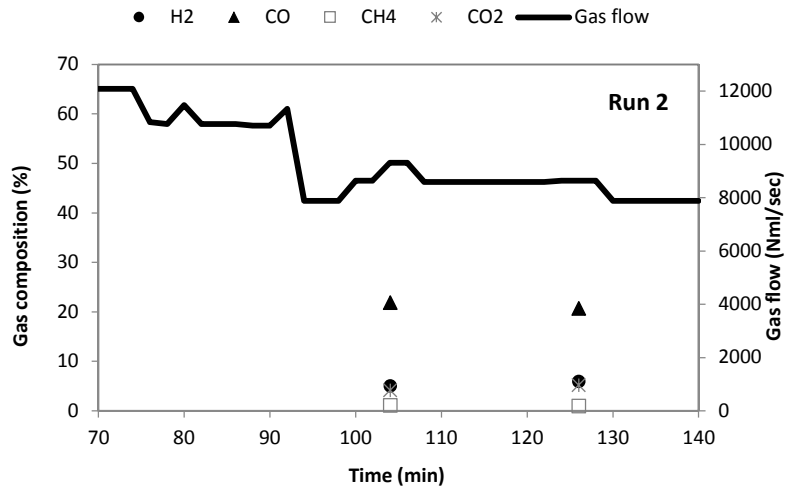

Supplement Figure 3.2 Producer gas evolution during the experimental run 2

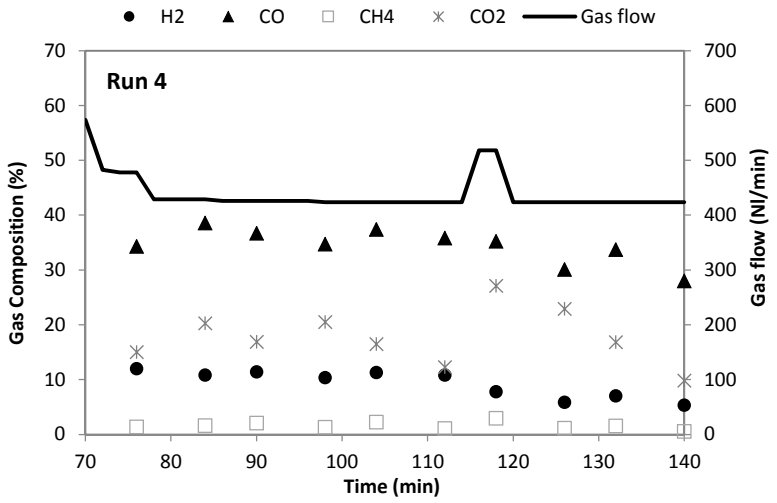

Supplement Figure 3.3 Producer gas evolution during the experimental run 4

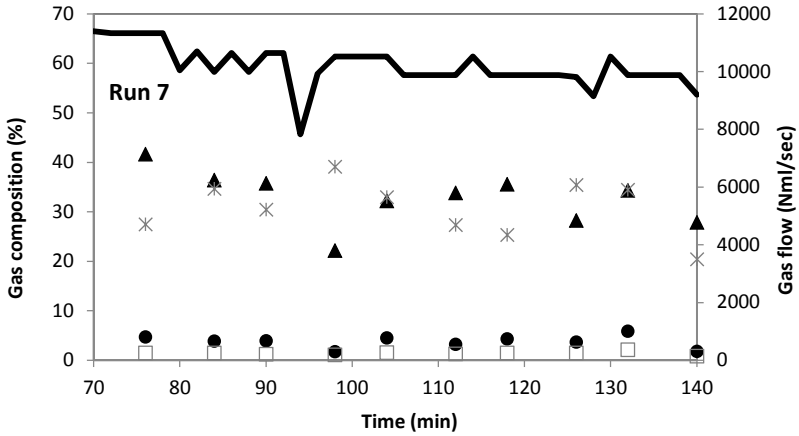

Supplement Figure 3.4 Producer gas evolution during the experimental run 6

Chapter IV

CO_2 recycled biomass gasification system for high efficiency and carbon-negative power generation

4.1 Introduction

Despite the previously investigated potential of CO_2 to be utilized as gasifying agent, only limited number of research works examined the comprehensive system including the CO_2 supply [1-3] and all were performed for coal feedstock. Oki [3] recently investigated the CO_2 recycle in the pressurized coal oxy-IGCC and successfully proposed a system with more than 40 % efficiency even after CO_2 sequestration. Based on that finding, a biomass based CO_2 recycled gasification system was developed. Simplification is proposed by doing the atmospheric gasification process and by deleting the steam turbine component and optimizing the utilization of hot gas turbine flue gas as a heat carrier as well as a gasifying agent. This simplification might be required since in some cases, small and distributed conversion is designated for processing biomass

In this chapter, the performance of the power system with CO_2 recycling to a gasifier and the gas turbine cycle was analyzed using the thermal equilibrium model. Validation and model adjustment were performed for the gasifier component by comparing the simulation results with the results of the previous chapter with comparable conditions. The analysis and optimization of the performance of the system as a function of the amount of the recycled CO_2 to the gasifier under various conditions were conducted. The gasifier temperature was varied from 750˚C to 950˚C, and the turbine inlet and exit temperature of the gas turbine were varied from 1000˚C to 1200˚C and 900 ˚C to 1000˚C, respectively. The comparison of the efficiency and CO_2 emission to those of the conventional air gasification was also performed.

4.2 Process modelling methodology

Fig.4.1 shows the scheme of the proposed CO_2 recycled gasification system. Aspen Plus software is utilized for developing the system and simulating its performance. The processes simulation was done based on the mass and energy balance and chemical equilibrium which were performed under these following assumptions:

- Chemical reactions reached the equilibrium condition. Kinetic and physical limitations are neglected.
- All gases are following the ideal gas properties.
- No pressure and temperature drop inside the components and during the transportation between components

The basic parameters of the involved components were set as follow:

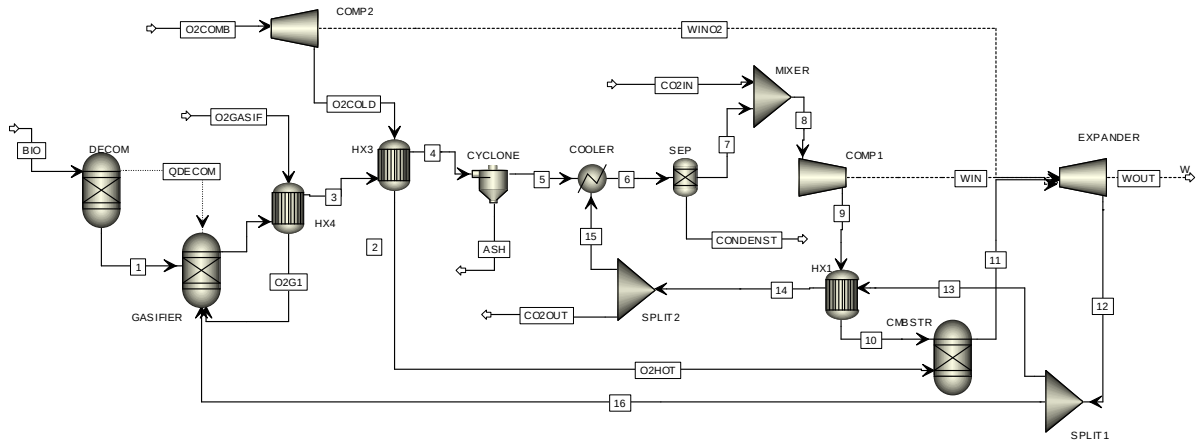

Figure 4.1 Scheme of the CO_2 recycled gasification system

4.2.1 Material and streams

Coconut shell sample utilized in the previous chapter was used as a biomass feedstock model (BIO stream) with the moisture content adjusted to 10 %. All of the material and stream from the outside of process were in ambient condition (25˚C, 1 atm.). The streams in the process were in the atmospheric pressure and the possible lowest temperature was 40˚C (after COOLER block). The feed rate was fixed at 100 kg/hr to simulate the small and distributed power generation system.

4.2.2 Gasifier

Gasifier component was simulated using the RGibbs reactor model. Syngas composition; consisted of C residue, H_2,CO, CO_2, H_2O, N_2, O_2, NO, NO_2, benzene, toluene, and phenol; and the temperature were calculated based on the minimization of the Gibbs free energy. Prior to the gasifier, a block for decomposition (DECOM block) is required when we use biomass as a feedstock since biomass is a non-conventional component in Aspen Plus. Decomposition block was simulated using RYield where the feedstock is converted into its components including carbon, H_2, O_2, H_2O, and N_2. The yield distribution

was specified based on the feedstock's ultimate analysis using a FORTRAN statement in Calculator block. The elements and heat generated from decomposition process were then go into the gasifier block. Oxygen supply to the gasifier was set as a dependent variable to maintain the gasifier at the target temperature, 750-950˚C, by setting the design specification and the manipulated variable limit in Design Spec block.

4.2.3 Gas turbine

The gas turbine was simulated as an arrangement of a compressor, a combustor, a turbine/expander, and a heat exchanger. The parameter setting of each component is shown in Table 4.1. The combustor was also simulated using RGibbs, so that the combustion products were calculated based on the minimization of the Gibbs free energy. Oxygen supply to combustor was specified to be in the exact amount for stoichiometric combustion of producer gas by specifying another FORTRAN statement in Calculator block. For the purpose of maintaining combustor at the targeted temperature (1000˚C-1200˚C), CO_2 supply to the compressor as a producer gas diluent was set as a dependent variable and manipulated by using Design Spec block specification Since there is no heat loss in the system, the turbine inlet temperature (TIT) was assumed to be the same as the combustor temperature. For the purpose of maintaining turbine exit temperature (TET) at the targeted temperature (900˚C -1000˚C), pressure ratio of the compressors were set as a dependent variable and manipulated by using another Design Spec block specification.

Table 4.1 Gas turbine parameter setting

Component	Parameter	Basic setting
Compressor	Isentropic efficiency	72 %
Turbine/Expander	Inlet temperature	1000˚C - 1200˚C
	Exit temperature	900˚C - 1000˚C
	Isentropic efficiency	80%
Heat exchanger	Minimum temperature approach	20 ˚C

4.2.4 Other auxiliary components

The other installed auxiliary components are two heat exchangers (HX2 and HX3), an oxygen compressor (COMP2), a cyclone (CYCLONE), a gas cooler (COOLER), a liquid separator (SEP), a gas mixer (MIXER), and two gas splitters (SPLIT1 and SPLIT2). The parameter setting of heat exchangers and the compressor were the same as those that were attached in the gas turbine. The cyclone and liquid separators separated all of ash and liquid from the producer gas stream, respectively. The gas cooler outlet temperature

was set to 40˚C. In order to simplify the system, the air separation unit was not simulated and the oxygen supply is assumed to come independently from the outside of the system (i.e. oxygen tank or cylinders). The energy requirement of oxygen supply, 0.576 MJ/kg_{O_2} was taken from the reference [7].

4.3 Result and discussion

4.3.1 Description of CO_2 recycled gasification system

As shown in Fig.4.1, the main improvement of the CO_2 recycled gasification system compared to the conventional air blown gasification system [8] are the recycle of high temperature flue gas from the gas turbine, which mainly consisted of CO_2, to the gasifier (stream 16) and to the gas turbine cycle (stream 15). To the gasifier, the recycled CO_2 was aimed to be the heat carrier and the additional gasifying agent. The Bouduard`s reaction (Eq.4.1) and the reverse water gas shift reaction (Eq.4.2) were expected to be the dominant reactions in the gasifier so that the produced CO and the unconverted CO_2 would be the major composition in the producer gas (stream 2). To the gas turbine cycle, the recycled CO_2 was aimed to be the producer gas diluent for controlling the turbine inlet temperature (TIT). Combustion of the diluted producer gas with oxygen would exhaust high concentration of CO_2, over than 98% mass, and small amount of water vapor so it can be recycled in the next process cycle (stream 12). The un-recycled part of the flue gas would go to the CO_2 sequestration. Since one of the main objective of this study is to find the optimum amount of recycled CO_2 to the gasifier and since CO_2 recycled to the gas turbine cycle is a dependent variable of TIT, the term of the CO_2 recycle ratio used hereafter in this manuscript is refer to the amount of recycled CO_2 to the gasifier relative to the amount of carbon in biomass in one process cycle, as shown in Eq. 4.3. Three heat exchangers were attached for recovering the heat from the recycled part of the flue gas to the turbine cycle (HX1) and from the producer gas (HX2 and HX3).

$$C + CO_2 \rightarrow 2CO \qquad \Delta H = 171.1 \text{ kJ/mol} \qquad (4.1)$$

$$CO + H_2O \leftrightarrow CO_2 + H_2 \qquad \Delta H = -41.1 \text{ kJ/mol} \qquad (4.2)$$

$$CO_2\, recycle\, ratio = \frac{CO_2 \ recycled\ to\ gasifier\ (mol)}{C\ in\ biomass\ (mol/kg_b) X\ \dot{m}_b\ (kg_b)} \qquad (4.3)$$

CO_2 inlet (stream CO2IN) was installed for supplying CO_2 at the initial stage. The inlet will be latter closed during the process cycle since the system is net CO_2 generating so that the supplied CO_2 would be sustained in the cycle. However during the operation cycles in this study, since the utilized simulation model cannot

accommodate the change of the operating mode, the CO_2 inlet tube was continuously operated to supply the producer gas diluent instead of splitting some of the flue gas back to the system by activating SPLIT2 block. Therefore, the net CO_2 output was calculated as a difference between the CO_2 output (stream CO2OUT) and the CO_2 input (stream CO2IN).

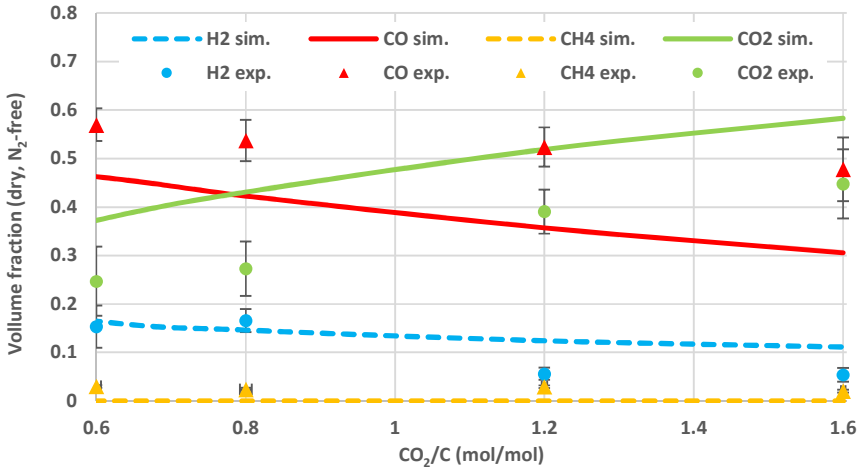

Figure 4.2 Comparison of the producer gas composition obtained from simulation and experiment

The validation analysis of this system was performed in the gasifier component by comparing the results of the simulation with the experiment results shown in chapter III. E/R was assumed to be fixed at 0.4. Fig.4.2 shows the comparison of the producer gas composition obtained in the simulation and the experiment. Compared with the experimental results, underestimation of CO along with overestimation of H_2 and CO_2 were observed in the simulation results. It implied that the water gas shift reaction (Eq.4.2) occurred in the experiment might be more than that was predicted in the simulation. The gas phase reaction in the freeboard seems to be significant in the real experiment. A slight underestimation of the CH_4 fraction was also shown by the simulation implying that the reactions in the real experiment was not perfectly reached the equilibrium. The root mean square (RMS) error between the simulation result and the experimental results was found as big as 6.045.

The gasifier model adjustment was performed by treating some part of CH4 as an inert gas from the gasifier and adding a water gas shift reactor block (WGSR) to simulate the freeboard reaction. The modified gasifier model configuration is shown in Fig.4.3. A constant yield of CH_4 was adjusted for every experimental run since previous researchers found that CH_4 generated from devolatilization is very stable and hardly affected by the secondary reaction [9, 10]. This CH_4 stream (stream 2B) then directly went to final stream of producer gas (stream 2D) after separated in SEP1 block. WGSR block was attached for accommodating the

extension of the water gas shift reaction. The calculation was performed under the equilibrium model with an equilibrium constant adjustment, f_{wgsr}, and parameters setting as suggested in the previous research [9], shown in Eq. 4.4. f_{wgsr} , empirically derived from the experiment results, is the correction factor of the equilibrium constant to accommodate the deviation from the equilibrium condition. WGSR block calculation was performed with the CSTR model block by previously adjusting the equilibrium constant in Reactions block specification in Aspen Plus. The optimization of CH_4 yield and f_{wgsr} to obtain the minimum RMS error from the experimental results, 3.819, were found to be -8 kg/kg-biomass and 10, respectively. The comparison of the producer gas composition obtained in the modified simulation and the experiment is shown in Fig.4.4. The modified model were utilized hereafter in this manuscript, however we found that it gave a very similar results to the pure equilibrium model for the system analysis.

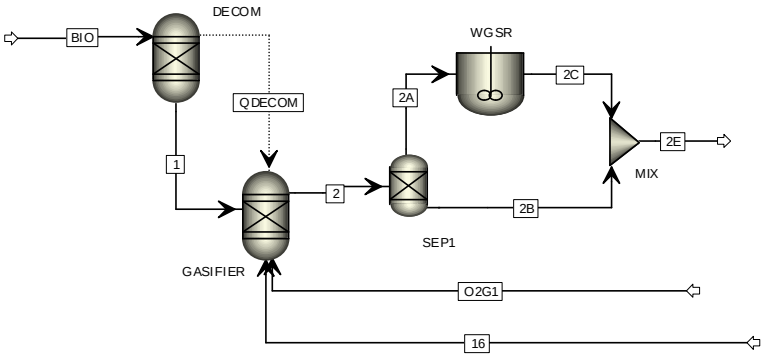

Figure 4.3 Scheme of the modified gasifier model configuration

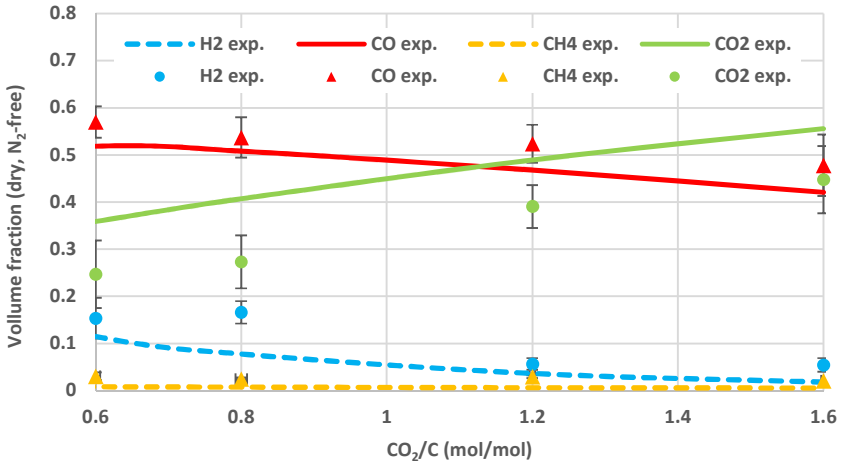

Figure 4.4 Comparison of the producer gas composition obtained from the modified simulation and the experiment

$$\frac{y_{H_2} y_{CO_2}}{y_{H_2O} y_{CO}} = f_{wgsr} \left(0.029 \exp\left(\frac{4094}{T}\right)\right) \quad (4.4)$$

4.3.2 Effect of the CO_2 recycle ratio on the operating variable and the thermal efficiency of the system at various gasifier temperature

Fig.4.5 shows the effect of the CO_2 recycle ratio on the required equivalence ratio (E/R) to maintain the gasifier at the target temperature of 750, 850 and 950˚C. In the first part of this study, the turbine inlet temperature (TIT) was kept at 1000˚C while the turbine exit temperature (TET) was kept at 900 ˚C. E/R is defined as the mole ratio of the supplied oxygen to the required oxygen for the stoichiometric combustion of the feedstock (Eq.4.5). The increased portion of the recycled CO_2 supplied into the gasifier generally resulted in a higher required E/R at the gasifier temperature of 850˚C and above. It implied that the existence of CO_2 increased the heat demand in the gasifier so that the higher extent of the feedstock oxidation was required to provide the heat for maintaining the target temperature. At 950˚C, where the increase is the most significant, the E/R increase was mainly caused by the lower temperature of CO_2 supply (900˚C) than the target so that it acted as a heat recipient. At 850˚C, where the increase was less significant than that at 950˚C, the E/R increase might be caused by the increase of endothermic reactions extent since the supply temperature is higher than the target temperature. A decreasing trend was observed at 750˚C since the heat carried by the recycled CO_2 was more than the heat demand to maintain the target temperature especially at the high CO_2 recycle ratio.

$$\text{Equivalence ratio } (E/R) = \frac{O_2 \ supply \ (mol)}{O_2 \ for \ stochiometric \ combustion \ (mol)} \quad (4.5)$$

Fig.4.6 shows the effect of the CO_2 recycle ratio on each producer gas specie at the gasifier temperature of 750, 850 and 950˚C. At all gasifer temperatures, the increase of CO was observed together with the decrease of H_2 and CO_2 as the CO_2 recycle ratio increased. The temperature played a positive role on the significance of those trends. These implied that the Bouduard's reaction (Eq.4.1) and the reverse water gas shift reaction (Eq.4.2) were the main reactions occurred in the gasifier and they were enhanced by the increase of CO_2 injection into the gasifier and the setting of the temperature. The yield of CH_4 was fixed at -8 kg/kg-biomass while the other gas species were minor under the examined condition.

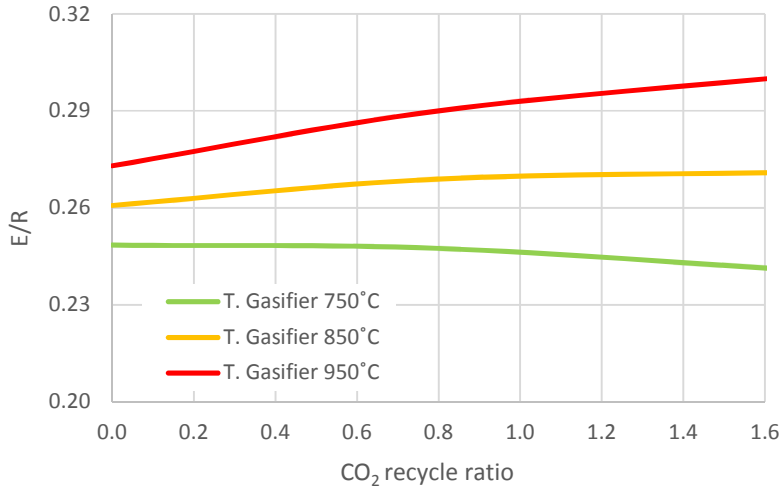

Figure 4.5 Effect of CO_2 recycle ratio on the required equivalence ratio at various gasifier temperatures

Fig.4.7 shows the gasifier efficiency and the gas turbine efficiency of the CO_2 recycled gasification as a function of the CO_2 recycle ratio under the various gasifier temperature setting. The efficiency of the gasifier is evaluated by the cold gas efficiency (CGE) and it is calculated as the low heating value (LHV) based ratio of the energy of the producer gas and the energy of the biomass supplied in one process cycle as shown in Eq.4.6. $\dot{m}$ is the mass flow rate while p subscript refer to producer gas and b subscript refer to biomass. The term of the gasifier efficiency is used in this paper to clearly distinguish it from the other term of the efficiency, i.e. the turbine efficiency and the system efficiency. The CO_2 recycle ratio positively affected the gasifier efficiency at 750˚C and 850˚C, with the more significant increase shown at the lower temperature. At the gasifier temperature of 750˚C, the gasifier efficiency increase as CO2 recycle ratio increased was strongly correlated with the reduced E/R. While at the gasifier temperature of 850˚C , the gasifier efficiency increase implied that the producer gas energy increased due to the enhancement of the Bouduard's and water gas shift reactions by introducing CO_2 into the gasifier was more than the producer gas energy reduced by the increase of the oxidized part of the feedstock. As previously explained, the increase of the CO_2 recycle ratio required higher extent of the feedstock oxidation, indicated by E/R, for maintaining the gasifier temperature. A higher extent of the feedstock oxidation on the other hand reduced the portion of the feedstock to be converted to the producer gas and resulted in a low energy yield. At 950˚C, the CO_2 recycle ratio trivially affected the gasifier efficiency which indicated the balance between the energy increases due to the progress of CO_2 involved reactions and the energy decrease due to the reduced feedstock for the producer gas precursor.

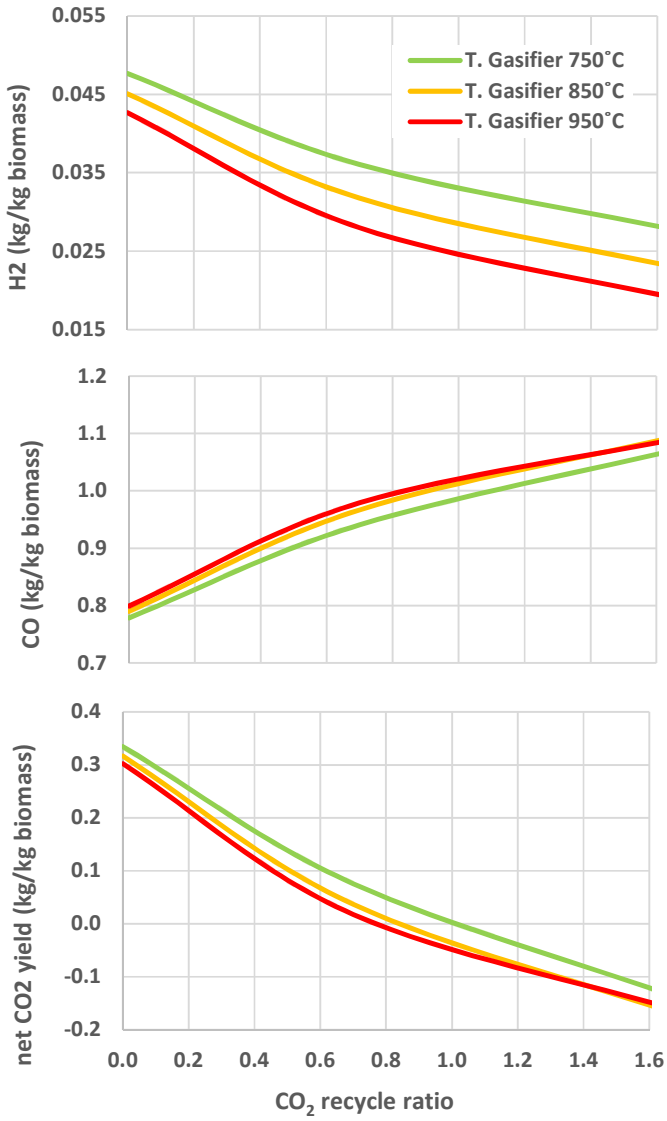

Figure 4.6 Effect of the CO_2 recycle ratio on the producer gas yield at various gasifier temperatures

The gas turbine efficiency is calculated as the ratio of the net of the work produced by the gas turbine (subtraction of the turbine work, W_t, and the compressor work for the producer gas,$W_{c,p}$) and LHV based energy of the producer gas, as shown in Eq.4.7. As shown in Fig.4.7, the gas turbine efficiency at all gasifier temperatures remained constant under the CO_2 recycle ratio below 0.8 and then significantly decreased as the CO_2 recycle ratio was increased. The decrease was related to the significant reduction of the exchanged heat from the flue gas recycled to the turbine cycle (stream 13) to the compressed gas (stream 9) when the

recycled portion of flue gas to the gasifier (stream 16) increased over the CO_2 recycle ratio of 0.8. Under the CO_2 recycle ratio below 0.8, the minimum temperature approach (the pinch temperature) applied between the hot inlet (flue gas, stream 13) and the cold outlet (compressed gas, stream 10) temperatures which allowed a maximum heat transfer to the cold stream. Meanwhile under the CO_2 recycle ratio of 0.8 and above, the minimum temperature approach applied between the hot outlet (stream 14) and the cold inlet (stream 9) temperatures. The temperature setting of the gasifier slightly increased the gas turbine efficiency under the CO_2 recycle ratio of 0.8 and below since the producer gases produced in high temperature had low energy content, indicated by the low gasifier efficiencies.

$$\text{Gasifier efficiency (\%)} = \frac{LHV_p\left(\frac{MJ}{kg_p}\right)x\ \dot{m}_p\ (kg_p)}{LHV_b\left(\frac{MJ}{kg_b}\right)x\ \dot{m}_b\ (kg_b)} \qquad (4.6)$$

$$\text{Turbine efficiency (\%)} = \frac{(W_t - W_{c,p})\ (MJ)}{LHV_p\left(\frac{MJ}{kg_p}\right)x\ \dot{m}_p\ (kg_p)} \qquad (4.7)$$

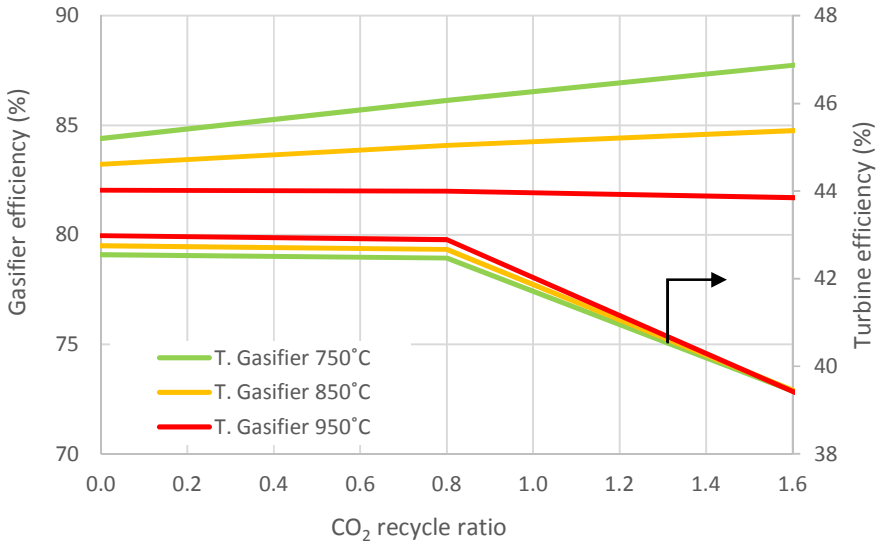

Figure 4.7 Effect of the CO_2 recycle ratio on the gasifier efficiency and the gas turbine efficiency at various gasifier temperatures

Fig.4.8 shows the overall efficiency of the CO_2 recycled gasification system as a function of the CO_2 recycle ratio under the various gasifier temperature setting. As shown in Eq.4.8, the system efficiency is calculated

as the ratio of the net of the work produced by the gas turbine (including the work of the O_2 compressor,W_{C,O_2}) and the energies of the supplied biomass and for supplying O_2 (multiplication of O_2 energy cost, E_{O_2} ,0.576 MJ/ kg_{O_2},with the mass flow rate of O_2, $\dot{m}_{O_2}$). The combination of the increase of the gasifier efficiency, the relatively constant energy for providing O_2 and the decrease of the gas turbine efficiency as the CO_2 recycle ratio increase, resulted in a peak of the system efficiency (34.78 %) under the CO_2 recycle ratio of 0.8 and the gasifier temperature of 750˚C. Similar trend with the lower values than those of at the gasifier temperature of 750˚C was observed at the gasifier temperature of 850˚C with the peak of the system efficiency of 34.11 %. Meanwhile, related to the low and trivial profile of the gasifier efficiency against the CO_2 recycle ratio, the system efficiency at 950˚C showed a low value compared with those at the lower temperatures and they were not increased as the CO_2 recycle ratio increased.

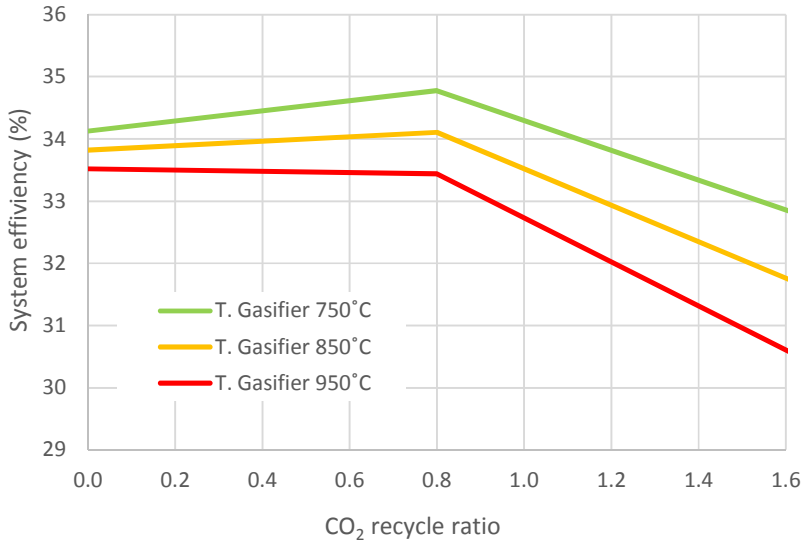

Figure 4.8 Effect of the CO_2 recycle ratio on the overall system efficiency at various gasifier temperatures

$$\text{System efficiency (\%)} = \frac{(W_t - W_{C,p} - W_{C,O_2})(MJ)}{LHV_b\left(\frac{MJ}{kg_b}\right)x\,\dot{m}_b\,(kg_b) + E_{O_2}\left(\frac{MJ}{kg_{O_2}}\right)x\dot{m}_{O_2}(kg_{O_2})} \qquad (4.8)$$

From the thermal equilibrium analysis of this CO_2 recycled gasification system, gasifier temperature as low as 750˚C was essential since CO_2 recycle at this condition produced some significant positive trend of the

system efficiency. However a problem might occur from the kinetic limitation of the CO_2-char reaction that is highly endothermic and slow. Our previous research in Chapter II indicated that 750˚C might be too low for expecting the optimum performance of CO_2 gasification. Other research also shown that catalyst is required to have the CO_2 gasification performance close to the equilibrium prediction at 750˚C [11]. Hence in this first part of study, 850˚C gasifier temperature with 0.7 CO_2 recycle ratio might be the most optimum condition for operating the CO_2 recycled gasification system.

4.3.3 Effect of the CO_2 recycle ratio on operating variables and the thermal efficiency of the system at various turbine inlet temperatures

Further study of the CO_2 recycled gasification performance was then performed by examining the efficiency of the system with higher applied turbine inlet temperature (TIT) micro gas turbines, 1100 and 1200˚C. These type of turbines have been developed using Si_3N_4 material over the past decades [4,5]. Higher TIT allow the turbine cycle to have higher pressure ratio at certain applied TET that in some extent will be resulted in higher turbine efficiency. Higher TIT also accept the turbine cycle to have higher applied TET so that the heat and material recovery by recycling CO_2 to the gasifier might become more advantageous. Performance optimization of the system was then conducted by varying the applied TET in the range of 900 ˚C -1000 ˚C and the applied TIT in the range of 1000 ˚C -1200 ˚C with the increments of 50 ˚C and 100 ˚C, respectively. 850˚C gasifier temperature was set as the basic condition for the hereafter examinations.

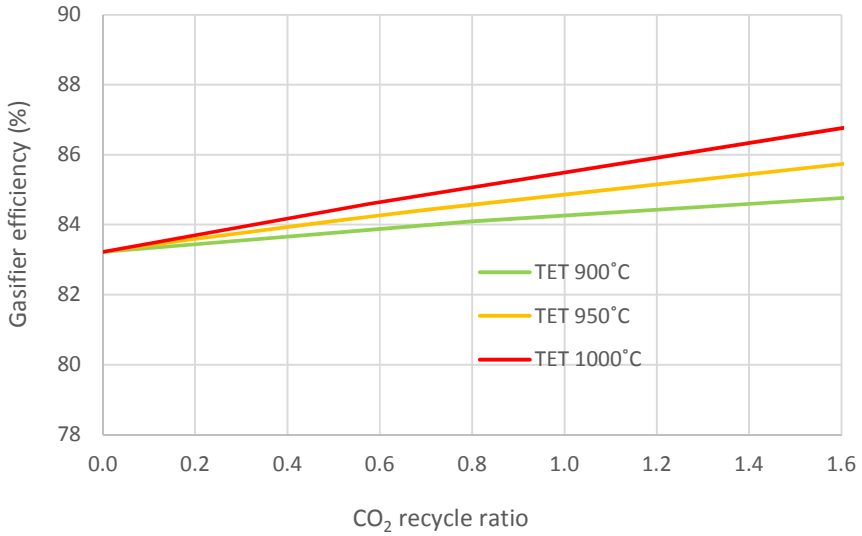

Figure 4.9 Effect of the CO_2 recycle ratio on the gasifier efficiency with the various TET

Fig. 4.9 showed the effect of CO_2 recycle ratio on the gasifier temperature at various TET, regardless the applied TIT. Related to the more significant heat supply to gasifier and the enhanced CO_2 to CO conversion especially through the Bouduard's reaction (Eq.4.1), the gasifier efficiency were more significantly increased by the CO_2 recycle ratio increase in the systems with the higher applied TET. However, as shwon in Fig. 4.10, the increase of gasifier efficiency by increasing applied TET were not in all conditions resulted in the higher efficiency of the system, particularly in the system with applied TIT of 1100 ˚C and below. With the applied TIT of 1000 ˚C, although the more significant effect of CO_2 recycle ratio was observed in the system with higher TET, low system efficiencies was shown by the system with the applied TET of 950˚C compared to those of with the applied TET of 900˚C. With the applied TIT of 1100 ˚C, the comparable yield of efficiency were produced by the system with the applied TET of 950 and 1000 ˚Cas the CO_2 recycle ratio increased to 0.6. The positive effect of applied TET was then observed as the efficiency of the system with the applied TET of 1000 was continuously increased by the CO_2 recycle ratio increase to 0.8 while those of the system with the lower applied TET were significantly decreased. The consistently positive effect of the applied TET was observed in the system with the applied TIT of 1200˚C where the high yield of efficiency was shown by the system with applied TET of 1000 ˚Ccompared with those of with the lower applied TET.

These occurrences implied that TET and TIT is not independently affecting the efficiency of the turbine and subsequently the overall system. The combination of these parameter that is corresponded in a certain pressure ratio was also the determining factor. Fig. 4.11 shows the relation between the turbine efficiency and the pressure ratio at various applied TIT and TET (the number on the data point shows the applied TET). It is shown that with all the examined applied TIT, the turbine efficiency was significantly increased by the pressure ratio increase to around 2.3 and moderately decreased afterwards. This peak come from the optimization between the increase of compressor work input and turbine/expander work output as the pressure ratio increased. However, the optimum pressure ratio of 2.3 might not be generally applicable and merely specific for the turbine condition examined in this study. The dependence of the work of compressor and turbine to the pressure ratio (ΔP) are shown in eqs. 4.9 and 4.10 where C_p is the specific heat capacity, CIT is the compressor inlet temperature ,TIT is the turbine inlet temperature ɲ is the isentropic efficiency, ΔP is the pressure ratio, and ɣ is the heat capacity ratio. p subscript refer to the producer gas f refer to the flue gas and t subscript refer to turbine/expander

$$W_c = -C_{p,p}\frac{CIT}{\eta_c}\left[\Delta P_c^{(\gamma-1)/\gamma} - 1\right] \qquad (4.9)$$

$$W_t = -C_{p,f}\,\eta_t TIT\left[1-\left(\frac{1}{\Delta P_t}\right)^{(\gamma-1)/\gamma}\right] \qquad (4.10)$$

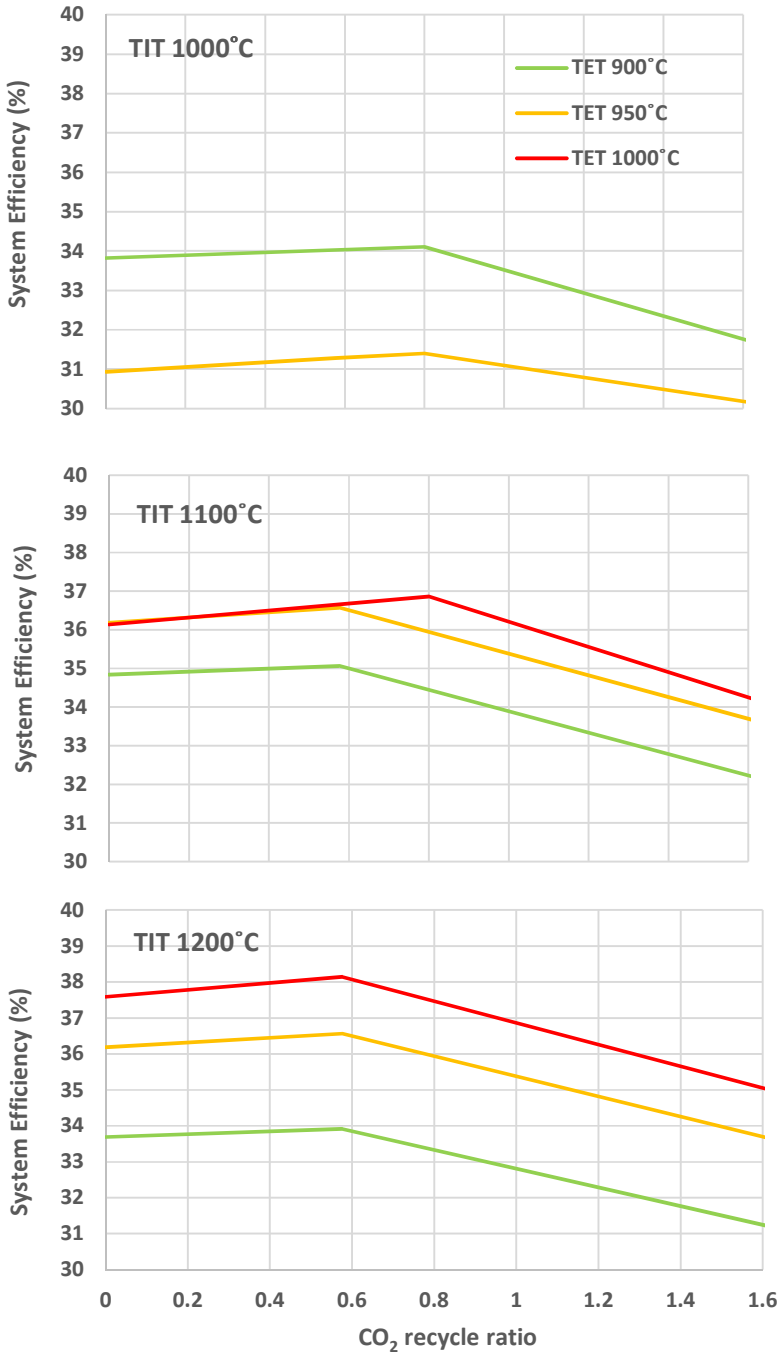

Figure 4.10 Effect of the CO_2 recycle ratio on the system efficiency with various applied TIT and TET

When 1000 ˚C TIT is applied, the increase of applied TET from 900 ˚C to 950 ˚C decreased the pressure ratio from 2.0 to 1.4 and since the values were less than 2.3, it is resulted in the significant decrease of turbine efficiency. When 1100 ˚CTIT is applied, the increase of applied TET from 900 ˚Cto 950 ˚Cdecreased the pressure ratio from 3.9 to 2.4 and resulted in the increase of turbine efficiency. Further increase of applied TET to 1000 ˚C decreased the pressure ratio to 1.8 and resulted in the slight decrease of turbine efficiency. The higher efficiency of the system with the applied of 1000 ˚C than that of with the applied TET of 950 ˚C, shown in Fig. 4.10, can be explained by the extended optimum CO_2 recycle ratio for the heat recovery in the turbine heat exchanger (HX1 block in Fig. 4.1) from 0.6 to 0.8 recycle ratio that allowed more heat to be supplied to the gasifier. This is related to the high heat content of the turbine exit stream (stream 12 in Fig. 4.1), which acted as the hot stream, and the relatively equal heat content of the compressed gas stream (stream 9 in Fig. 4.1), which acted as the cold stream, of the system with the applied of 1000 ˚C compared with those of the system with the applied TET of 950 ˚C.

With the applied TIT of 1200 ˚C, the application of TET in the range of 900 ˚C-1000 ˚C resulted in the pressure ratio over 2.3 thus their decrease were resulted in the continuous increase of turbine efficiency. However, the increase of applied TET did not increase the system efficiency corresponded CO_2 recycle ratio. This is since the heat content decrease of the compressed gas stream was significant and balanced the heat content increase of turbine exit stream. With the applied TIT of 1200 ˚C, the decrease of pressure ratio by the comparable applied TET increase is more significant than that of with the lower applied TIT; therefore, the more significant temperature decrease is also obtained.

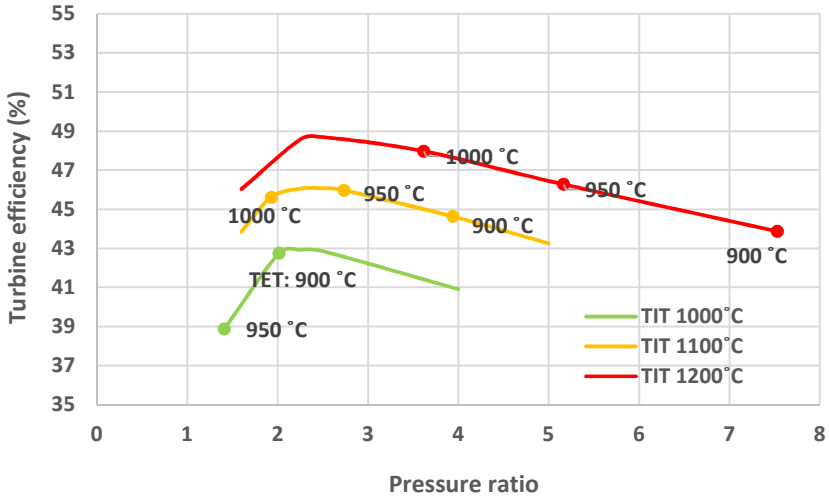

Figure 4.11 Effect of pressure ratio on the gas turbine efficiency with various applied TIT and TET

At the comparable pressure ratio, the higher TIT was resulted in the higher efficiency since the applied TIT is linearly related to turbine work, shown in eq. 4.10. Thus under the examined conditions, the optimum condition for gaining highest system efficiency, 38.14 %, is under 0.6 recycle ratio with applied the TET and TIT of 1000 ˚Cand 1200 ˚C. By observing the trend of the turbine efficiency against the pressure ratio, the application of higher TET and higher TIT than the current optimum condition might be favorable for gaining higher efficiency of the CO_2 recycled gasification system. However some technical difficulties might occur regarding the long time operation of the high temperature turbine and CO_2 stream with the current commercially available technology.

4.3.4 Performance comparison of the CO_2 recycled gasification system and the conventional air gasification system

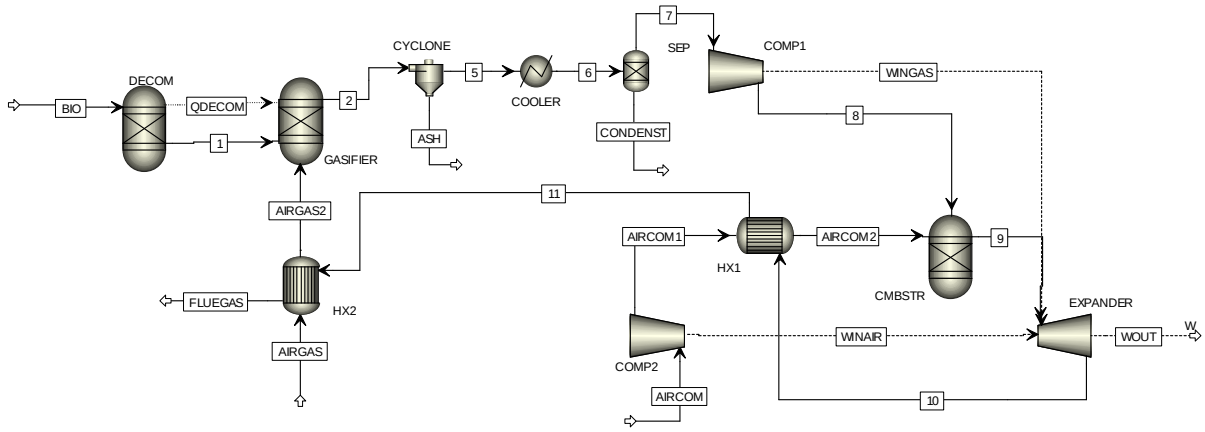

Figure 4.12 Scheme of the conventional air gasification system

As the comparison base for the proposed system, the conventional direct gasification system with air as a gasifying agent was simulated. Fig.4.12 shows the scheme of the conventional air gasification system. In this system, the heat source of the gasification process mainly came from the partial combustion of the feedstock while some heat was added from the recovery of the flue gas heat. The producer gas was then undergo the cooling, cleaning, and compressing processes before eventually fully oxidized with air in the gas turbine to generate electric power and exhausted as a flue gas. Two heat exchangers were attached for recovering heat in the flue gas to the compressed gas in the gas turbine (HX1) and to the gasifying agent (HX2).

Considering the kinetic limitation and the range of beneficial CO_2 recycle ratio, the representative condition for the CO_2 recycled was selected to be at the gasifier temperature of 850˚C and under 0.8 recycle ratio. Gas turbine was specified to be operated with TET of 1000˚C. For the conventional air gasification system in which the kinetic limitation might not be significant, 750˚C gasifier temperature, commonly obtained by supplying air at around 0.25-0.3 E/R, was consider as the optimum condition as suggested in the reference [12]. Refering to the specification micro gas turbine manufactured by Power Works™ (Ingersoll-Rand 70 kW type), the operated gas turbine was specified with TET of 700˚C and the efficiency around 30 %. For the comparison of the two system the applied TIT was fixed at 1100˚C

The streams condition of the CO_2 recycled gasification system is shown in Table 4.2 while that of the conventional air gasification system, shown in Table 4.3. Related to designated applied TET, the temperature difference between the flue gas of the gas turbine (stream 12) and the compressed gas (stream 9) of the CO_2 recycled gasification system (895˚C) is bigger than that in the conventional direct gasification system (between stream AIRC1 and stream 8) (374˚C). The higher temperature difference implied the opportunity for more efficient flue gas heat recovery in the CO_2 fed gas turbine than that in the conventional air fed gas turbine as well as highlighted the importance of the heat exchanger utilization in the CO_2 fed gas turbine for gaining a high efficiency. In addition, since the diluent flow of the CO_2 gasification system was almost twice higher than that of the conventional air gasification system, the volumetric turbine capacity is also needed to be almost twice bigger.

Table 4.4 shows the comparison of the optimum operating condition and the performance between the proposed CO_2 recycle gasification system and the conventional air gasification system. The proposed CO_2 recycle gasification system produced 11.93 % higher efficiency than the conventional air gasification under the compared condition. These were the result of the higher efficiencies of the gasifier and the turbine gas as CO_2 was introduced in those components. In the gasifier, the CO_2 recirculation to the system allow better heat recovery and provide more producer gas precursor than the merely flue gas heat recovery in the air gasification system. In the gas turbine, the usage of CO_2 as a diluent allow better heat recovery of the flue gas to the compressed gas than that of when N_2 is utilized. Hence under the certain applied TIT, a high amount of the diluent flow, which resulted in a high work output, is allowable for the CO_2 diluted fuel gas compared to that of N_2 diluted fuel gas.

Table 4.2 Stream conditions in the CO_2 recycled gasification system under the gasifier temperature=850˚C, CO_2 recycle ratio=0.6, TIT=1100˚C and TET=1000˚C (refer to Figs. 4.1 and 4.3)

Review item	Stream Name													
	2	2A	2B	2C	2D	3	4	5	6	7	8	9	10	11
Mass flow (kg/hr)														
H_2	3.08	3.08	-	3.08	3.08	3.08	3.08	3.08	3.08	3.08	3.08	3.08	3.08	-
CO	98.92	98.92	-	98.92	98.92	98.92	98.92	98.92	98.92	98.92	98.92	98.92	98.92	0.41
CO_2	126.44	126.44	-	126.44	126.44	126.44	126.44	126.44	126.44	126.44	8683.57	8683.57	8683.57	8840.56
CH_4	0.80	0.72	0.08	0.72	0.80	0.80	0.80	0.80	0.80	0.80	0.80	0.80	0.80	-
H_2O	24.38	24.38	-	24.38	24.38	24.38	24.38	24.38	24.38	-	-	-	-	29.30
N_2	0.15	0.15	-	0.15	0.15	0.15	0.15	0.15	0.15	0.15	0.15	0.15	0.15	0.15
O_2	-	-	-	-	-	-	-	-	-	-	-	-	-	0.23
Ash	2.48	2.48	-	2.48	2.48	2.48	2.48	-	-	-	-	-	-	-
Temp. (˚C)	850	850	850	850	850	787	638	638	40	40	40	105	980	1100
Pressure (atm.)	1.00	1.00	1.00	1.00	1.00	1.00	1.00	1.00	1.00	1.00	1.00	1.93	1.93	1.93

Review item	Stream Name													
	12	13	14	15*	16	O2G	O2G1	O2C	O2C1	O2C2	CO2OUT	CONDENST	ASH	CO2IN
Mass flow (kg/hr)														
H_2	-	-	-	-	-	-	-	-	-	-	-	-	-	-
CO	0.41	0.40	0.40	-	0.01	-	-	-	-	-	0.40	-	-	-
CO_2	8840.56	8714.49	8714.49	-	126.07	-	-	-	-	-	8714.48	-	-	8557.12
CH_4	-	-	-	-	-	-	-	-	-	-	-	-	-	-
H_2O	29.30	28.89	28.89	-	0.42	-	-	-	-	-	28.89	24.38	-	-
N_2	0.15	0.14	0.14	-	-	-	-	-	-	-	0.14	-	-	-
O_2	0.23	0.23	0.23	-	-	29.76	29.76	84.13	84.13	84.13	0.23	-	-	-
Ash	-	-	-	-	-	-	-	-	-	-	-	-	2.48	2.48
Temp.(˚C)	1000	1000	126	-	-	830	830	28	112	767	126	40	638	40
Pressure (atm.)	1.00	1.00	1.00	-	1.00	1.00	1.00	1.00	1.92	1.92	1.00	1.00	1.00	1.00

**stream is bypassed*

Table 4.3 Stream conditions in the conventional air gasification under the gasifier temperature=750˚C, TIT=1100˚C, and TET=700˚C (refer to Fig. 4.12)

Review item	Stream Name							
	2	3	4	5	6	7	8	9
Mass flow (kg/hr)								
H_2	4.73	4.73	4.73	4.73	4.73	-	-	-
CO	75.51	75.51	75.51	75.51	75.51	-	-	-
CO_2	38.84	38.84	38.84	38.84	38.84	157.99	157.99	157.99
CH_4	0.19	0.19	0.19	0.19	0.19	-	-	-
H_2O	10.56	10.56	10.56	-	-	42.71	42.71	42.71
N_2	107.03	107.03	107.03	107.03	107.03	1803.04	1803.04	1803.04
O_2	-	-	-	-	-	432.94	432.94	432.94
Ash	2.484	-	-	-	-	-	-	-
Temperature (˚C)	750	750	40	40	336	1101	700	388
Pressure (atm.)	1.00	1.00	1.00	1.00	6.79	6.79	1.00	1.00

Review item	Stream Name							
	AIRG	AIRG1	AIRC	AIRC1	AIRC2	FLUEGAS	CONDENST	ASH
Mass flow (kg/hr)								
H_2	-	-	-	-	-	-	-	-
CO	-	-	-	-	-	-	-	-
CO_2	-	-	-	-	-	157.99	-	-
CH_4	-	-	-	-	-	-	-	-
H_2O	-	-	-	-	-	42.71	10.56	-
N_2	106.89	106.89	1696.72	1696.72	1696.72	1803.04	-	-
O_2	32.46	32.46	515.19	515.19	515.19	432.94	-	-
Ash	-	-	-	-	-	-	-	2.48
Temperature (˚C)	28	368	28	326	680	370	40	750
Pressure (atm.)	1.00	1.00	1.00	6.79	6.79	1.00	1.00	1.00

Table 4.4 Comparison of the operating condition and the performance between the conventional air gasification system and the CO_2 recycled gasification system

Comparison item	Conventional air gasification	CO_2 recycled gasification
Condition		
Gasifier temperature (˚C)	750	850
Equivalence ratio	0.3	0.26
CO_2 recycle ratio (mol/mol ˚C)	0.0	0.6
TIT (˚C)	1100	1100
TET (˚C)	700	1000
Pressure ratio	6.8	1.9
Performance		
Gasifier efficiency (%)	80.87	85.07
Turbine efficiency (%)	30.82	45.51
System efficiency without CCS (%)	24.93	36.86
System efficiency with CCS (%)	-	30.67
CO_2 output (g/kwh)	1372.23	888.98

The CO_2 recycled gasification system exhausted 484.25 gCO_2/kWh lower CO_2 emission than the conventional air gasification at the examined condition. Hence considering the carbon-neutral property of biomass, this emission reduction can be realized as the implementation of the carbon-negative power plant. Moreover, unlike those of the air gasification, the exhaust gas of the CO_2 recycled gasification was in the form of high purity CO_2 (over than CO_2 98%mass) which was favorable for the sequestration process. If the sequestration is applied, the system would potentially have the negative carbon intensity up to -1372.23 gCO_2/kWh.

Up to 6.19 % efficiency penalty might be required for sequestration which mainly come from the CO_2 pressurizing process (considering the pressure for underground CO_2 injection, 150 atm.; the penalty should be less if only transporting is considered). However, the system efficiency of the CO_2 recycled gasification with CCS is still higher than that of the air gasification without CCS while the air gasification might require higher energy penalty due to the complexity of the applicable CCS techniques.

The oxy fuel combustion mode of CO_2 recycled gasification gas turbine is also adaptable to the higher applied TIT from the point of view of NO_x formation since the main diluting agent of gas turbine is CO_2. Thermal equilibrium analysis of CO_2 recycled gasification system under the conditions described in table 4.4 showed that the system maximally emitted 0.0017 gNO_x/kwh. This level was much lower than the NO_x emission intensity of most power plant [13].

4.4 Conclusion

A biomass fed power system utilizing CO_2 recycled to the gasifier and the gas turbine cycle was proposed and analyzed by using the thermal equilibrium model. For the first part of the study, the effect of the CO_2 recycle ratio was examined on the system with various gasifier temperatures, 750˚C, 850˚C, and 950˚C, and the specified turbine inlet temperature, 1000˚C and turbine exit temperature 900˚C. The increase of the CO_2 recycle ratio to the gasifier decreased the heat demand for maintaining the gasifier temperature at 750˚C, indicated by the decrease of required E/R, while it increased the heat demand for maintaining gasifier temperature the 850˚C and above, Moreover, CO_2 recycle enhanced the Bouduard's and reverse water gas shift reactions that were indicated by the increase of the CO yield and decrease of H_2 and CO_2 yields. The increase of gasifier efficiency as the CO_2 recycle ratio increased was observed at the gasifier temperature of 750˚C and 850˚C, while they were not observed at 950˚C. The gas turbine efficiency at all conditions was significantly decreased when the CO_2 recycle ratio increased over 0.8 due to the significantly reduced heat recovery in the gas turbine cycle. Peak of system efficiency were observed under the CO_2 recycle ratio of 0.8 at the gasifier temperature of 750˚C, 34.78 %, and 850˚C, 34.11 %, while it is not observable at 950˚C.

Performance optimization of the system was conducted by varying the applied TET in the range of 900 ˚C-1000˚C that is mixt by the application of TIT in the range of 1000˚C -1200˚C. 850˚C gasifier temperature was set as the basic condition. The gasifier efficiency were more significantly increased by the CO_2 recycle ratio increase in the systems with the higher applied TET. Additionally, the combination of TET and TIT that is corresponded in a certain pressure ratio was importantly determining the turbine efficiency and eventually system efficiency. The turbine efficiency was significantly increased by the pressure ratio increase to around 2.3 and moderately decreased afterwards. Under the examined conditions, the optimum condition for gaining highest system efficiency, 38.14 %, is under 0.6 recycle ratio with applied the TET and TIT of 1000˚C and 1200˚C.

Performance comparison of the proposed system with the conventional air gasification showed that the proposed system produced 11.93 % higher efficiency and exhausted 484.25 gCO_2/kWh CO_2 emission than the conventional air gasification. In addition, the exhausted CO_2 is in the form of high purity CO_2 stream which is suitable for sequestration or further utilization. Thus, considering the carbon neutrality of biomass feedstock, the system potentially implement carbon-negative power generation with the intensity around -484.25 to -1372.23 gCO_2/kwh. However, up to 6.12 % efficiency penalty might be required for the sequestration process.

Nomenclatures

C_p specific heat capacity (MJ/Kg˚C)

CIT compressor inlet temperature (˚C)

E production energy

f correction factor (dimensionless)

LHV low heating value (MJ/kg)

ṁ mass flow rate (kg/hr)

T temperature (K)

TIT turbine inlet temperature (˚C)

W work output (MJ/hr)

y molar fraction of gas specie in producer gas (kmol/kmol)

ΔP pressure ratio

ɲ isentropic efficiency (%)

ɣ specific heat capacity ratio

Subscript

b biomass

c compressor

f flue gas

p producer gas

t turbine

References

1. Marco J. Castaldi, John P. Dooher, Investigation into a catalytically controlled reaction gasifier (CCRG) for coal to hydrogen, International Journal of Hydrogen Energy, Volume 32, Issue 17, December 2007, Pages 4170-4179,
2. Michael E. Walker, Javad Abbasian, Donald J. Chmielewski, and Marco J. CastaldiDry Gasification Oxy-combustion Power Cycle, Energy Fuels, 2011, *25* (5), pages 2258–2266
3. Yuso Oki, Jun Inumaru, Saburo Hara, Makoto Kobayashi, Hiroaki Watanabe, Satoshi Umemoto, Hisao Makino, Development of oxy-fuel IGCC system with CO2 recirculation for CO2 capture, Energy Procedia, Volume 4, 2011, Pages 1066-1073
4. Claire Soares, Microturbines: Applications for Distributed Energy Systems, Butterworth-Heinemann, 2011
5. F. David Doty, Phase I Development of an Advanced, Intercooled, Ceramic Gas Microturbine, Unsolicited Proposal Submitted to the U.S Department of Energy, 2002 http://dotynmr.com/download/pubs/2003_Doty_DOE_CGMT.pdf
6. I. Takehara, T. Tatsumi, Y. Ichikawa Summary of CGT302 Ceramic Gas Turbine Research and Development Program, Journal of Engineering for gas turbine power, Volume 124, Issue 3, June 2002, Pages 627-635
7. Jean-Pierre Tranier, Richard Dubettier, Arthur Darde, Nicolas Perrin, Air separation, flue gas compression and purification units for oxy-coal combustion systems, Energy Procedia, Volume 4, 2011, Pages 966-971
8. Carolina Font Palma, Alastair D. Martin, Model based evaluation of six energy integration schemes applied to a small-scale gasification process for power generation, Biomass and Bioenergy, Volume 54, July 2013, Pages 201-210
9. A. Gómez-Barea, B. Leckner, Estimation of gas composition and char conversion in a fluidized bed biomass gasifier, Fuel, Volume 107, May 2013, Pages 419-431
10. S. Jarungthammachote, A. Dutta, Thermodynamic equilibrium model and second law analysis of a downdraft waste gasifier, Energy, Volume 32, Issue 9, September 2007, Pages 1660-1669
11. L Garcia, M.L Salvador, J Arauzo, R Bilbao, CO_2 as a gasifying agent for gas production from pine sawdust at low temperatures using a Ni/Al coprecipitated catalyst, Fuel Processing Technology, Volume 69, Issue 2, February 2001, Pages 157-174
12. T. Reed, A. Das. Handbook of Biomass Downdraft Gasifier Engine Systems. The Biomass Energy Foundation Press. 1988

13. Osamu Ito, Emissions from coal fired power Generation, Workshop on IEA High Efficiency Low Emissions Coal Technology Roadmap Date: 29 November 2011 Location: New Delhi http://www.iea.org/media/workshops/2011/cea/Ito.pdf

Chapter V

Conclusion and Recommendation

5.1 Conclusion

This thesis focused on the implementation of biomass CO_2 gasification for applying the high efficiency and carbon-negative power generation. In more detail this study was divided into three parts: first is the study of the basic biomass CO_2 gasification characteristics in a lab scale experiment, then the examination of the operability and performance of biomass CO_2 gasification in a pilot scale downdraft gasifier, and finally the proposal of the CO_2 recycled biomass gasification system. The followings are the summary of findings in this thesis.

In Chapter II, the effect of steam replacement by CO_2 for producing nitrogen-free producer gas was investigated in a lab-scale downdraft gasifier. The results showed that substitution of steam with CO_2 would generally lower the H_2 yield and enhance the CO yield. Inhibition of the CO_2-char reaction was observed under the presence of steam. It was confirmed by a significant CO evolution under pure CO_2 atmosphere. Positive effect of the CO_2 mixing ratio on the thermal efficiency of the gasifier was observed at the temperature of 850ºC and above. For the indirect gasification (without O_2 supply), the highest thermal efficiency of the gasifier (52%) was gained under the CO_2-only atmosphere at 850 ºC. For the direct gasification (with O_2 supply), the highest thermal efficiency (60%) was gained under the CO_2-O_2 atmosphere at 950º C. This calculation result shows that the gasification process with CO_2 as a gasifying agent and a heat carrier, especially in the direct gasification process, is potentially be more efficiently utilized in the N_2-free producer gas production than steam. The kinetics and diffusional limitations of CO_2-char reaction were significant at the reaction temperature of 750ºC. At the reaction temperature of 850ºC and above, the limitations were less so that the experimental CGE of CO_2-O_2 gasification results were close to the equilibrium prediction.

In Chapter III, the operability and the performance of the CO_2-O_2 gasification in a pilot scale downdraft gasifier were examined. The CO_2-O_2 gasification was stably operated for around 70 minutes in a pilot scale downdraft gasifier under 0.6 - 1.6 CO_2/C ratios and around 0.4-0.6 equivalence ratio. The progress of CO_2 to CO conversion mainly through the CO_2-char reaction and the dry reforming was indicated by the less significant decrease of the CO fraction than the increase of the CO_2 fraction in the producer gas as the CO_2/C ratio increased. Owing to the dilution effect of unreacted CO_2, LHV of the producer gas was

decreased by the increase of the CO_2/C ratio. Nevertheless, LHV of the producer gas of CO_2-O_2 gasification is still higher than those of air gasification even at the comparable amount of O_2 diluent in the gasifying agent. CO_2-O_2 gasification did not bring significant improvement of the H_2/CO ratio compared with air gasification that implied the suitability of its producer gas for heat and power generation fuel gas. A statistically significant effect of the CO_2/C ratio was hardly observed on the cold gas efficiency of the gasifier. However, the cold gas efficiencies of CO_2-O_2 gasification were consistently higher than those of air gasification at the examined CO_2/C range.

In Chapter IV, the CO_2 recycled biomass gasification system was proposed and optimized using the thermal equilibrium model that was adjusted with the results from the previous chapter. With 900˚C applied turbine exit temperature, the beneficial effect of CO_2 recycling was only significant at the gasifier temperature of 750ºC and it was less at the gasifier temperatures of 850ºC and 950ºC. This is because the recycled CO_2 temperature was not so high to give a substantial amount of heat to the gasifier with the target temperature of 850ºC and above. On the other hand, our previous finding in Chapter II showed that 750ºC might be too low to expect the optimum performance of CO_2 gasification because of the kinetic and physical limitations. Performance optimization of the system was then conducted by varying the applied TET in the range of 900 ˚C -1000 ˚C that is mixt by the application of TIT in the range of 1000˚C -1200˚C. 850˚C gasifier temperature was set as the basic condition. The gasifier efficiency were more significantly increased by the CO_2 recycle ratio increase in the systems with the higher applied TET. Additionally, the combination of TET and TIT that is corresponded in a certain pressure ratio was importantly determining the turbine efficiency and eventually system efficiency. The turbine efficiency was significantly increased by the pressure ratio increase to around 2.3 and moderately decreased afterwards. Under the examined conditions, the optimum condition for gaining highest system efficiency, 38.14 %, is under 0.6 recycle ratio with applied the TET and TIT of 1000˚C and 1200˚C. The proposed system produced 11.93 % higher efficiency and exhausted 484.25 gCO_2/kWh CO_2 emission than the conventional air gasification. In addition, the exhausted CO_2 is in the form of high purity CO_2 stream which is suitable for sequestration or further utilization. Thus, considering the carbon neutrality of biomass feedstock, the system potentially implement carbon-negative power generation with the intensity around -484.25 to -1372.23 gCO_2/kwh.

5.2 Recommendations for future research

Some research focus might be developed based on the present works as follows:

1. The examination of the gas yield and the thermal efficiency of the pilot scale CO_2 gasification still needs to be performed since our gas flow measurement in the pilot scale experiment might be imprecise. A more precise gas flow meter than the orifice meter should be utilized.
2. The behavior of tar under various conditions of CO_2 gasification can be an important topic to be researched either in lab scale or more essentially in pilot scale.
3. Regarding the proposed CO_2 recycled biomass gasification system, the broaden utilization of the producer gas to chemical synthesis processes can be simulated and it might be also an interesting topic.
4. Furthermore, the development of the proposed system in lab scale and eventually pilot scale physical facility needs to be performed.
5. Eventually another thermochemical processes such as fast pyrolysis with CO_2 can be the alternative of gasification if the product is more important than power.